THESIS FOR THE DEGREE OF DOCTOR OF PHILOSOPHY

On Optimization Based Control of Distributed Energy Resources in Power Systems

Electricity Markets and Voltage Regulation Perspectives

by

PAVAN BALRAM

Division of Electric Power Engineering
Department of Energy and Environment
CHALMERS UNIVERSITY OF TECHNOLOGY
Gothenburg, Sweden 2016

On Optimization Based Control of Distributed Energy Resources in Power Systems
Electricity Markets and Voltage Regulation Perspectives
PAVAN BALRAM
ISBN 978-91-7597-515-3

Technical Report at Chalmers University of Technology
Technical Report No. 4196
ISSN 0346-718X

Division of Electric Power Engineering
Department of Energy and Environment
Chalmers University of Technology
SE-412 96 Gothenburg
Sweden
Telephone: +46 (0)31-772 1000

Printed by Chalmers Reproservice
Gothenburg, Sweden 2016

♡ *To Shweta*

On Optimization Based Control of Distributed Energy Resources in Power Systems
-Electricity Markets and Voltage Regulation Perspectives
PAVAN BALRAM
Department of Energy and Environment
Chalmers University of Technology

Abstract

Distributed energy resources are increasingly being integrated into power systems around the world. These resources, typically connected at the distribution system level, are already changing the pattern of power flow from being unidirectional to multidirectional. Treating them as negative loads would only limit their further integration and could add to grid investment costs, while optimally controlling their output could potentially reverse that position. The latter approach is of significance to electricity markets and stakeholders that trade electrical energy as a commodity, as well as distribution systems and their operators, whose primary responsibility is to deliver electricity reliably and securely to customers. This dissertation deals with modeling and investigating the effects of price-based scheduling of aggregated electric vehicle energy for electricity markets and their coordinated control along with other distributed energy resources for voltage control in electrical distribution systems.

Investigations from an economic perspective include the effects on electricity prices in day-ahead and regulating power markets, impact on retailer's profits, electricity pricing to variable and fixed retail contract customers and associated savings in charging cost for vehicle owners. For this purpose, an electric vehicle aggregator model is developed under day-ahead, regulating power and retail market paradigms. Results show that electrifying all vehicles in the Nordic area and performing price-based control of charging could lead to flattening of day-ahead electricity market price curve when compared to simpler charging strategies that could lead to higher peak prices over the day. In a regulating power market, the aggregator was found to potentially help the system during up-regulation by reducing active power losses due to local production, also reducing the corresponding cost for balancing the power system during operational hour. An electricity retailer performing a two-stage stochastic planning while accounting for price-responsive scheduling by an aggregator could potentially increase their profits with greater number of electric vehicle customers. For the latter, the charging cost savings were found to be higher when more than 30% of the customers opt for variable retail contracts, while for the remaining consumers, the price for fixed retail contracts was found to increase by up to 2 Euros per MWh.

Technical issues investigated include the adoption of centralized and distributed model predictive control-based coordinated voltage regulation using distributed energy resources and their comparison in terms of reactive power utilized and influence on active power loss within a network. Distributed resources considered were solar photovoltaics and battery energy storage systems that could be controllable due to power converter interfacing with the grid. Results from case studies indicate that the developed centralized and distributed model predictive control strategies function according to the design criteria and are able to control bus voltages across the distribution network satisfactorily. The

proposed distributed model predictive control strategies, while providing potential practical advantages, utilize around 1.3% more reactive power reserves compared to centralized control strategy for voltage control, also resulting in greater active power losses.

Field validation was also performed in this thesis wherein, the reactive power ouput of a voltage source converter was controlled using the developed voltage control algorithm to maintain a remote bus voltage in the distribution system within specified bounds. Results from the tests indicate that the developed control algorithm functions successfully and as intended within a practical setting.

Keywords: Electric vehicles, battery energy storage, photovoltaics, electricity markets, coordinated voltage control, model predictive control and distribution systems

Acknowledgements

This work has been carried out at the Division of Electric Power Engineering, Department of Energy and Environment, Chalmers University of Technology, Gothenburg, Sweden. The financial support provided by E.ON Sverige AB is gratefully acknowledged.

I would like to thank my examiner and main supervisor during the second half of the project, Prof. Ola Carlson for his constant support and guidance. I express my sincere gratitude to Dr. Tuan Le, who was my co-supervisor for the entire length of the project for his tremendous patience, constant guidance, stimulating discussions and critical comments regarding the work. I would also like to thank Prof. Lina Bertling Tjernberg for her help and encouragement during the first two and a half years of the project.

I am extremely grateful to my reference group from E.ON Sverige AB consisting of Pierre Andersson-Ek, Ingmar Leisse, Malin Johnsson and Demijan Panic, who have been instrumental in their feedback that helped refine the work during the second half of the project. I would also like to thank Lars Bierlein and Peder Berne from E.ON Sverige AB for their involvement and feedback during the first half of the project. Special thanks also goes to Michael Bayer, David Csongor, Johan Karlsson and Stephan Sprenger for hosting me at E.ON, Energy Trading, Düsseldorf during my study visit and for walking me through various practical aspects of energy trading in Nordic power market. In addition, I appreciate the help provided by Ola Ölme of Göteborg Energi DinEl AB regarding retail electricity market in Sweden.

I am much obliged to my colleagues at Electric Power Engineering division of Chalmers, especially my fellow office mates Joachim Härsjö, Nicolas Espinoza, Pinar Tokat, Pramod Bangalore and Daniel Pehrman for providing a wonderful and memorable working environment. I would specially like to convey my appreciation towards David Steen for his help and cooperation.

I am greatly indebted to my wife, Shweta Tigga for her friendship and unconditional love that has enriched my life. Finally, I cannot even begin to express the gratitude that I have for my parents and brother, for unselfishly loving and always believing in me.

Pavan Balram
Göteborg, Sweden
December 2016

List of Abbreviations

ACOPF	Alternating-current Optimal Power Flow
AMI	Advanced Metering Infrastructure
ASM	Aggregator Scheduling Method
BESS	Battery energy storage system
BRP	Balance Responsible Party
CVaR	Conditional Value at Risk
DAM	Day Ahead Market
DCOPF	Direct-current Optimal Power Flow
DER	Distributed Energy Resource
DG	Distributed Generator
DR	Demand Response
DSO	Distribution System Operator
EV	Electric Vehicle
GAMS	General Algebraic Modelling System
HEV	Hybrid Electric Vehicle
ICE	Internal Combustion Engine
ICT	Information and Communication Technology
IEA	International Energy Agency
ITL	Incremental Transmission Loss
JSM	Joint Scheduling Method
LMP	Locational Marginal Price
LV	Low Voltage
LVC	Local Voltage Control
MPC	Model Predictive Control
MV	Medium Voltage
NTC	Net Transfer Capacity
OPF	Optimal Power Flow
PCC	Point of Common Coupling
PCVC	Predictive Centralized Voltage Control
PDVC	Predictive Decentralized Voltage Control
PHEV	Plug-in Hybrid Electric Vehicle
P-PDiVC	Parallel Predictive Distributed Voltage Control
PI	Proportional-Integral

PV	Photovoltaics
RP	Retailer Planning
RPM	Regulating Power Market
SOC	State-of-Charge
S-PDiVC	Sequential Predictive Distributed Voltage Control
TSO	Transmission System Operator
VSC	Voltage Source Converter

List of Symbols

Sets

T	Set of time periods in the planning horizon
N	Set of buses in the system
N_G	Set of generator buses in the system
N_L	Set of transmission lines in the system
N_V	Set of EV buses in the system
H	Set of hourly time periods in EV aggregator model
W	Set of scenarios
Y	Set of planning years
Q	Set of planning quarters
M	Set of planning months

Parameters

SOC^{max}	Aggregated maximum energy level of battery vehicles [MWh]
SOC^{min}	Aggregated minimum energy level of battery vehicles [MWh]
SOC^{ini}	Aggregated initial energy level of battery vehicles [MWh]
E_t^{next}	Aggregated energy required by battery vehicles for next day travel at time t [MWh/h]
C_t^L	Aggregator forecasted conventional load at time t [MWh/h]
SOC_i^{max}	Aggregated maximum energy level of battery vehicles at bus i [MWh]
SOC_i^{min}	Aggregated minimum energy level of battery vehicles at bus i [MWh]
SOC_i^{ini}	Aggregated initial energy level of battery vehicles at bus i [MWh]
$E_{i,t}^{next}$	Aggregated energy required by battery vehicles for next day travel at bus i at time t [MWh/h]
$E_{i,t}^{up}$	Planned up-regulating energy to be discharged at bus i at time t [MWh/h]
P_i^{max}	Maximum active power output of generator at bus i [MW]
P_i^{min}	Minimum active power output of generator at bus i [MW]
Q_i^{max}	Maximum reactive power output of generator at bus i [MVAr]
Q_i^{min}	Minimum reactive power output of generator at bus i [MVAr]
V_i^{max}	Maximum voltage magnitude limit at bus i [kV]
V_i^{min}	Minimum voltage magnitude limit at bus i [kV]

$L_{i,j}^{max}$	Maximum active power capacity of transmission line between buses i and j [MW]
P^{R+}	Reserve requirement for up regulation [MW]
P^{R-}	Reserve requirement for down regulation [MW]
$P^{dev}i$	Real time deviation in active power at bus i [MW]
$B_{i,j}$	Susceptance element (i,j) of ac network admittance matrix [p.u]
$PL_{i,t}$	Active power demand at bus i at time t, respectively [MW]
$QL_{i,t}$	Reactive power demand at bus i at time t, respectively [MVAr]
$DP_{i,t}$	Aggregated battery discharging power of vehicles at bus i at t [MW]
$CP_{i,t}$	Aggregated battery charging power of vehicles at bus i at time t [MW]
$ptdf_{i,j,k}$	Change in flow over line between buses i and j from power injection at bus k
$E_t^C(w)$	Conventional demand at time t in scenario w [MWh/h]
E_h^{next}	Aggregated energy required by battery vehicles for next day travel at time h [MWh/h]
$\pi_t^S(w)$	Estimated spot price at time t in scenario w [€/MWh]
π_h^S	Estimated spot price at time h [€/MWh]
π_t^{Ybase}	Base yearly forward price at time t [€/MWh]
π_t^{Qbase}	Base quarterly forward price at time t [€/MWh]
π_t^{Mbase}	Base monthly forward price at time t [€/MWh]
ρ^Y	Slope of yearly forward price function [€/MW^{2}h]
ρ^Q	Slope of quarterly forward price function [€/MW^{2}h]
ρ^M	Slope of monthly forward price function [€/MW^{2}h]
$prob(w)$	Probability of scenario w
vy_{yt}	Binary parameter to indicate maturity of yearly forward contract at time t in year y
vq_{qt}	Binary parameter to indicate maturity of quarterly forward contract at time t in quarter q
vm_{mt}	Binary parameter to indicate maturity of monthly forward contract at time t in month q
$P_t^D(w)$	Total end user demand at time t in scenario w [MWh/h]
$E_t(w)$	Charging energy of EVs scheduled at time t in scenario w of RP model [MWh/h]
P^{maxF}	Maximum power traded with fixed retail contract [MWh/h]
P^{maxV}	Maximum power traded with variable retail contract [MWh/h]
ν^F	Fraction of customer demand with fixed price contracts
ν^V	Fraction of customer demand with variable price contracts
θ^F	Slope of fixed retail contract price determination curve [€/MW^{2}h]
θ^V	Slope of variable retail contract price determination curve [€/MW^{2}h]
$R_t^V(w)$	Revenue from variable contract at time t in scenario w [€/h]
$\lambda_t^V(w)$	Selling price for variable contract at time t in scenario w [€/MWh]
α	Confidence level for calculation of $CVaR$
β	Risk weight factor [0,1]

Variables

E_t	Aggregated charging energy to be scheduled at time t [MWh/h]

SOC_t	Aggregated energy level of battery vehicles at time t [MWh]
$\hat{\pi}_t^s$	Day-ahead price forecasted using supply function at time t [$/MWh]
ACC	Total charging cost estimated by aggregator [€]
$SOC_{i,t}$	Aggregated energy level of battery vehicles at bus i at time t [MWh/h]
$DAEC$	Total day-ahead cost estimated by aggregator using DCOPF [€]
DAC_t	Total day-ahead cost from ACOPF at time t [€]
$C_i(P_{i,t})$	Production cost function of generator at bus i [€]
$P_{i,t}$	Active power output of generator at bus i at time t [MW]
$E_{i,t}$	Aggregated charging energy to be scheduled by EV aggregator model at bus i at time t [MWh/h]
$L_{i,j}$	Active power flow over line between buses i and j from spot market scheduling [MW]
V_i	Voltage magnitude at bus i [kV]
$\delta_{i,t}$	Voltage angle at bus i at time t [rad]
ΔEV_i^+	Total up regulating power from EVs at bus i [MW]
ΔEV_i^-	Total down regulating power from EVs at bus i [MW]
ΔP_i^+	Up regulating power volume by BRP at bus i [MW]
ΔP_i^-	Down regulating power volume by BRP at bus i [MW]
RP	Total cost of obtaining regulating power [€]
c_i^+	Up regulating price by BRP at bus i [€/MWh]
c_i^-	Down regulating price by BRP at bus i [€/MWh]
ac_i	Adjusted up or down regulating price at bus i [€/MWh]
ITL_i	Incremental transmission loss at bus i
PF_i	Penalty factor at bus i
RPO	Objective function of retailer planning model [€]
E_h	Charging energy of EVs to be scheduled at time h in EV aggregator model [MWh/h]
SOC_h	Energy level in EV batteries at time h [MWh/h]
C_t^F	Cost from forward contracts at time t [€/h]
$C_t^S(w)$	Cost from spot market purchase at time t in scenario w [€]
π_t^{FY}	Unit price of yearly forward contracts [€/MWh]
π_t^{FQ}	Unit price of quarterly forward contracts [€/MWh]
π_t^{FM}	Unit price of monthly forward contracts [€/MWh]
P_t^{FY}	Power purchased through yearly forward contracts at time t [MWh/h]
P_t^{FQ}	Power purchased through quarterly forward contracts at time t [MWh/h]
P_t^{FM}	Power purchased through monthly forward contracts at time t [MWh/h]
P_y^Y	Power purchased through yearly forward contracts over the year y [MWh]
P_q^Q	Power purchased through quarterly forward contracts over the quarter q [MWh]
P_m^M	Power purchased through monthly forward contracts over the month m [MWh]
$P_t^S(w)$	Power purchased from spot market at time t in scenario w [MWh/h]
$R_t^F(w)$	Revenue from fixed contract at time t in scenario w [€/h]
$\lambda_t^F(w)$	Selling price for fixed contract at time t in scenario w [€/MWh]
CVO	Objective function of CVaR optimization problem [€]
ξ	Auxiliary variable used for calculation of $CVaR$ [€]
$\eta(w)$	Second auxiliary variable used for calculation of $CVaR$ [€]

Contents

Part I

Introduction

Chapter 1

Introduction

This chapter provides an overview of the background and motivations behind the presented research work, the main contributions of the thesis and resulting scientific publications.

1.1 Background and Previous Work

The electric distribution systems are faced with continually developing challenges with regards to large-scale integration of distributed energy resources (DER) such as wind and solar photovoltaic (PV) resources on the generation-side and battery energy storage systems (BESS) on the demand-side. According to the International Energy Agency (IEA), their integration is only expected to increase in the future [1], [2], [3], [4]. The total installed capacity of renewable-based energy sources of power generation has close to doubled over a period of 10 years as shown in Figure 1.1 [5]. These renewable sources of energy include hydro (including pumped storage), wind, solar, biofuels and geothermal power. Out of these, solar PV and wind power contribute to 10% and 20% of the total renewable-based installed capacity around the world, respectively.

Large integration of such sources of energy into electric power systems could create new challenges in terms of operation and control. With wind power, the uncontrollable nature of its production could make such sources less valuable to transmission system operators than dispatchable power from hydro or gas turbines. The variable and intermittent nature of wind power would necessitate the operators to more actively manage power delivery to the loads, which could increase cost of balancing production and consumption or lower system reliability and security [6]. In case of solar PV and power converter interfaced wind turbines, an inherent loss of inertia is encountered. Without any form of control, it could lead to frequency issues seen in Germany [7] or other related challenges such as frequent voltage variations, voltage regulation and protection system issues could possibly occur [8].

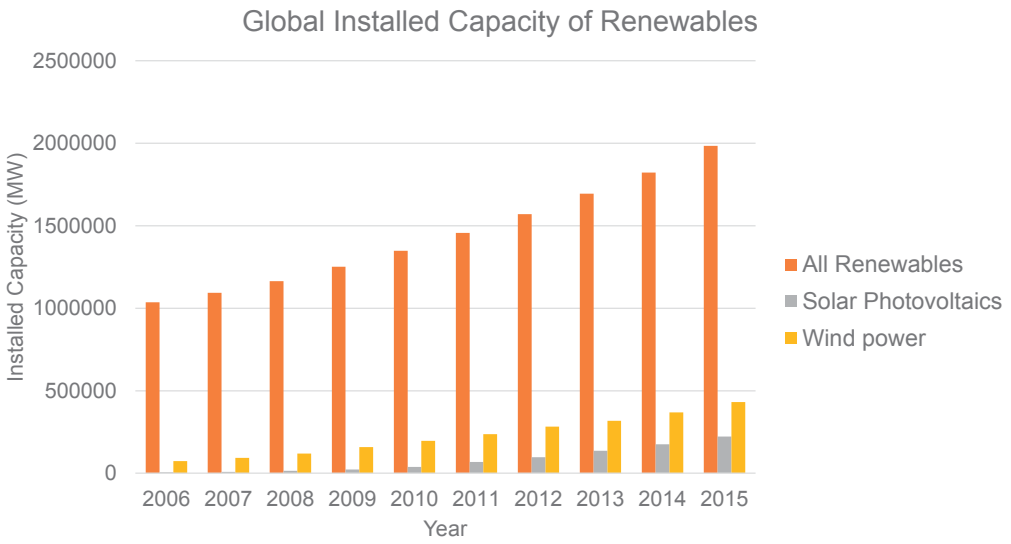

Figure 1.1: Installed capacity of renewables in the world. Data source: IRENA [5]

1.1.1 Distributed Generation

One possible solution to challenges with integration of distributed generators (DG) is to control their output in order to provide frequency and voltage control services. For example, the 50.2 Hz problem in Germany enabled recommendations by Association for Electrical, Electronic and Information Technologies to retrofit 315000 medium-to-large PVs connected at the low voltage (LV) distribution system with frequency-dependent active power control [9]. Furthermore, localized voltage rise and fluctuation issues, including under-voltage during peak load, low PV generation periods could occur on distribution system feeders that have relatively higher PV generation due to cloud effect [10]. Low voltage customers could possibly view frequent voltage variations due to changes in active power output from the DGs. The distribution system operators (DSO) typically have no measurement feedback available from the low voltage customer side to correct any voltage variation issues. These factors combined have resulted in DSOs imposing technical requirements on PV systems to perform active power curtailment and provide reactive power compensation at a certain power factor to improve grid operations [11].

Voltage control could be performed using on-load tap controllers on low voltage (LV) distribution transformers. But this could result in significant additional cost as tap controllers typically do not exist in current distribution systems on the low voltage level and would need to be installed. Better communication and measurement infrastructure in distribution systems could provide a (possibly) cheaper alternative wherein exiting DGs could be utilized more efficiently and reactive reserves between areas could be shared to improve voltage control by coordinating their response [12]. Automating the coordination with the help of optimization-based control strategies could offer a great

advantage because, with large number of DGs, it could be extremely difficult to manually determine the optimal outputs from the devices. With optimization-based control it would be possible to readily define a new objective, augment the model to include any new components in the system and hence, additional control variables to the optimization problem.

But challenges remain within the area of optimization-based coordinated control. The controller could be a single, central optimizer that handles the overall objective function of the system and determines optimal set-point changes to all the control devices or it could be multiple, decentralized optimizers controlling only a few devices in an area. Either way, a shift from a local, equipment-level control to an additional layer of central, system-level control structure is possible. Now, a central controller would give the optimal performance for a defined objective taking into consideration all interactions that occur within the system. But it could have multiple drawbacks, the biggest being decreased reliability in case of controller malfunction along with increasing processing times with very large number of control variables and great complexity in practical implementation. With decentralized strategy, each optimizer handles a limited number of control devices in an area but has no knowledge about its interactions with other optimizers. The major advantage of decentralized control is that it could be much more practically implementable and maintainable when compared to the central control strategy. However, as it loses information about interactions with other areas, it might be unable to perform well when control variables are at their limits. In between these two lies the distributed control strategy that maintains the decentralized control architecture and could offer performance similar to that of central controller since it also takes interactions between the optimizers into consideration [13].

In [14], local voltage control (LVC) strategies to regulate active and reactive power output from PVs to increase their hosting capacity into LV distribution system are investigated. Strategies already available commercially along with other advanced LVC techniques yet to be made available commercially for PV connected to LV distribution systems have been compared. Centralized coordinated voltage control strategies involves a single optimizer that regulates the set-points of control devices across the distribution network under consideration. In [12] and [15], the authors propose a single central coordinator agent that controls the setpoint values to the local controllers of tap changers in transformers and DGs, including wind power plant and PV system. Both of these coordinators perform static, single time-step optimization.

With the help of model predictive control (MPC) [16], it is possible to perform dynamic, multi-time step optimization thereby accounting for response of local controllers of devices with different time constants. In [17], the authors propose a MPC-based central optimizer that utilizes a linearized model to regulate voltages across a medium voltage network by varying the set-point to local controllers of PV systems and tap changing transformers. For all the advantages that centralized controllers provide, they also face two big challenges that could potentially hinder their widespread adoption- one, reliability of the controller becomes questionable when its failure occurs and two, maintaining the measurement, control and communication infrastructure between a central controller and local controllers becomes difficult as greater number of dispersed devices are considered. A compromise can

be reached by designing and operating an optimizer for each area of the distribution system that coordinates and controls only a few devices within that area while communicating with other optimizers about the actions it has taken. This type of arrangement is referred to as distributed coordination and is gaining momentum in process industry application [18], [19]. This has gained traction in power system research as seen in [20], where centralized, decentralized and distributed MPC strategies to regulate active power of a BESS for power market participation have been studied.

1.1.2 Demand Resources

Another possible solution to overcome the challenges of increasing DGs could be to increase the level of controllability on the demand side to effectively make the intermittent DG resources dispatchable and extend their functionalities over wider time periods [21]. This could partly alleviate the challenge of immediate need for network reinforcement for accommodating large amounts of variable DG in the distribution system [22]. Demand-side resources could include controlling loads such as energy storage elements including thermal storage, battery energy storage systems (BESS) in future electric vehicles (EV) and large battery energy storage solution owned and controlled by system operators. These potential solutions are facilitated by advanced measurement and communication systems by obtaining real-time estimation of energy consumption by demand side elements and through the use of power electronic devices to achieve the necessary level of controllability in active and reactive power exchange with the network.

Furthermore, regulations on power trading platforms need to enable the participation of small and medium scale demand resources in electricity markets. This could result in a host of possibilities such as: a viable business case for the resource owners, more efficient use of resources within the market, provide greater benefits for the customers and ultimately, further integration of variable, renewable resources [8]. Methods for electrical energy storage have always been considered as an attractive prospect by engineers. The challenge has been to store electrical energy in an economical way. Large scale roll-out of electric vehicles and smart metering devices coupled with the integration of advanced information and communication infrastructure in the power system could result in a new potential for storing electricity in vehicle batteries. By aggregating and controlling the charging and discharging of these storage elements, it could be possible to provide greater opportunities for demand response [23] while reducing the impacts of increased energy consumption from these new power system elements.

Over the past few years, the yearly share of electric cars (battery electric vehicles and plug-in hybrids) compared to all new cars sold around the world has steadily increased to approximately 1%. In a sharp contrast, some countries such as Norway and Netherlands have observed a significant increase in electric cars' share to 23% and 10%, respectively. This can be seen in Figure 1.2 and could be mostly attributed to monetary incentives provided by their respective governments [24].

Foreseeing the increase in EVs, research work has been previously carried out to study the impact of large scale introduction of EVs on power systems [25], [26], [27], [28]. In

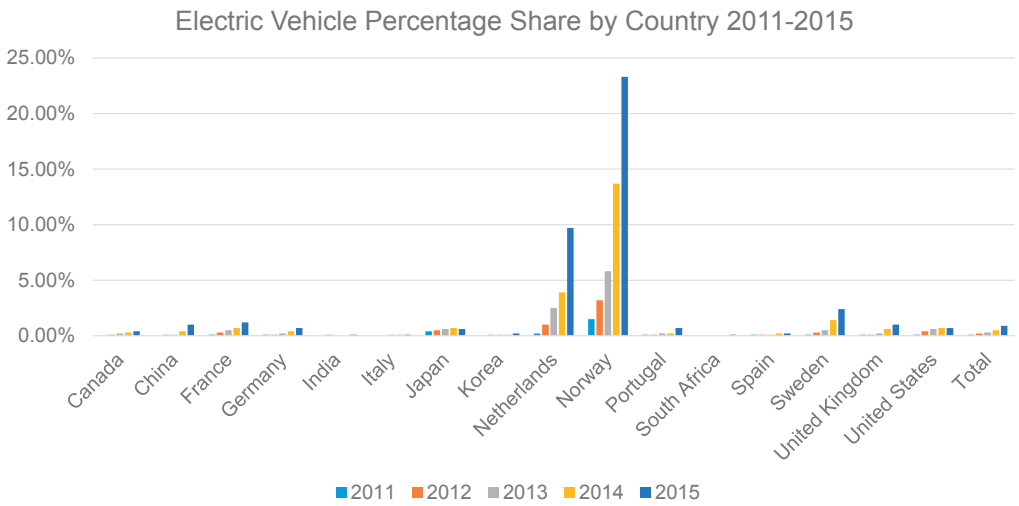

Figure 1.2: Yearly share of electric cars sold in selected countries around the world between 2011-2015. Data source: IEA [24]

[29], an EV charging control scheme is proposed by obtaining demographic statistical data and estimating the charging behavior to study the impacts on the distribution network. In [30], an optimization framework is proposed, in which, demand response resources are aggregated and their consumption schedules are optimized for their participation in day-ahead markets. The authors in [31] propose an optimization algorithm for EV flexibility planning and participation in reserve markets while authors in [32] have developed an approach to optimize the charging schedules for day-ahead and secondary reserve markets. Papers [33], [34] have proposed optimal biding strategies for EV participation in day-ahead electricity markets. Results from these works have indicated the need for aggregation and controlled charging of vehicles in order to reduce the stress created by large-scale roll out of these new types of demand on the transmission and distribution systems. However, the question still remains as to the impacts of EVs and their scheduled demand on market price of electricity and a need to quantify the impacts, if any, on various stakeholders such as electricity retailers, customers and the power system operators.

1.1.3 Measurement and Communication

As discussed previously, one of the main enablers of automation in future distribution systems is advanced metering infrastructure (AMI) that opens up the possibility for the distribution system operator for communication with the end customers. The role out of AMI is a reality today with electricity laws in place that require customers to be billed on an monthly basis. As an example, Göteborg Energi AB, a DSO in Sweden completed a mass roll out of these devices for 270000 end customers by 2009 [35]. Two possibly important properties of these metering systems could be listed as follow [36]:

- Interval metering- regular measurements that could range from hourly to real-time. This would open up opportunities for the DSO to improve the efficiency of system operation, especially on the low voltage distribution system and also impose condition-based network tariff, e.g., in case of network congestion.
- Two way communication between customer and DSO- this is a function that is generally included within the measurement units even though it is not an explicit metering functionality. This allows the possibility to provide electricity prices to customers in real-time as well as control the consumption and production of DER if required.

Hence, measurements would provide the DSO with feedback on the state of the system variables such as voltages and currents, while bi-directional communication would enable the control of said variables via the active and reactive power output from DER devices. This could result in a host of system services such as frequency and voltage control. It could also enable the customers to be more proactive and perform electricity market price-based scheduling of their demand for monetary benefits.

1.2 Motivation

From the previous sections, it could be reasoned that new power system devices such as EVs would lead to a possibility for flexible shaping of the demand profile through controlled charging and discharging, which in turn is made possible by AMI with bidirectional communication. This opens up opportunities to dynamically schedule the EV energy according to price of electricity in order to minimize the cost of charging for the EV owners. A question now arises as to what the effect of such scheduling would have on the market price of electricity. Because, the cost of charging for EV owners is either directly, or indirectly, related to the electricity price in power markets. Hence, it is vital to develop models for optimally scheduling EV battery energy and to observe the effect of controlled EV demand on market price in the day-ahead and regulating power market. Additionally, it is also vital to develop an energy portfolio optimization model for an electricity retailer, who is a critical actor for representing and trading customer demand in various electricity markets. This optimization model for the retailer should account for the customer-side scheduling and also reflect the monetary benefits for customers offering their demand flexibility.

Furthermore, large scale integration of EVs and PVs into the power system could bring about challenges to voltage control in distribution systems to which they are coupled. These active power sources close to the loads could create voltage variations that, a DSO today, would typically not be able to observe because of the non-existence of measurement devices on the LV part of the distribution system. A drive towards AMI would provide a feedback to the DSO regarding voltage magnitudes on the customer level and hence, control it dynamically using existing DER, possibly utilizing distribution system resources more efficiently instead of opting for the obvious, possibly costly, alternative, i.e., network reinforcements. The question now arises as to what degree of control is required. While,

LVC by DER is a possibility, its effect is limited to controlling voltage at the DER's point of common coupling (PCC). Coordinated voltage control provides an option for the DSO to systematically respond to voltage fluctuations at many points in the network using multiple DERs, possibly operating close to their limits because of their much smaller capacities than traditional generating plants.

MPC is an optimization-based control technique that has been widely employed in the process industry due to its distinct advantages in terms of naturally handling multivariable control problems, inherently accounting for constraints on inputs, states and outputs of the controlled system thereby allowing efficient, profitable system operation closer to constraints [16]. Thus, identical patterns and similar challenges could be identified between process industries and coordinated voltage control in rapidly evolving distribution systems with DER, which might need to function with greater efficiency and cost effectiveness.

Previous work by researchers indicates that MPC could be successfully used for coordinated voltage control in distribution systems. However, most of the work with MPC for voltage control has been done assuming a centralized control architecture, which DSO might not prefer due to a variety of reasons such as loss of reliability during controller failure, complexity of communication and control with large number of DER etc. Instead, they might prefer to utilize distributed control architecture consisting of more controllers with lesser communication requirements and/or better fall-back strategies. For such cases, distributed MPC could prove to be a suitable technique as its model-based approach inherently estimates control predictions that could be exchanged with other controllers, thereby naturally coordinating with each other without the need for a central coordinator. Hence, distributed MPC approach could be adapted for the coordinated voltage control problem for distribution systems. Once developed, it would also be vital to investigate how well the distributed control strategy performs against centralized control using MPC and subsequently, with local voltage control strategy in terms of important indicators for the DSO, i.e., reactive power used and active power losses in the network. Furthermore, to establish a proof of concept, it is imperative to verify that the developed MPC-based voltage control algorithm works in practice when implemented in a real distribution system.

1.3 Objectives and Main Contributions

The first half of the thesis focuses on development of optimization-based scheduling of EV energy for participation in electricity markets. Specifically, day-ahead, regulating power and retail markets have been addressed. To accomplish this, mathematical models to schedule EVs' energy by an aggregator for its participation in day-ahead, regulating power and for contracting electricity from the forward market have been proposed.

The second half of the thesis deals with the challenge of coordinated voltage control in distribution systems by utilizing MPC-based strategies to regulate power output from PV and BESS. Furthermore, it describes the implementation of the MPC voltage control

algorithm within a real distribution system setting in order to verify its functioning according to the design criterion. The main contributions of this thesis could be summarized as follows:

- Models for optimal EV energy scheduling have been developed and its effects have been studied under three market arenas- retail market, day-ahead market and regulating power market.
- MPC-based coordinated voltage control strategies have been developed and compared under three different control architectures- centralized, decentralized and distributed.
- The MPC algorithm for voltage control has been implemented in a field test to verify the functioning of the controller according to design criterion.

1.4 Thesis Outline

The thesis is divided into four parts. The first part provides an introduction to the thesis, the second part details the optimal scheduling of electric vehicle energy within electricity markets, the third part describes the MPC-based coordinated voltage control strategies and the fourth part lists the conclusions and suggestions for future work. The corresponding chapters within the thesis are as follows:

- **Chapter 2** provides a background to the conceptual framework and a context to the developed models within this thesis. An overview of Nordic electricity markets, demand-side control for market participation and voltage regulation services is also described.
- **Chapter 3** describes methods for EV energy scheduling by an aggregator developed under two different day-ahead market paradigms. The first, named as the joint scheduling method, considers a joint dispatch of generators and EV battery energy while the second, named as the aggregator scheduling method, considers independent planning by the aggregator.
- **Chapter 4** details the development of a planning model for EV aggregator's participation in regulating power market. In this model, the aggregator scheduling method is extended to also plan for the deviations that could occur after the clearing of the day-ahead market. Additionally, a modified clearing mechanism of the regulating power market is proposed where the regulating power resources are activated based on a re-valued regulation price that reflects the resource's impact on active power loss within the transmission network.
- **Chapter 5** proposes an approach for an electricity retailer to presume the market functions of an aggregator and plan for medium-term hedging against the price volatility and energy demand uncertainty in the forward market. The mathematical model developed for this purpose also determines the retail market prices that the retailer could offer to its end consumers based on two types of retail contracts.

- **Chapter 6** proposes coordinated voltage control in distribution systems using centralized, decentralized and distributed model predictive control strategies. The mathematical models and the performance of these controllers have been tested using a CIGRÉ European LV distribution network and compared with local voltage control strategy.
- **Chapter 7** presents and discusses results from an experimental setup to validate the online optimization using the proposed MPC-based voltage control algorithm.
- **Chapter 8** presents the main conclusions of the thesis and provides potential ideas for future research work.

1.5 List of Publications

This thesis is based on the appended papers listed below.

Papers related to electricity market perspectives:

I **Pavan Balram**, Le Anh Tuan, and Lina Bertling Tjernberg, "Centralized Charging Control of Plug-in Electric Vehicles and Effects on Day-Ahead Electricity Market Price," Book Chapter in *Plug In Electric Vehicles in Smart Grids*, Series on Power Systems, Springer Singapore, 2015, pp.267-299

II **Pavan Balram**, Le Anh Tuan, and Lina Bertling Tjernberg, "Effects of plug-in electric vehicle charge scheduling on the day-ahead electricity market price," 3rd IEEE PES International Conference on Innovative Smart Grid Technologies (ISGT Europe), Berlin, Oct., 2012.

III **Pavan Balram**, Le Anh Tuan, and Lina Bertling Tjernberg, "Stochastic programming based model of an electricity retailer considering uncertainty associated with electric vehicle charging," 10th International Conference on the European Energy Market (EEM), Stockholm, May, 2013.

IV **Pavan Balram**, Le Anh Tuan, and Lina Bertling Tjernberg, "Modeling of Regulating Power Market Based on AC Optimal Power Flow Considering Losses and Electric Vehicles," IEEE PES International Conference on Innovative Smart Grid Technologies (ISGT Asia), Bangalore, Nov., 2013.

V David Steen, **Pavan Balram**, Le Anh Tuan, Lina Reichenberg and Lina Bertling Tjernberg, "Impact Assessment of the Coordination between Wind Power and Demand Side Management on Spot Market Prices," IEEE PES International Conference on Innovative Smart Grid Technologies (ISGT Europe), Istanbul, Oct., 2014.

Papers related to voltage regulation perspectives:

VI **Pavan Balram**, Le Anh Tuan and Ola Carlson, "Predictive voltage control of batteries and tap changers in distribution system with photovoltaics," Power Systems Computation Conference (PSCC) 2016, Genoa, Jun. 2016.

VII **Pavan Balram**, Le Anh Tuan, Ola Carlson, Ingmar Leisse, Pierre Andersson-Ek, Demijan Panic and Malin Johnsson, "Coordinated Voltage Control in LV Distribution Systems with Photovoltaics using MPC," Submitted to Journal of Electric Power Systems Research.

VIII **Pavan Balram**, Le Anh Tuan and Ola Carlson, "Distributed MPC-based Coordinated Voltage Control in Multi-area Active Distribution Systems," Submitted to Journal of Energy Conversion and Management.

IX **Pavan Balram**, Le Anh Tuan and Ola Carlson, "Comparative study of MPC based coordinated voltage control in LV distribution systems with photovoltaics and battery storage," Submitted to International Journal of Electrical Power and Energy Systems.

X **Pavan Balram**, Ola Carlson and Le Anh Tuan, "Demonstration of Voltage Control in a Real Distribution System using Model Predictive Control," Submitted to IET Journal of Generation, Transmission and Distribution.

Chapter 2

Conceptual Framework

This chapter presents the conceptual framework, which lays the basis for the work in the thesis. This framework constitutes current Nordic electricity markets, the aggregator agent and its functions within the markets, interactions of the aggregator with other stakeholders and possible augmented functions of a distribution system operator in the context of future distribution networks with large number of distributed energy resources.

2.1 Overview of Nordic Electricity Markets

The electricity market is an arrangement for purchase and sale of electrical energy as a commodity between various market participants- producers, consumers, retailers and traders. Additional power system stakeholders such as transmission system operators (TSO) and distribution system operator (DSO) facilitate the functioning of electricity markets and the subsequent delivery of electrical energy to end consumers. Power generated by the producers is delivered to consumers through transmission and distribution networks. As the electricity network acts as a common platform for the delivery of energy, the network owners are generally established monopolies that are independent and neutral. The producers and consumers pay a fee known as the 'point tariff' to the network owners for every kWh of electric energy exchanged with the grid. This ensures that the market mechanism is facilitated, while ensuring financial compensation to the TSO/DSO for managing network related operations [37]. An overview of market participants along with the various types of contracts they could enter into is shown in Figure 2.1.

Many of the electricity markets within the European Union (EU) and other parts of the world have a structure similar to that of the Nordic electricity market and are constantly evolving. However, considering the EU level plan of a harmonized electricity market to facilitate cross-border trading [38], it could be reasonably assumed that future developments would not drastically change the framework of electricity markets from the present.

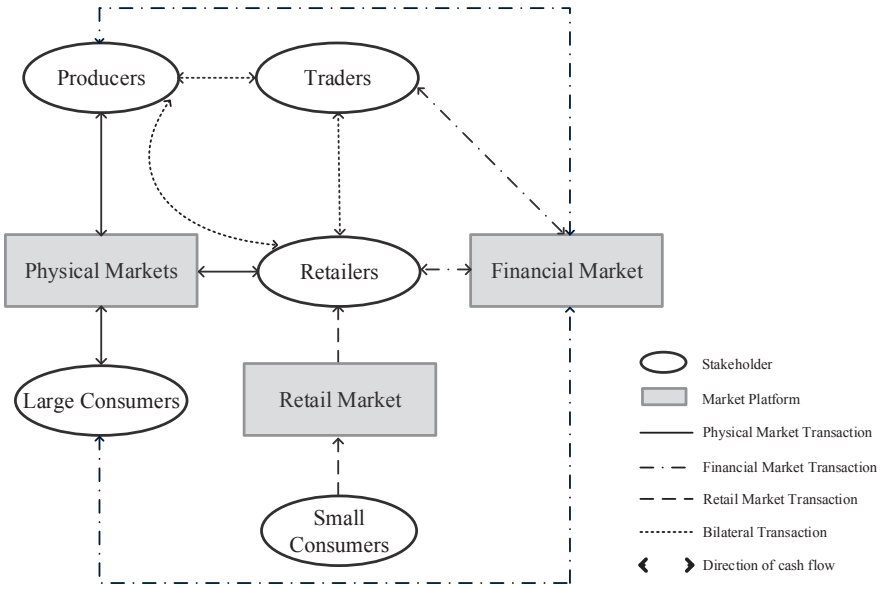

Figure 2.1: Market participants and their interactions within an electricity market framework

Currently, market participants can enter into various power contracts that are further described in the following sections within the context of the Nordic electricity market. It is important to mention that the financial and physical markets are operated on a time-based hierarchy. Financial markets are cleared days, weeks, months or years ahead of delivery as opposed to physical markets that are generally cleared 45 minutes to one day-ahead. An overview of the time-line for Nordic physical and financial markets operation is shown in Figure 2.2.

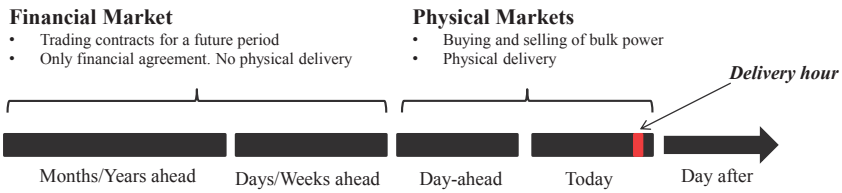

Figure 2.2: Overview of timeline of Nordic physical and financial markets

2.1.1 Physical Electricity Markets

Like many other commodities, electricity could also be traded within a wholesale market framework. A common day-ahead market (DAM) called Elspot exists for the Nordic and Baltic countries where the market participants trade bulk of the energy production and consumption. The clearing of Elspot results in a production and/or consumption plan for each participant with a delivery obligation, which requires them to abide by their individual plans.

Electrical energy is however, dynamic, in the sense that energy has to be instantaneously available when there is demand with few economically viable storage options. This singular characteristic along with the fact that Elspot is cleared one day ahead of the delivery time of electricity necessitates the use of forecasting methods by the participants to estimate their production and consumption. The resulting power deviations that could occur due to forecasting errors, component failures etc., need to be rectified. The participants are provided an opportunity to do this through the continuously traded Elbas market that is available to balance out their individual deviations from their Elspot plans.

It is still possible that last minute imbalances could occur due to failure of components or various faults within the power system. The responsibility of maintaining power balance within the power system during delivery period rests on the TSOs, who jointly operate the regulating power market (RPM) to provide a mechanism for correcting the resulting imbalance during delivery period and ensure the desired level of security of supply within the power system. This market is settled after the adjustment of imbalance through active power regulation.

There is a physical obligation associated with these electricity markets, i.e., it has to be ensured that the energy traded in the market is delivered to the end consumers during the specified delivery period. Hence, the Elspot, Elbas and regulating power markets are collectively known as *physical markets*.

Market participants could also enter into more conventional bilateral contracts that involve a direct trade between a buyer and seller of electrical energy. Considering around 84% of power consumption in the Nordic and Baltic countries have been traded at the DAM [39] as of 2013, it can be seen that the platform of electricity markets is becoming more appealing to the market participants.

2.1.2 Financial Electricity Markets

It is imperative that the market participants are able to quantify and hedge against monetary risks associated with their participation in the physical markets. The financial electricity market provides a platform to manage risks by hedging against price fluctuations in the physical markets. Numerous contracts could be made available in a financial electricity market [40]. Specifically, four contract types are offered to participants in the Nordic financial market-

- Power Futures

- Power Deferred Settlement Futures (formerly termed as 'Power Forward')
- Electricity Price Area Differentials (formerly termed as Contracts for difference)
- Power Options

Within this thesis, only 'deferred settlement futures' or 'power forward' contract is considered within the conceptual framework. The goal is to develop a framework for portfolio optimization considering hedging against price and volume risks in the presence of scheduling by an aggregator. If necessary, other types of contracts could also be considered similar to that of Power Forwards within the framework.

2.2 Stakeholders in Electricity Markets

All the stakeholders in the electricity markets could be broadly classified based on the nature of their activities as either commercial or non-commercial. The former engage in competitive behavior within the electricity market environment while the latter are regulated monopolies that are typically responsible for the secure and reliable operation of the power system. More details regarding various stakeholders within each of these categories are described below.

2.2.1 Commercial Stakeholders

Producers

A producers is an entity that is able to supply electricity to the power system. This could include traditional generating technologies with less variability such as hydro, thermal and gas power plants or renewable technologies such as wind and photovoltaics that are inherently variable and intermittent in nature. With the increased integration of latter generating technologies, electricity markets that operate closer to the operating hour such as Elbas and RPM could see an increase in power trading. This is due to the fact that operating schedule for these technologies generally has lower error close to the operating hour due to availability of better forecasts. Hence, a smaller planning window closer to the operating hour could be more favorable for these variable generation sources.

Consumers

These are the stakeholders that essentially require electrical energy for end-use. They typically enter into contracts with electricity retailers to purchase the necessary electrical energy. They could be small consumers consisting of residential customers or large consumers consisting of commercial and industrial customers that typically have greater consumption patterns. A new class of consumers could be large number of electric vehicle (EV) owners who could act not only as end consumers but could also participate in

providing system services such as active power regulation or also provide other system support actions such as voltage control at the request of the DSO. This is facilitated by a combination of battery energy storage system within the EVs, active and reactive power control using full power converters along with better measurement and communication within the power network in the future with the help of AMI.

Traders

A trader is an entity in electricity markets who temporarily owns electricity during the trading process [37], typically with the intention of performing arbitrage. Generally, a trader has a large footprint within the financial electricity market and does not directly interact with the end consumers.

Electricity Retailers

A retailer is a stakeholder that buys electrical energy from the electricity markets and ultimately sells it to end consumers and also to producers (typically for balance adjustment). A figurative description of the participation of a typical retailer in various markets within the considered conceptual framework is shown in Figure 2.3.

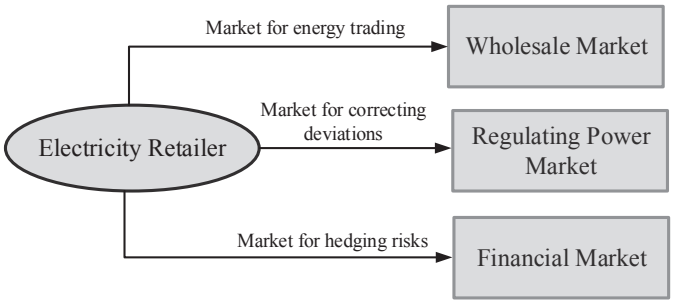

Figure 2.3: Overview of retailer participation in physical and financial markets

2.2.2 Non-commercial Stakeholders

Transmission System Operator

The TSO is a regulated stakeholder who is responsible for operating the transmission network infrastructure, which typically includes parts of the power grid operating at high voltage levels [41]. A major responsibility of the TSOs is to also procure system services to ensure security of supply, which includes frequency reserves from other stakeholders

and minute-to-minute balance between supply and demand. To achieve this, the RPM is jointly operated by all TSOs within the Nordic system to adjust, regulate and settle the balance between production and consumption within their individual control areas during the operating hour shown in Figure 2.2.

Distribution System Operator

DSOs are owners and operators of power grids typically operating at low and medium voltage levels, closer to the consumer demand [41]. The DSO is primarily responsible for developing and maintaining their network in order to ensure high levels of system security, reliability and quality-of-supply to end consumers. The emphasis in network management for the DSO is typically on distribution congestion and voltage control. According to the EU-wide directive [38], DSOs serving more than 100000 end consumers cannot trade energy within the electricity markets and are hence, unbundled from generation, transmission and retail operations. The exception to this rule is if the DSO has self-production to cover the network losses within its control area [42]. Apart from owning production units to cover its losses, the DSO has two other ways to procure the expected losses within its area- electricity markets and bilateral contracts. DSO then obtains its revenue by charging a tariff to its customers, which is usually dependent on the quality-of-supply and also includes the cost of services and losses.

2.3 Price Based Demand Response

Conventionally, end consumers have been exposed to fixed average electricity rates and hence, shielded from short-term variations in prices due to varying cost of electricity generation. As a result, consumers could over-consume during demanding hours without any control from network owners. E.g., during winter season, when surrounding temperature drops, the electric heating load could drastically increase within all domestic households leading to a significantly greater demand for electricity. In a hydro power dominated region, the water availability in the reservoirs is typically moderate during winter, which could increase generation from other fossil fuels that have significantly higher marginal costs. The opposite situation of under-consumption during summer season when reservoir levels are relatively high could lead to very low market price since the value of hydro power production depends on its opportunity cost.

Demands could respond to price of electricity in the market to consume during low price hours as opposed to high price hours. Alternatively, response from demand could also be used to support network operation through frequency regulation, voltage control, black start capability, voluntary load shedding etc. Such programs involving control of demand-side have historically been utilized but limited to large industrial consumers. With the roll out of AMI, greater real-time control of domestic consumers' consumption could also be achieved. This could result in greater demand side participation in electricity markets, possibly leading to more efficient use of generation resources, while also reducing

the stress on transmission network during peak consumption periods. Consumers who are willing to respond to incentive-based signals are referred to as active consumers. An active consumer could be either a large industrial consumer or a small domestic consumer. Since, the consumption levels of domestic consumers are small compared to the volumes traded in electricity markets, an agent similar to a retailer could become essential to represent the needs of domestic consumers in electricity markets. With controllable resources, however, this agent generally referred to as an 'aggregator' could possibly assume new functions that might require it to control consumer appliances in real-time.

Within the context of the Nordic system, the physical electricity markets provide opportunities for price dependent demand to compete directly with generation. This is especially the case with large scale industrial consumers who have the flexibility to bid for energy directly on the market on an hourly basis and to adjust their consumption in order to prevent being exposed to very high prices. When it comes to small and medium sized consumers, there is a plan to move towards a common retail electricity market with the Nordic region [43] that offers the option of variable retail pricing for consumers directly based on the price of electricity in DAM. In this regard, the installation of AMI has been adapted [44] to measure real-time consumption pattern of domestic and commercial consumers of electricity.

2.4 Electric Vehicles as Flexibility Resource

Electrification within the transportation sector has been highlighted to provide good opportunities for demand control in future power systems [45]. With battery energy storage systems (BESS), EVs provide flexibility regarding the sources of electrical energy for charging. Hence, if global policies are driven towards tapping renewable resources such as wind, solar, biomass, biogas etc. for power production, then power sources with lower carbon footprint could be used to charge the vehicles. With EVs, greater flexibility could be achieved by storing renewable energy when it is available, and then re-using it during times of greater power imbalance between renewable energy and customer demand. Therefore, EVs could also be utilized to offset some of the shot-term variability in power production from renewable sources.

Main types of Electric Vehicles

Internal combustion engines (ICE) have been the heart of the automotive industry around the globe for over a century. The drawback of ICE is that they have predominantly used fossil fuels as an energy source. More recently, electric vehicles are being introduced by auto makers as an environment friendly alternative to ICEs run on petrol or diesel. In general, EVs consist of a battery for energy storage, an electric machine for propulsion, a power electronic control system and a mechanical transmission system. Based on the configuration of these subsystems, EVs could be classified into three main types as described below [46].

1. *Hybrid Electric Vehicle* (HEV)- employ a traditional ICE engine supplemented by an electric motor and battery in order to increase the overall fuel efficiency as shown in Figure 2.4. The battery in this type of EV is not recharged from the electric grid but from the combustion engine and regenerative braking. This limits the choice for battery charging source as compared with other types of EVs.

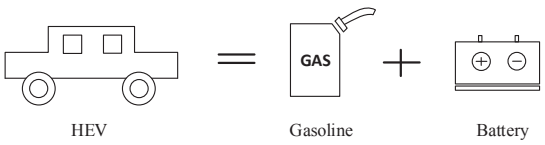

Figure 2.4: Hybrid electric vehicle

2. *Plug-in Hybrid Electric Vehicle* (PHEV)- is similar to the HEV as it uses two power sources to propel the vehicle. However, the battery capacity of the PHEV is relatively higher with an added advantage that the battery could be connected and directly charged from an electricity outlet. This is shown in Figure 2.5. In addition, the battery could also be charged by using the combustion engine and regenerative breaking, similar to an HEV.

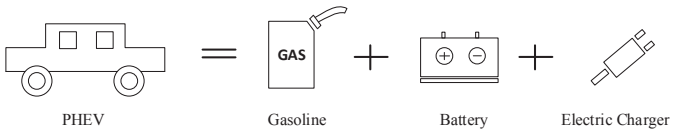

Figure 2.5: Plug-in hybrid electric vehicle

3. *Battery Electric Vehicle* (BEV)- are completely electric. Their propulsion is solely due to the functioning of an electric motor powered by a battery. The battery could be charged from an electricity outlet and has a capacity that is significantly larger than that of a PHEV or HEV. A representation of BEV is shown in Figure 2.6.

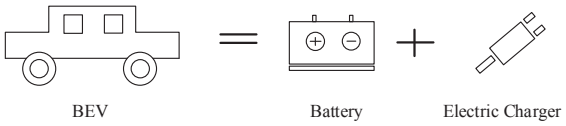

Figure 2.6: Battery electric vehicle

The PHEV and BEV class of vehicles could be collectively referred to as plug-in electric

vehicles (PEV) since they have a common functionality of connecting to the power system for charging (and potentially, discharging). In this thesis, the term EV is used interchangeably with PEV as these classification of vehicles have the greatest potential for dominance in the future.

2.5 Voltage Control in Distribution Systems

In addition to active power regulation with the help of demand-side components, voltage control support is vital component in operating the power system in a secure and reliable manner. Large penetration of DG within a localized part of a distribution network could have adverse effects on its bus voltages due to variations in active power output as the latter typically have low X/R ratios [12]. This could necessitate active power curtailment and/or reactive power output regulation by the DG in order to maintain their point-of-common-coupling voltages [11].

With the integration of new demands such as BESS, the possibility for these resources to provide voltage control support arises, which could either be provided within a market environment [47] or through grid codes as a mandatory requirement from controllable components connecting to the distribution network. In the future, if BESS including those in EVs reach a stage where they could perform arbitrage in certain electricity markets, stakeholders such as producers or consumers could install these battery systems based purely on commercial interests. This could further add to the arsenal of controllable demand-side components available to the DSO for voltage control services.

2.6 Developed Models within Conceptual Framework

In this thesis, models have been developed considering two aspects from a future power system point of view:

- New controllable demands such as EVs and battery storage systems in general, when aggregated, would be able to provide active power regulation flexibility through the help of price signals from electricity markets. In this regard, scheduling models have been developed for DAM and RPM with focus on EVs as flexibility agents. Also, the portfolio optimization of an electricity retailer, who could potentially be a critical stakeholder, is also developed considering scheduling possibility of EVs.
- Renewable DG and battery energy storage systems, including grid-connected EVs in the future, could provide voltage control support by regulating their reactive power output. The actions of all these components could be coordinated with the help of the DSO who is primarily responsible for network management.

It is considered that control/curtailment of active power output from battery storage systems/renewable DG is decoupled from that of reactive power. Hence, control of active power output based on scheduling of EV energy for market participation is considered to be performed independent of voltage control during real-time operation. Correspondingly, models for optimal scheduling of aggregated EV energy are developed in the first part of the thesis.

There is an imbalance cost associated with deviations from the plan for market participation, regulation of reactive power output is considered for voltage control during real-time operation while discouraging any deviations from the energy schedule developed within the market model. Hence, the maximum reactive power available at any time from each of these components for voltage control is subsequently limited by their active power output (likely based on market schedule) and the total power rating of the converter. It is also considered that active power output from battery storage systems could be controlled for voltage control service. However, the cost associated with this is assumed to be high within the developed control schemes reflecting the idea that it is to be regulated only in critical circumstances by the DSO. Furthermore, there are additional requirements to be met in order to enable aggregator scheduling for market participation and voltage control by DSO. These are described below.

2.6.1 Enabling the Aggregator

Most of the small consumers including future EV owners do not have a means to directly trade in electricity markets. In order to trade their flexibility, they would require the services of an aggregator agent that gathers the flexibility offered by many consumers and pools in the total active power demand to be traded as a single resource. The aggregator could also generate agreements with consumers to adjust their energy consumption with advance notice. If an aggregator is dedicated for trading flexibilities offered by EVs, it is referred to as an 'EV aggregator'. Within the context of electricity markets, the functions of the EV aggregator are similar to that of a retailer. Hence, its interaction with other market participants could be described using Figure 2.7.

There are notable challenges that exist for domestic consumer participation in the current Nordic electricity markets [48]. Though an aggregator agent could be a legal entity in current Nordic DAM, intra-day and financial electricity markets, barriers could arise when the aggregator would want to participate in the RPM. This is due to the fact that aggregator would need to assume the role of a balance responsible party (BRP) in order to directly participate in RPM, or contract with another BRP. There could be further limitations due to the rules and regulation regarding aggregation of demand in general and also, concerning a new market player possibly taking the role of a BRP. Another barrier that could hinder the participation of an aggregator is the minimum bid volume requirement by the TSO in RPM, which is currently 10 MW [49]. This could prove to be a large volume for aggregators, especially in trading areas with net surplus production. Hence, some additional requirements might need to be accommodated in order to enable the concept of an aggregator within the electricity market [25] and its

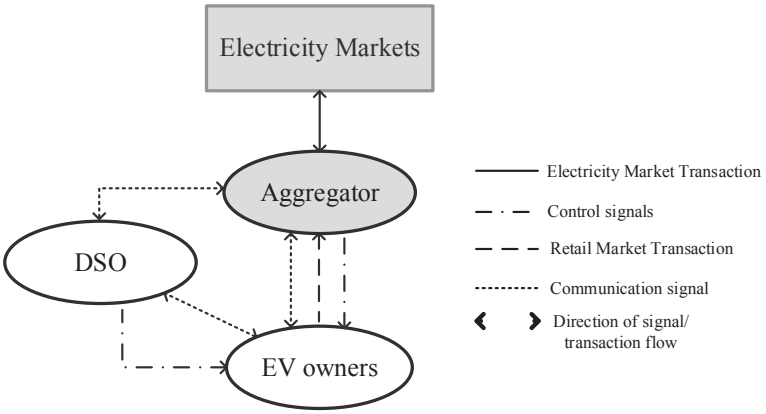

Figure 2.7: Aggregator and its interaction with electricity markets and other stakeholders

subsequent implementation. Some of the main requirements that could be highlighted are as follows:

- There should be necessary communication infrastructure in place for the aggregator to obtain near real-time electricity consumption measurement, vehicle battery state-of-charge and consumption needs of EV owners [50].
- There should be a mechanism in place for the control of output from EV batteries. The batteries could be controlled directly by an aggregator with energy schedule validation by the DSO if the necessary automatic control infrastructure is established and the regulatory framework permit the same. However, if the rules impose strict separation of power system operation and business aspect of the aggregator, then it could be possible for the DSO to take over the function of EV output control based on the energy scheduling plan communicated to the DSO by the aggregator [25]. Both of these control possibilities are depicted in Figure 2.7.
- It might become necessary to introduce shorter time periods of around 30 minutes or less between market closure and operating hour in order to reduce forecast errors by the aggregator [51]. The same requirement could easily extend to electricity systems with large penetration of wind and solar PV generation.
- For higher participation of small consumers represented by many aggregators, especially within the RPM, it might become necessary to reduce the minimum volume submitted to the market to values lower than 1 MW [51].

Within the models developed in the electricity market perspective part of this thesis, all the necessary communication and control infrastructure are assumed to be available in order to perform flexible load shaping by scheduling of energy within the batteries of EVs. It is imperative that the individual EVs providing the active power flexibility be controlled to follow the optimal scheduling performed by the aggregator. As described in

the possible requirements above, the responsibility for control implementation could rest either with the aggregator or DSO, depending on the regulatory framework. Regardless, within the conceptual framework of this thesis, it is assumed that the control of EVs based on aggregator's optimal scheduling would be implemented with no errors. It is further considered that an electricity retailer could most likely assume the market related functions of an EV aggregator and a retailer planning (RP) model is developed incorporating the flexibility scheduling aspect of the aggregator within its portfolio optimization.

2.6.2 Augmented Functions of DSO

Increasing renewable DG and BESS could pose considerable challenges on the DSO's responsibility for a secure network operation and management. Engaging customers to respond to price signals from electricity markets could necessitate dynamic operation and control of the distribution system.

An aspect towards this is to ensure that the DSO is able to manage congestion within the network through future market mechanisms and perform voltage control in the medium and low voltage networks with the help of DG and battery storage systems aggregation including EVs. Along with the two short-term operational services of congestion management and voltage control, the DSO should be able to observe long-term goals of maximizing the integration of renewable DG and the efficiency of grid operations [52]. All of the service procurements could be enabled by a combination of market mechanisms or through grid code revisions. The latter would impose mandatory requirements on DG, battery storage systems, EVs etc to regulate their output in order to help the operation of distribution systems and would specifically be useful in the context of voltage control. This aspect is addressed in the second part of this thesis, where coordinated voltage control strategies are developed assuming availability of necessary measurement and bi-directional communication infrastructure for controllability of PV and BESS.

Part II

Electricity Markets Perspective

Chapter 3

EV Energy and the Day-ahead Market

This chapter gives an overview of the role of future electric vehicles and their scheduling models for participating in the day-ahead electricity market.

3.1 Related Work

With the expected mass adoption of EVs in the coming decades as reported by the IEA in [53], the increase in total electrical load in a system can be significant if the charging of EVs is uncontrolled [54]. To reduce the impacts of such an increase in EV demand, certain measures of control and coordination could become necessary.

Charging strategies of EVs based on real-time price have been discussed in e.g., [55], [56], [57] and the charging of EVs can be scheduled and coordinated by an aggregator agent during periods of low electricity price as shown in [29]. In these works, the EVs are considered to have no influence on the market price for electricity. However, large fleets of EVs could result in changes to the shape of the daily load curve appearing in the electricity market which could in turn influence the cleared market price.

A locational marginal price-based impact assessment has been done in [58] to show the effects of controlled and uncontrolled EV charging on the market price. However, it is necessary to observe these effects in a pool-based electricity market setup such as the Nordic electricity power exchange NordPoolSpot [37]. In such a setup, the charging schedule of the EVs would need to be submitted to the market by an aggregator agent or electricity retailer. Hence, the scheduling of EV charging is performed before the scheduling of the generators. This market structure is implemented in this chapter using the proposed aggregator scheduling method (ASM). Furthermore, with adequate infrastructure for control and communication in place, the market can advance to a situation wherein, the

individual EV owners can directly interact with it, thereby, eliminating errors that arise due to scheduling of EV charging by the aggregator. This idea is implemented using the proposed joint scheduling method (JSM).

3.2 Modeling Approach

In this section, two methods for incorporating EV energy and their charge scheduling in day-ahead electricity markets have been developed and described. The main difference between the two is in the way the scheduling of EV energy is done. In the JSM, EV demand is considered to influence the electricity price and the total energy needs of the EVs is scheduled simultaneously with the generation units with the objective function being minimization of total generation cost.

In ASM, EV energy is first scheduled independently by an aggregator agent based on the estimated electricity market price. The charging schedule, which represents the EV energy demand, is submitted to the market in the same way as other conventional loads. In so modeling EV charging energy, the effects of EV energy demand on electricity market price is assessed and compared among cases with and without EVs, including the results from joint scheduling method. It should be noted that while EVs can provide reserve capacity and energy back to the grid (known as vehicle-to-grid service) as considered by many recent studies such as [59], [60], in this chapter, we focus only on the charging of EVs from the grid. The main reason for this is that EVs are primarily consumption devices that are used for driving purposes by their owners. Hence, treating them as such within a power market environment and scheduling their consumption needs would give an idea of the impacts they could have on electricity prices.

3.2.1 Joint Scheduling Method

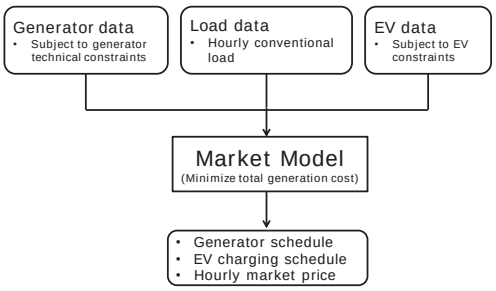

Figure 3.1: Overview of JSM

In JSM, the EV energy scheduling is considered to be performed by a central market operator that also plans for the dispatch of the generators. The market operator is

assumed to receive data related to the generators and EV batteries. The operator could then schedule both the generators and the EV charging energy demand by minimizing the total cost of generation. In a scenario where advanced methods of communication and control are feasible, individual EV owners could directly interact with the market by submitting the necessary EV data. In this scheduling method, the central operator is assumed to receive the following three sets of information:

1. Generator marginal costs along with its technical constraints
2. Daily EV driving energy requirements, driving pattern data and aggregated EV battery energy limits.
3. Hourly conventional load data, which represents the inflexible demand data.

Using these three sets of information, the market model jointly schedules the generators and EV charging demand to minimize the total generation cost within a unit commitment framework [61] subject to generator constraints, EV constraints and power balance constraints. This is shown in Figure 3.1.

The generators are assumed to provide their true marginal cost of generating electricity and the market is settled with the minimum generation cost objective [47]. Demand, except that of EVs, is considered to be perfectly forecasted a priori, and is then fixed for each hour.

3.2.2 Aggregator Scheduling Method

In ASM, the EV aggregator is assumed to function similar to an electricity retailer in the market. The aggregator plans for DAM participation by independently scheduling EV energy based on its objective of minimizing the total cost of charging. This is considered as Stage 1 for ASM. For the scheduling, the EV aggregator is assumed to have the following three sets of information:

1. Daily EV driving energy requirements, driving pattern data and aggregated EV battery energy limits.
2. Hourly conventional load data, which represents the inflexible demand from all other loads other than EV demand.
3. Estimated supply function.

Using the above sets of data, the aggregator schedules the charging energy of EVs such that the total cost of charging is minimized as shown in Figure 3.2.

EV Aggregator Model: The EV aggregator ensures that the charging and discharging events of the vehicle's aggregated battery is scheduled considering the unavailability of EVs due to driving needs. Batteries within EVs are essentially loads that are required to be charged with sufficient energy to ensure smooth operation of the vehicle according to the driver's needs. Hence, it could be reasonable to assume that the main position held by

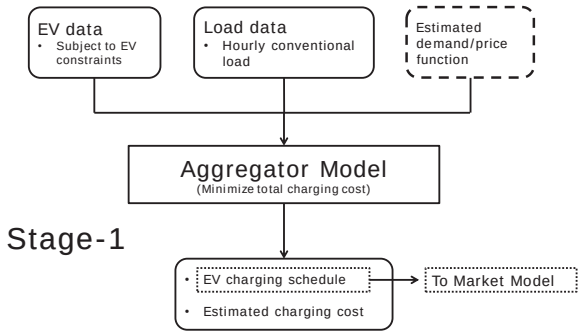

Figure 3.2: Overview of ASM:Stage 1

the EV aggregator is as a consumption entity within the electricity market. Considering such a stance, the objective function of the aggregator would then be to make sure that the cost from energy purchased for charging of all the EVs is minimized while accounting for the driving needs of the EVs. Due to its participation in the DAM, the charging energy price would depend on the market price of electricity. If hourly market prices are directly imposed on the EV owners as charging price, the objective function could then be represented using (3.1).

$$Minimize \quad ACC = \sum_{t=1}^{T} \hat{\pi}_t^s E_t \tag{3.1}$$

where, $\hat{\pi}_t^s$ is the day-ahead price forecasted by the EV aggregator at time t based on the estimated supply function. Depending on the structure and organization of the day-ahead market, it is possible that the charging price used by the EV aggregator is either an endogenous variable or an exogenous parameter. If the market structure is such that it requires the aggregator to plan the hourly charging needs before submitting its energy requirements to the market, then the electricity price would need to be estimated and it would identify itself as an exogenous parameter within the aggregator model. The objective function in (3.1) is subject to constraints imposed by the needs of vehicle owners along with the technical limitations of the battery as described in Section 3.2.3. The estimated supply function gives an approximation of how the market price varies with changes in total demand. This function is important to identify the effect of total EV demand on the market price when it is scheduled. The estimated supply function is modeled to be dependent on the total demand within the system as is shown in (3.2).

$$\hat{\pi}_t^s = f(C_t^L, E_t) \tag{3.2}$$

Where CL_t is the total forecasted conventional load and E_t is the EV charging energy to be scheduled. This estimated function can also be obtained from historical data on price and demand level cleared in the market.

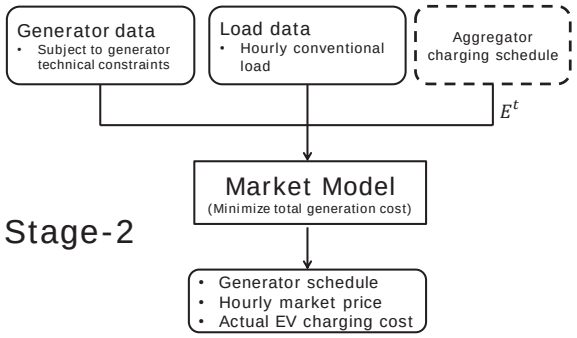

Figure 3.3: Overview of ASM:Stage-2

Market Model: The EV charging schedule E_t from ASM:Stage-1 is then provided to the market model in ASM:Stage-2 as an input parameter, where the generators are scheduled to meet the total demand from the conventional load and the scheduled EV energy in a way so as to minimize the total generation cost within a unit commitment framework. This is shown in Figure 3.3.

3.2.3 EV Constraints

Within both the methods, restrictions that essentially reflects the temporal energy needs of EV owners along with the physical capacity restrictions imposed on batteries of EVs is expressed in the form of mathematical constraints for the optimization problems. In the developed model, the individual batteries are assumed to be aggregated and treated as a single battery. The constraints essentially reflect the charging and discharging operation of the aggregated vehicle battery while accounting for the traveling energy needs of EV owners based on their aggregated driving pattern. It is further assumed that the vehicles are available to the grid for charging at all times when they are not traveling.

Minimum Energy Requirement: It is considered that the EV owner provides information about how much travel is intended for the next day in kilometers. An aggregator or central market operator could then estimate the charging energy required based on the characteristics of the EVs. The aggregator/central market operator would schedule only that amount of charging energy necessary over its initial state-of-charge (SOC) of the battery as shown in (3.3).

$$SOC^{ini} + \sum_{t=1}^{T} E_t \geq SOC^{min} + \sum_{t=1}^{T} E_t^{next} \tag{3.3}$$

Where, E_t^{next} is the energy required by the EV for next day travel during hour $t \in T$, T is the optimization period length, SOC^{ini} is the initial state of energy in the battery

and SOC^{min} is the minimum energy requirement imposed by the EV owner on the battery.

Charging Period Limit: It is assumed that the EV owner provides information about the time and duration of traveling intended for the upcoming day. The aggregator/central market operator could use the provided driving information to generate an aggregated driving profile of its EV customers that would, in turn, provide the unavailability of the vehicles. The aggregator/central market operator then needs to schedule the charging of the EV in such a way that the aggregated battery is charged during hours $tf = (1, 2, ..., t-1)$ before expending energy for travel during hour t for all values of $t \in T$.

$$\sum_{tf=1}^{t-1} E_{tf} - E_{tf}^{next} \geq E_t^{next} \tag{3.4}$$

Battery State: Charging and discharging of the battery during consecutive hours results in a change in its state-of-charge (SOC) or energy level. This is formulated as:

$$SOC_t = \begin{cases} SOC^{ini} + E_t - E_t^{next} & \forall t \in \{1\} \\ SOC_{t-1} + E_t - E_t^{next} & \forall t \in \{2, 3..., T\} \end{cases} \tag{3.5}$$

Battery Energy Limits: The energy state in the battery should not deviate from its minimum and maximum limits, SOC^{min} and SOC^{max}, respectively.

$$SOC^{min} \leq SOC_t \leq SOC^{max}; \;\; \forall t \in (1, 2, ..., T) \tag{3.6}$$

3.3 Case Studies and Results

The scheduling methods described in the previous sections are tested on a modified IEEE 30-bus test system and a Nordic test system. The input data related to EVs used for both the JSM and ASM case studies were obtained from a report published by the *Grid for Vehicles* (G4V) project under the European commission's 7^{th} framework programme [62], and are shown in Figure 3.4 and Table 3.1, respectively.

The driving pattern shown in Figure 3.4 is dependent on vehicle users and it is reasonable to assume that the driving behavior would not change drastically with the introduction of EVs. Hence, the conventional vehicle user behavior is considered to be representative of the expected EV user behavior. The battery capacity and energy consumption in Table 3.1 are calculated based on the expected composition, at high penetration levels, of BEVs and PHEVs, and represent a weighted average value.

The battery charging and discharging characteristics are highly non-linear and depend on the type of battery. Li-ion batteries are considered here as they appear to be the

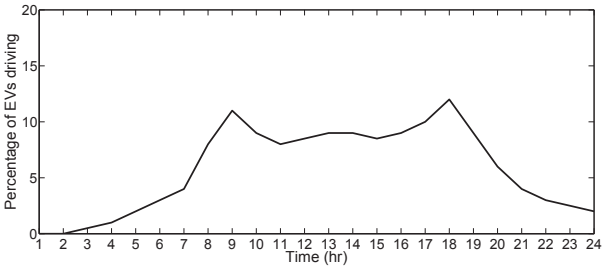

Figure 3.4: Driving pattern of EVs based on conventional vehicle data

most promising type for EV application [63]. Their charging curve indicates that the charging power is nearly constant within a certain range of their SOC [64]. Hence, the values of SOC^{min} and SOC^{max} are fixed at 20% and 85% of the battery capacity for all simulations.

Table 3.1: EV related parameter values

Battery Capacity	24 kWh
Energy Consumption (per km)	0.192 kWh/km
Average Distance Traveled	40 km/day
Energy Consumption (per day)	7.68 kWh/day
Charging Power Available	3.68 kWh/h

3.3.1 IEEE 30-bus system

The presented JSM and ASM have been tested using a modified IEEE 30-bus test system [65] to observe the effects of EV aggregator demand scheduling on the price of electricity. The test system consists of nine generating units that are subjected to the following general technical constraints [61]: minimum and maximum generation limit, minimum up and down time, up/down ramp rate limits and start-up/shut-down ramp limits.

The penetration level of EVs is defined as the ratio of total number of EVs to the total number of vehicles in the system. An estimated total of 170000 EVs would, in addition to the conventional load, result in energy requirements that would lead to the flattening of the daily load curve at a level corresponding to the peak demand. Since, information about vehicles in this test system is not readily available; the above estimate is referenced to as the total number of vehicles in the system.

The resulting hourly load from ASM is compared with the result from JSM for 100% EV penetration and is shown in Figure 3.5. It can be seen that ASM results in lower EV load to be scheduled between hours 2 to 7 when compared with the JSM due to the error in estimation of charging price. This under-scheduling of EV load during the early hours results in greater EV load being scheduled between hours 9 to 21.

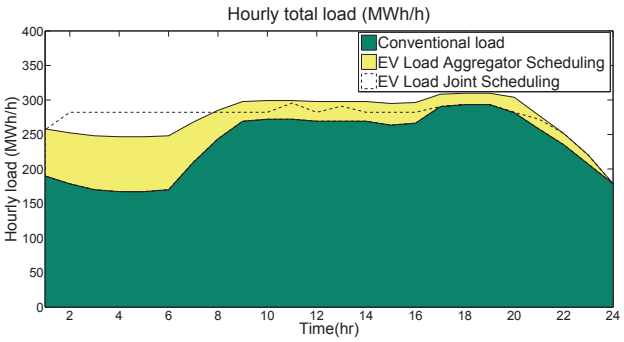

Figure 3.5: ASM and JSM comparison result- system demand at zero and 100 % EV penetration

The corresponding changes in market price can be seen in Figure 3.6. This price directly reflects the errors in charging price forecasting by the aggregator on electricity market price. It is lower by about 4 $/MWh during hours 2 to 7 but, consequently, increases by 4 $/MWh during the later hours 9 to 21 when compared to JSM results.

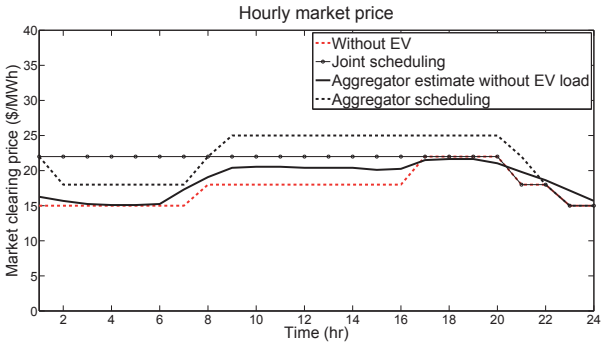

Figure 3.6: ASM and JSM comparison result- market price at zero and 100 % EV penetration

From these results, it could be concluded that compared to ASM, JSM provides a better utilization of generating resources and also schedules the EV charging according to the energy needs.

3.3.2 Nordic test system

The proposed JSM is used to simulate the effect of EV charging in the Nordic day-ahead market called Elspot, which consists of five participating countries from the Nordic region, namely- Norway, Sweden, Finland and Denmark. Market players who want to trade

electricity on the Elspot market must submit their sell offers and/or buy bids for every hour of trading to the market, no later than 12:00 hours, on the day before the power delivery. These bids are submitted via the internet to the website of NordPoolSpot. The collected sell bids are cumulated in increasing order of price to form a supply curve and the buy bids are cumulated in decreasing order of price to form a demand curve- for every hour. The intersection of the two curves gives the market price of electricity for that hour. More information on the operation of Elspot can be found in [37].

Due to the physical restrictions imposed on energy trading by transmission lines, the Nordic electricity market area is divided into a number of bidding areas. The TSO decides on the criteria and number of bidding areas. Since, the operations of a TSO are generally limited to one country, a bidding area does not traverse political boundaries between countries in the Nordic region. Currently, Norway is split into 5 bidding areas- NO1 to NO5; Sweden into four- SE1 to SE4; Denmark into two- DK1 and DK2; and Finland into one- FI.

The total installed generating capacity in Nordic region is 96 GW. The share of total installed generation capacity based on the bidding areas in the Nordic region (excluding Estonia, Latvia and Lithuania) is shown in Figure 3.7 [66].

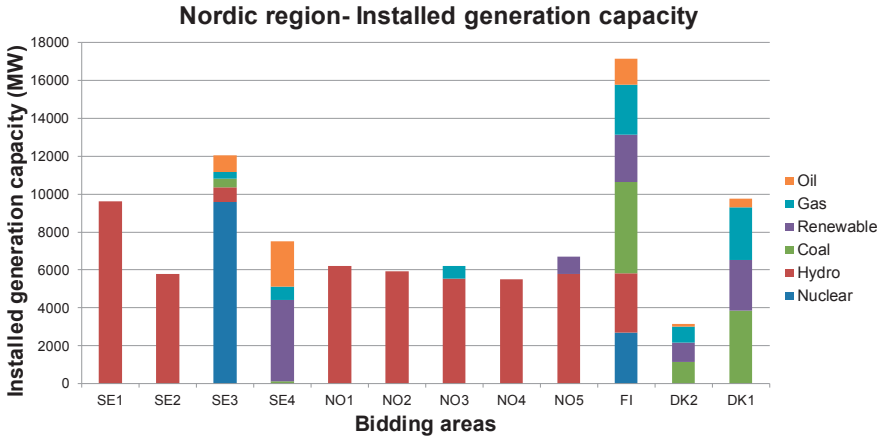

Figure 3.7: Generating capacity distribution by bidding area in the Nordic region

Installed generation capacity data for units greater than 100 MW for all four countries is obtained from [67], based on the type of generating technology. The variable cost of power generation based on different technologies in [68] is used and and scaled to reflect the average system prices in Nord Pool Spot for the year 2012 [69], after which the aggregated supply curve in the Nordic test system can be obtained as shown in Figure 3.8.

The aggregated supply curve is based on installed generation capacity in four countries- Norway, Sweden, Finland and Denmark. A normal market situation is considered, where, all the installed generation capacity is available. Two generation technologies that influence

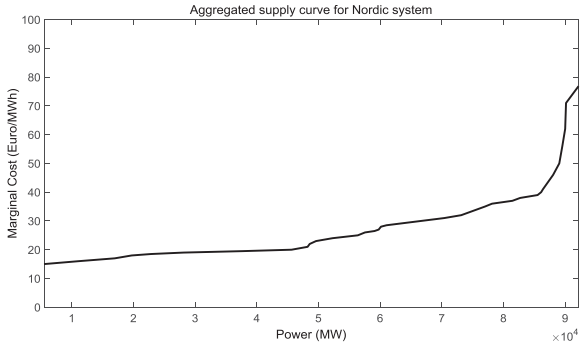

Figure 3.8: Generator marginal cost curve for the Nordic test system

this assumption critically in the Nordic market are- hydro and nuclear power. With respect to hydro power, it reflects a situation when there is sufficient inflow to the hydro power station reservoirs in Norway and Sweden. This can further be classified as a normal winter that occurs every other year. This is in line with a study on vulnerabilities of the Nordic power system where, 90% hydro availability is assumed in Norway and Sweden during normal hydro conditions [70]. Similarly, due to the low probability of forced outages of nuclear power generation in Sweden and Finland, 100% availability is assumed.

The vehicle data required to simulate the participation of EVs in the Nordic market is based on statistics available for conventional fuel driven vehicles and is obtained from [71], [72], [73], [74]. The resolution of this data currently available is for each county present in each of these countries. The total number of conventional vehicles in the Nordic area is found to be around 12.7 million. These are approximately segmented according to bidding areas and the resulting distribution is shown in Figure 3.9.

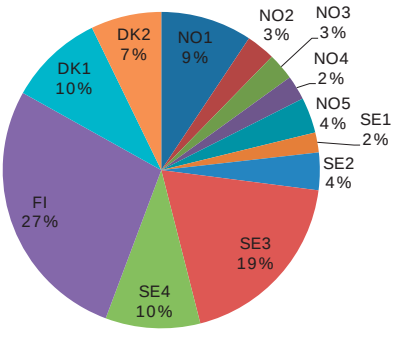

Figure 3.9: Conventional vehicles' distribution based on bidding areas

It is difficult to estimate the elasticity of conventional demand in the short-term since this elasticity would occur in special circumstances, where, the price of electricity is very high over a sustained period of time (days or weeks). Hence, the conventional demand is assumed to be inelastic as shown for the case of peak demand in Figure 3.8.

The impact of the assumptions made in this study on the final results and its analysis is optimistic, while at the same time, reflecting a highly expected market situation. It is imperative to mention that the simulation models are designed for a single auction market while the Nordic market is, in fact, a double auction market where a number of market players determine the outcome. A direct consequence of this may be a lower resulting market price due to better utilization of generating resources.

The external interconnection capacities between countries within and outside of the Nordic area are included as inelastic demand thereby representing an export scenario from the Nordic countries. This is indicative of an anticipated market situation, though, in reality, the complete transmission capacity may not be utilized.

The JSM has been used in the following two cases for the Nordic test system:

1. Unconstrained case: when the trading of electricity is not limited by the interconnection capacities between different bidding areas in the Nordic region.
2. Constrained case: trading of electricity is limited by the interconnection capacities between different bidding areas in the Nordic region, which are modeled based on the net transfer capacity (NTC) values from the year 2014 [75].

Only the JSM is used for the case study of the Nordic market, because the ASM is heavily dependent on the accuracy of the estimated supply function given by (3.2). The accuracy of this function could be improved by modeling the price as a polynomial function of demand, although, by doing so, the complexity of the optimization function increases and the resulting model might not necessarily provide a solution. The consequence of such an assumption is the results being more optimistic, where the available generation and flexible demand are utilized more resourcefully.

3.3.2.1 Unconstrained Case

Theoretically, if there were no upper limits on interconnection capacities, one supply and one demand curve would be used for the clearing of the whole Nordic day-ahead market. In a single auction market, it would translate into a single supply curve for the entire Nordic market. This would then be matched with the demand curve during that particular hour to obtain the market price for electricity.

The demand profile for this system was obtained using the data in [76] for a Tuesday during week 51 with an aggregated peak demand of 69 GW [66]. In such a context, if EVs are introduced into the system and their charging energy traded in the Nordic market as flexible demands, the corresponding changes to the electricity price in the day-ahead market, for various penetration levels of EVs, can be obtained as shown in Figure 3.10.

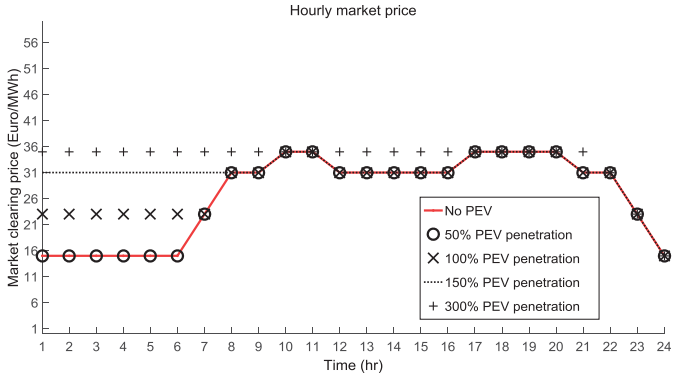

Figure 3.10: Unconstrained case result- changes in market price by the introduction of EVs

It can be observed that even if all the 12.7 million conventional vehicles were replaced by EVs, the market price would increase by 8 €/MWh during low demand periods. It would require an introduction of at least 37 million EVs before the system price during most hours corresponds to the peak load price of 35 €/MWh during hour 18. Hence, the Nordic market could be considered to be resilient towards the introduction of EVs. The changes in hourly total load and market price, with the introduction of 12.7 million EVs in the Nordic region, are shown in Figure 3.11 and Figure 3.12, respectively.

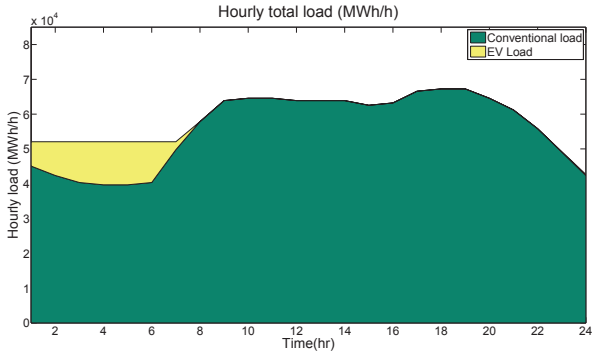

Figure 3.11: Unconstrained case result- total load at 100 % EV penetration

3.3.2.2 Constrained Case

With interconnection capacities in place, area prices apply when power traded between at least two areas in the market exceeds the total available transmission capacity between those areas. The area market prices in the Nordic market for the constrained case are

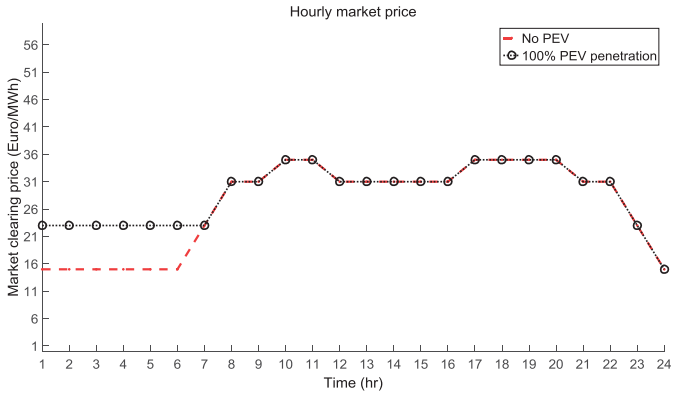

Figure 3.12: Unconstrained case result- market price at 100 % EV penetration

shown in Figure 3.13. Y-axis denotes the area prices; x-axis denotes the 12 bidding areas and the colored bars from blue to red denote the 24 hours under consideration for each area. It can be seen in Figure 3.13 that areas FI, SE4 and DK2 already suffer from

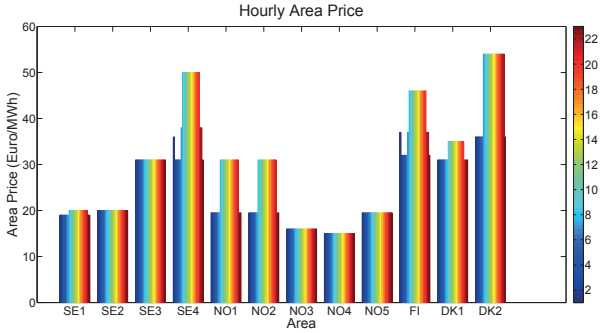

Figure 3.13: Constrained case result- area prices with only conventional load

high prices compared to other areas primarily due to the dominant fossil fuel-based local generation. Prices in most of the areas are different indicating that the interconnections between these areas have been fully utilized. In areas NO1 and NO2, it can be observed that the prices during all of the 24 hours are the same indicating that the available transmission capacity is not completely utilized.

Extension of the model to include scheduling of EV charging results in area prices as shown in Figure 3.14, for 100% penetration of EVs in the market. In hydro power dominated areas- SE1, SE2, NO1-NO5, it can be seen that the market price remains relatively the same during all hours even with a high penetration of EVs. It is also found that mainly two areas, namely- SE4 and DK2 are affected by the high levels of EV penetration. At 100% EV penetration level, the electricity price in DK2 increases to 54 €/MWh even

during the low demand hours 1-7, whereas it increases to 38 €/MWh in SE4 during the same hours. Further introduction of EVs would result in a market price higher than 54 €/MWh in DK2 that corresponds to the price at peak demand with only conventional demand.

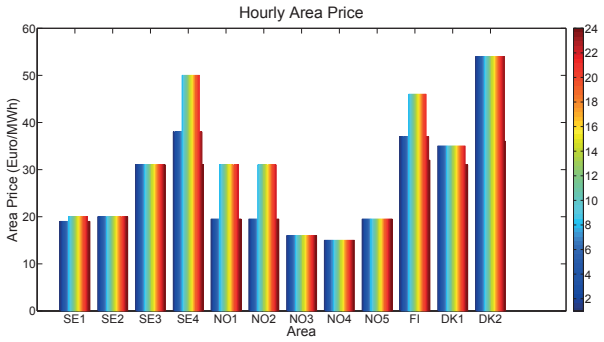

Figure 3.14: Constrained case result- area prices with 100 % EV penetration

Area price for SE4 at different penetration levels is shown in Figure 3.15. Similarly, for the bidding area DK2, the area price at different penetration levels is shown in Figure 3.16.

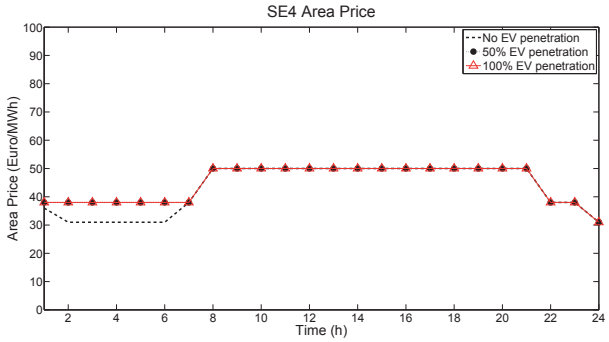

Figure 3.15: Constrained case result- SE4 area price at different EV penetration levels

It can be seen that the area prices in SE4 and DK2 increase with an increased penetration of EVs in the Nordic system. This may be attributed to a number of factors, for e.g., these two areas are dominated by thermal generators which are generally more expensive, capacity of transmission lines connecting them to generator surplus areas are insufficient and greater population in these areas account for relatively higher number of EVs being integrated at higher penetration levels.

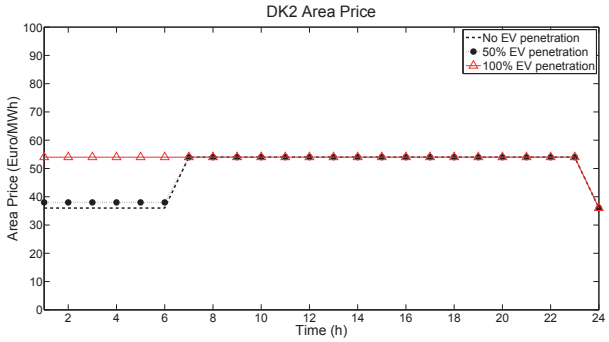

Figure 3.16: Constrained case result- DK2 area price at different EV penetration levels

3.4 Summary

In this chapter, joint scheduling and aggregator scheduling methods were proposed that could be used to evaluate the effects of EVs scheduling on the overall system load shape and the effects on electricity market price. JSM could prove useful in a market setup where there is a possibility to schedule both the generation and demand side resources; whereas ASM could be useful where market players would require performing their individual energy scheduling.

The two methods were applied to an IEEE 30-bus test system and a Nordic test system to find the effects of EV energy scheduling on market price of electricity. From the case study on the IEEE 30-bus test system, it was found that market integration of EVs might lead to an increase in market price at higher penetration levels. The proposed JSM may require changes in the operational structure of electricity markets, but the model could result in better utilization of resources as it simultaneously schedules both the generation and demand resources.

In the unconstrained case, the Nordic market was found to be highly resilient toward integration of EVs. Transmission network constraints, however, would directly influence the penetration level of the EVs that can be accommodated in the system before a significant increase in market price.

The day-ahead market is generally cleared 24-36 hours prior to the operating hour. It is the responsibility of transmission system operators to maintain the balance between production and consumption. To ensure this, the transmission system operators request generators and demand resources to bid in the regulating power market (RPM). The EV aggregator could also participate in the RPM to provide balancing services and possibly generate more revenue in the process. The market framework and EV energy scheduling for RPM is described in the next chapter.

Chapter 4

EV Participation in the Regulating Power Market

This chapter describes an optimization model for scheduling energy by electric vehicle aggregator for its participation in the regulating power market. A market framework based on nodal pricing is assumed. A mechanism for clearing the market while considering the effect of power injection at nodes on transmission network losses is proposed. Finally, a case study on a Nordic 32-bus test system is performed and the results are presented.

4.1 Related Work

The dispatch of balancing resources in a power system is based on the imbalance between supply and demand during real-time operation, which is reflected by system frequency. From the beginning of 2013, three levels of frequency control are being employed in the Nordic power system [77]. Tertiary control or manual reserve resources are procured via bids in the regulating power market (RPM) and the lowest cost bids are normally activated when necessary. Such a procurement of balancing resources might not be the most effective since power losses in the system are not considered during activation [78] and the system might incur additional regulation costs. Hence, it is necessary to include the effect of transmission losses and network constraints while selecting the regulation bids.

In [79], a model for RPM based on incremental DC optimal power flow (DCOPF) considering marginal transmission loss is presented and it is shown that this approach could lead to a better utilization of reserves in RPM. The present chapter extends the application of this approach by further modeling the participation of possible demand-side flexibility from electric vehicles (EV) in the future. A model of the RPM is proposed wherein the activation of regulating power resources is performed based on re-valued

regulation price, reflecting the regulating power's contributions to active power losses in the network. The effect of changes in active power injection at various generator and EV buses on the transmission line limits are also modeled as constraints during the activation process. This approach is implemented within an AC optimal power flow (ACOPF) framework where the power flows and system loss can be precisely evaluated. Furthermore, demand-side participation by EVs in providing regulating power in the market is incorporated in the RPM model. A case study is carried out based on the proposed model using a modified Nordic 32-bus system. Results from the proposed market model will be compared with those of the current approach used in the Nordic RPM based on a merit list without loss consideration. Also, effects of EVs participation in regulating power market will be studied.

4.2 Market Framework and Modeling Approach

The objective of RPM is to make sure that active power imbalances arising from forecasting and other unplanned errors are balanced during real-time operation. Hence, deviations from the production and consumption plans from DAM need to be modeled to characterize the response of generators in the RPM. With new players in the electricity market from the demand-side such as EV aggregator [80], the planning stage before the DAM participation becomes ever more important if they are to partake in arbitrage. Consequently, it is necessary to mathematically model the EV aggregator's planning and its subsequent participation in the day-ahead and regulating power market. The framework used in this work and hence, the relationship between the markets are shown in Figure 4.1.

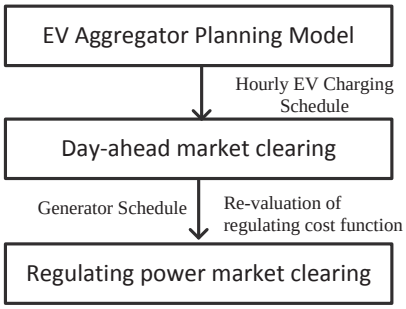

Figure 4.1: Relationship between the models

The following approach is used to characterize the relationship between the models:

- Use EV aggregator planning model to find the hourly aggregated charging schedule of EVs over the planning horizon.
- The hourly charging schedule of EVs is then taken as a fixed demand along with the conventional demand and used in the ACOPF model to obtain the actual generation

dispatch while considering the major operating constraints. The ACOPF performed also gives the incremental transmission losses at every bus in the system.

- The incremental transmission loss (ITL) is used to calculate the loss penalty factor, which in turn is used to modify the up and down regulation incremental cost functions. Doing this will reflect the effect of increment or decrement of power at a bus on the total transmission loss in the system. The re-valued incremental cost functions are used in the RPM model to finally determine the necessary regulating power.

4.3 EV Aggregator Planning Model

4.3.1 Objective Function

The EV aggregator model characterizes the flexibility available from the batteries of EVs and schedules their charging energy. It is imperative to have good estimate of the electricity price profile for planning the scheduling of EV charging. Considering an electricity market with nodal pricing, the price of electricity depends on the generation technology mix, the demand profile and the topology of the transmission system. A DCOPF framework [81] is used to account for these factors in the aggregator planning model and a global analysis is assumed to be performed by the aggregator. Therefore, it is assumed that the aggregator has the information with regards to generator cost functions, conventional load profile and the transmission network parameters. Based on the estimated data, the EV aggregator simulates the scheduling of generators and simultaneously plans for EV charging energy in a way so as to minimize the total cost of power generation as shown in (4.1).

$$Minimize \quad DAEC = \sum_{i \in N} \sum_{t \in T} C_i(P_{i,t}) \tag{4.1}$$

The objective function of the EV aggregator formulated in (4.1) is subject to the constraints (4.2)-(4.5) by the EV batteries and also constraints (4.6)-(4.8) imposed by the power system.

4.3.2 EV Related Constraints

The EV aggregator estimates the amount of energy that the EVs would need for travel during the battery charge scheduling horizon. Considering that the EV aggregator participates in RPM, it is necessary for the aggregator to forecast the regulating power volume and the regulating direction (i.e., up or down regulation) during the participating hour. If up regulation is provided using vehicle-to-grid (V2G) concept, the aggregator needs to plan for the additional energy charging needed for participating in the RPM.

Based on this charging requirement information and plan for participation in RPM, the batteries are charged only that amount of energy necessary over their initial state. Note that vehicles may travel more or less than the average distance considered. A minimum charge in the battery is always maintained to provide a possibility of backup energy in case the distance traveled needs to be higher than the average distance as shown in (4.2).

$$SOC_i^{ini} + \sum_{t=1}^{T} E_{i,t} = SOC_i^{min} + \sum_{t=1}^{T} (E_{i,t}^{next} + E_{i,t}^{up}); \qquad \forall i \in N_V \tag{4.2}$$

The EV aggregator needs to schedule the charging of the EVs in such a way that the battery is charged before travel during hour t. Additionally, the battery also needs to be charged with the extra energy needed for up regulation before the participating hour t. This constraint is formulated as shown in (4.3).

$$\sum_{h=1}^{t-1} E_{i,h} - E_{i,h}^{next} - E_{i,h}^{up} \geq E_{i,t}^{next} + E_{i,t}^{up}; \qquad \forall t \in T, i \in N_V \tag{4.3}$$

Charging and discharging of the battery during consecutive hours results in a change in its energy level. This is formulated as shown in (4.4).

$$SOC_{i,t} = \begin{cases} SOC_i^{ini} + E_{i,t} - E_{i,t}^{next} - E_{i,t}^{up} & \forall t \in \{1\}, i \in N_V \\ SOC_{i,t-1} + E_{i,t} - E_{i,t}^{next} - E_{i,t}^{up} & \forall t \in \{2, 3..., T\}, i \in N_V \end{cases} \tag{4.4}$$

The energy level in the battery should not deviate from its minimum and maximum limits as shown in (4.5).

$$SOC_i^{min} \leq SOC_{i,t} \leq SOC_i^{max}; \quad \forall t \in T \tag{4.5}$$

4.3.3 Other Constraints

It has to be ensured that the total power injected at a bus is equal to the total power withdrawn from the bus as shown in (4.6). The demand at bus $i \in N_V$ also includes the EV demand that is scheduled and is one of the results from the optimization model.

$$P_{i,t} - PL_{i,t} - E_{i,t} - \sum_{j \in N} B_{i,j} \delta_{j,t} = 0; \quad \forall i \in N, t \in T \tag{4.6}$$

It is imperative that the generators observe the minimum and maximum values of their active power generation limits as shown in (4.7).

$$P_i^{min} \leq P_{i,t} \leq P_i^{max}; \quad \forall i \in N, t \in T \tag{4.7}$$

There is only a certain amount of power that can be transmitted over the transmission lines and these limits are satisfied by using (4.8).

$$B_{i,j}(\delta_{i,t} - \delta_{j,t}) \leq L_{i,j}^{max}; \qquad \forall i, j \in N_L \tag{4.8}$$

4.4 Day-Ahead Market Model

The day-ahead market is represented using an ACOPF in this chapter for the following reasons:

1. To estimate the actual state of the power system before the regulation hour.
2. To accurately characterize the associated transmission loss and its incremental deviation with respect to changes in the injected power at various buses during the regulating hour.

For any regulating hour $t' \in T$, the results of actual generation scheduling and line flows can be obtained as described below.

4.4.1 Objective Function

Within the ACOPF framework, the day-ahead market model is cleared with the objective of minimizing the total cost of generation to supply the demand as shown in (4.9) subject to the system constraints shown in (4.10)-(4.17).

$$Minimize \quad DAC_t\Big|_{t=t'} = \sum_{i \in N} C_i(P_{i,t}\big|_{t=t'}) \tag{4.9}$$

4.4.2 Power System Constraints

It has to be ensured that both the active and reactive power balance at each bus is satisfied. The power injected into the bus should be equal to the power withdrawn from the bus at any time $t = t'$ as shown in (4.10) and (4.11) for active and reactive powers, respectively. For the ACOPF, the planned energy consumption $E_{i,t}$ from the EV aggregator model is provided as an input parameter for every time $t = t'$.

$$P_{i,t}\big|_{t=t'} - PL_{i,t}\big|_{t=t'} - E_{i,t}\big|_{t=t'} - P(V,\delta) = 0; \quad \forall i \in N \tag{4.10}$$

$$Q_i - QL_i - Q(V,\delta) = 0; \quad \forall i \in N \tag{4.11}$$

The voltage at every bus in the power system has to be within the specified limits as shown (4.12).

$$V_i^{min} \leq V_i \leq V_i^{max}; \quad \forall i \in N \tag{4.12}$$

It should also be ensured that the total power transmitted over the transmission lines do not exceed the maximum possible limit as shown in (4.13).

$$L_{i,j} \leq L_{i,j}^{max}; \quad \forall i,j \in N_L \tag{4.13}$$

4.4.3 Generator Constraints

Each generator has a maximum amount of active and reactive power that it can produce for each time $t = t'$ as shown in (4.14) and (4.15), respectively.

$$P_i^{min} \leq P_{i,t}\big|_{t=t'} \leq P_i^{max}; \quad \forall i \in N \tag{4.14}$$

$$Q_i^{min} \leq Q_i \leq Q_i^{max}; \quad \forall i \in N \tag{4.15}$$

4.4.4 Reserve Constraints

There should be sufficient active power reserves available within the power system in order to ensure its secure operation during emergency imbalance conditions. This is obtained using (4.16) for up-regulating reserves and (4.17) for down-regulating reserves.

$$\sum_{i \in N_G} (P_i^{max} - P_{i,t}\big|_{t=t'}) \geq P^{R+} \tag{4.16}$$

$$\sum_{i \in N_G} (P_i^{min} - P_{i,t}\big|_{t=t'}) \leq P^{R-} \tag{4.17}$$

4.4.5 Penalty Factor Calculation

After solving the optimization problem with the objective function in (4.9) subject to the constraints (4.10)-(4.17), the results yield the associated transmission losses and the corresponding incremental transmission loss (ITL) [81] as shown in 4.18.

$$ITL_i(P_{i,t}\big|_{t=t'}) = \frac{\partial P_{loss}}{\partial P_i}; \tag{4.18}$$

The penalty factor to be used in re-valuing the incremental cost functions of generators and EV aggregator can be calculated from ITL at bus i as shown in (4.19).

$$PF_i = \frac{1}{1 - ITL_i(P_{i,t}\big|_{t=t'})} \tag{4.19}$$

The calculated penalty factor could then be used to re-value the marginal price of regulating power within the regulating power market model as shown in (4.25). The re-valuation reflects the effect of transmission loss from regulating power injection at bus i on the associated changes in regulation costs due to the same.

4.5 Regulating Power Market Model

4.5.1 Objective function of RPM

The objective function of the RPM is to minimize the total cost of power balancing [82]. It can be mathematically formulated as in (4.20).

$$\textit{Minimize:} \quad RP = \sum_{i=1}^{N_G}[c_i^+ \Delta P_i^+ - c_i^- \Delta P_i^-] + \sum_{i=1}^{N_V}[c_i^+ \Delta EV_i^+ - c_i^- \Delta EV_i^-] \quad (4.20)$$

The objective function of RPM model is subjected to constraints (4.21) - (4.27).

4.5.2 Regulating power limits

There is a regulating range within which power can be up or down regulated by a production balance responsible party (BRP) at any node i in the system and is shown in (4.21) and (4.22), respectively.

$$\Delta P_i^+ \leq (P_i^{max} - P_{i,t}\big|_{t=t'}); \quad \forall i \in N_G \quad (4.21)$$

$$\Delta P_i^- \geq (P_i^{min} - P_{i,t}\big|_{t=t'}); \quad \forall i \in N_G \quad (4.22)$$

Based on generator scheduling in the day-ahead market, the available regulating power can be obtained. It is assumed that all the regulating power available in the system during an operational hour is made available to the RPM.

Modeling of EV participation in the day-ahead market is done as described in Section 4.3. Additionally, the up and down regulating power available from the EVs after the day-ahead market clearing can be obtained as shown in (4.23) and (4.24), respectively.

$$\Delta EV_i^+ \leq min[E_{i,t}^{up}\big|_{t=t'}, DP_{i,t}\big|_{t=t'}]; \quad \forall i \in N_V \quad (4.23)$$

$$\Delta EV_i^- \geq max[(SOC_{i,t}\big|_{t=t'} - SOC_i^{max}), -CP_{i,t}\big|_{t=t'}]; \quad \forall i \in N_V \quad (4.24)$$

The up regulating power from EVs is a net aggregate of V2G discharge power from the battery during the regulating hour.

4.5.3 Re-valued price

The regulating power prices in the RPM are determined based on re-valued incremental cost function of the BRP to take into account the additional costs due to transmission losses within the network [83]. This is described in (4.25).

$$c_i^+, c_i^- = \frac{\partial C_i(P_{i,t})}{\partial P_{i,t}} PF(i); \qquad \forall t = t' \quad (4.25)$$

4.5.4 Transmission Line Limits

The transmission line constraint is formulated as shown in (4.26). This indicates that the change in active power flow over the line should not exceed its maximum limit.

$$L_{i,j} + \sum_{k}^{N} ptdf_{i,j,k}(\Delta P_k^+ + \Delta P_k^- + \Delta EV_k^+ + \Delta EV_k^-) \leq L_{i,j}^{max};\ \forall i,j \in N_L \quad (4.26)$$

4.5.5 Active power balance

It should be noted that the net changes in active power injection at any bus i should be equal to zero. This is formulated as shown in (4.27)

$$\sum_{i}^{N}[\Delta P_i^+ + \Delta P_i^- + \Delta EV_i^+ + \Delta EV_i^-] - \sum_{i}^{N} P_i^{dev} = 0 \quad (4.27)$$

4.6 Case Study and Results

The proposed RPM model with EVs is applied to a case study using a modified Nordic 32-bus test system [84] shown in Figure 4.2. This test system is representative of the Swedish high voltage transmission network connecting the abundant hydro generators in the North to the load-centric South.

4.6.1 Data Setup

Quadratic cost functions were used for the generators present in the system and were obtained from [85]. Transmission line flow limits of 800MVA-1000MVA were assigned for these simulations where not explicitly provided in [84]. For DCOPF model, it was considered that the system must be N-1 contingency compliant and the MVA capacity was assumed to be limited to 80% of the value provided in the test system data. Additionally, it was also assumed that the system load was operating at an overall lagging power factor of 0.9 during normal operation. Hence, the active power transmission capacities were limited to $(0.9 * 0.8 \approx 0.7)$, i.e., 70% of the 800-1000 MVA values during the planning stage.

The load profile over the day was obtained from [86] for the third Monday in December, 2012 and normalized to be made usable for the test system. It was further assumed that the conventional demand at all the nodes experienced the same profile over the day.

Considering planning for day-ahead and regulating power markets, the planning horizon for the EV aggregator model is assumed to be 24 hours. The EV related parameters used in the case study were obtained from [87]. The value of SOC_i^{min} was fixed at 20% of

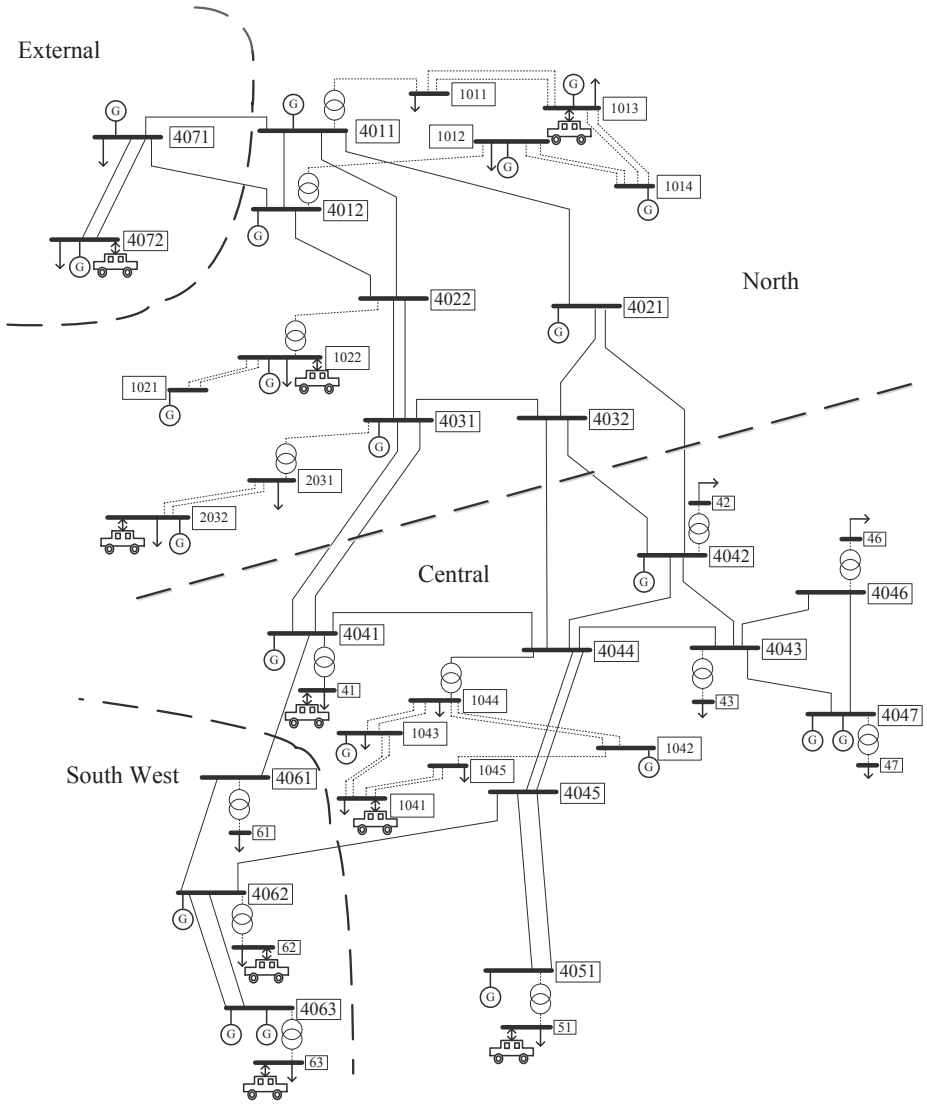

Figure 4.2: Nordic 32-bus Test System [84]

battery capacity to allow for a reserve in case the distance traveled needs to be higher than 40 km. Similarly, SOC_i^{max} was fixed at 85% of battery capacity to account for the changes in aggregated battery capacity limits when a significant number of vehicles are unavailable to the aggregator while traveling. The EV demand was assumed to be present mostly at the load-centric buses. The following buses were assumed to share the aggregated EV

demand: 4072, 1013, 1022, 2032, 1041, 41, 51, 62 and 63. The total number of vehicles present at these buses were assumed to be 50000 with 10% EV penetration. This is estimated to be the maximum amount of EV penetration in the Swedish automobile market by 2030 in the 'current control measure' scenario provided in [88].

The magnitude of total real time deviation for the case of up regulating power was assumed to be 159 MW and for the case of down regulating power, it was taken to be 147.9 MW. These values are approximately half of the reserve requirement in the Nordic system of around 1620 MW [89] when scaled down to be consistent with the Nordic 32-bus test system.

4.6.2 Results

4.6.2.1 Scheduling by EV aggregator

The EV aggregator planning model schedules the charging of EVs in such a way that they charge during the low electricity price hours. Since, it is assumed that all the EVs not driving during a particular hour are available for charging, the EVs are scheduled for charging by the aggregator in all the scenarios considered occurs between hours $t1 - t6$ of the day. Hence, the EVs are charged even the energy necessary for up regulation through V2G and available for activation during the rest of the hours between $t7 - t24$.

4.6.2.2 Day-ahead market clearing

The generation dispatch and corresponding locational marginal price (LMP) results from the ACOPF are shown in Table 4.1. It can be seen that most of the generators are running at their maximum capacity. Furthermore, the difference in LMPs of the buses in the North and South regions of the test system are significant due to difference in marginal production cost and additional congestion in the network. It can be seen that the LMP at load buses is significantly high making it difficult for EVs to compete in the RPM, especially for up regulating power. But, with the EV aggregator model, the EVs can charge $E_{i,t}^{up}$ during low price periods and re-sell it for up regulation during high price periods with a margin. A similar approach would apply for down regulation by EVs.

4.6.2.3 Regulating power activation

Considering the existing operation of RPM in the Nordic region, manual reserves are activated based on the merit order. This is subject to the condition that there is no congestion caused due to the activation of these reserves. The results, when applied to the test system considered, are compared with the results obtained using the RPM model proposed in this chapter, with and without EV participation. This is done for

Table 4.1: Result from day-ahead market model: Hour 18

Bus [$No.$]	Power Generation [MW]	LMP [€/MWh]
4072 (EV)	1561.4	23.5
4071	500.0	23.3
4011	1000.0	23.8
4012	800.0	22.6
4021	300.0	60.9
4031	350.0	67.9
4042	700.0	73.2
4062	207.0	84.5
4063	219.9	85.3
4051	700.0	77.6
4047	1200.0	74.1
2032 (EV)	850.0	62.9
1013 (EV)	268.8	21.9
1012	528.9	18.2
1014	700.0	21.3
1022	0.0	22.8
1021	207.7	21.6
1043	200.0	77.8
1042	400.0	73.7
1041 (EV)	0.0	80.2
41 (EV)	0.0	74.2
62 (EV)	0.0	84.5
63 (EV)	0.0	85.3
51 (EV)	0.0	77.5

two scenarios- one where the TSO requests up regulating power and two, where the TSO requests down regulating power.

Up Regulation Scenario: In the first scenario, the TSO request up regulating power from the generators and EV aggregator for the hour 18. The total active power deviation in the system that results in the request for up regulting power is assumed to be 159 MW. The resulting comparison of up regulating power activation is shown in Table 4.2. The comparison is done for three cases- activation using merit order, RPM model without regulating power from EV and RPM model with regulating power from EV. The corresponding up regulation prices and regulation costs incurred by the TSO are shown in Tables 4.3 and 4.4, respectively. It can be seen that the total regulation costs incurred by the TSO decreases when the effect of transmission losses are considered with the inclusion of the loss penalty factor. The EVs present near the load centre are particularly effective in reducing the costs by injecting power close to the load centres.

Table 4.2: Result: Up regulating power at hour 18

Bus $[No.]$	Merit Order $[MW]$	RPM, without EV $[MW]$	RPM, with EV $[MW]$
4062	29.8	32.6	21.9
4063	23.4	19.5	9.2
1012	105.8	105.9	106.8
2032 (EV)	-	-	5
1041 (EV)	-	-	5
41 (EV)	-	-	5
51 (EV)	-	-	5
ΔP	159.0 MW	158.0 MW	157.9 MW
ΔP_{loss}	11.1 MW	10.1 MW	10.0 MW

Table 4.3: Result: Up regulating power prices at hour 18

Bus $[No.]$	Merit Order $[€/MWh]$	RPM, without EV $[€/MWh]$	RPM, with EV $[€/MWh]$
4062	86.267	86.432	85.797
4063	86.649	86.421	85.806
1012	18.700	18.701	18.706
2032 (EV)	-	-	67.970
1041 (EV)	-	-	85.192
41 (EV)	-	-	79.204
51 (EV)	-	-	82.547

Table 4.4: Result: Total up regulation cost at hour 18

Merit Order[€]	RPM, without EV [€]	RPM, with EV [€]
6576.80	6483.33	6240.74

Down Regulation Scenario: In the second scenario, the total active power deviation in the system is assumed to result in down regulating power request by the TSO. The magnitude of power deviations is considered to be 147.9 MW. Similar to the previous scenario, three cases of down regulating power activation are compared- activation from merit order, RPM model without down regulating power from EV and RPM model with down regulating power from EV. The down regulating power activation results are compared in Table 4.5 and the corresponding down regulation prices and regulation costs for the TSO are shown in Tables 4.6 and 4.7, respectively. In the case of down regulating power activation, there is only a small difference in the cost between the merit order activation method and the proposed RPM model with EVs. This could be seen as advantageous from both the system perspective, where EV participation in down regulation does not significantly increase the cost of balancing, as well as from EV perspective as their batteries could be charged at a price generally lower than the day-ahead price.

Table 4.5: Result: Down regulating power at hour 18

Bus [$No.$]	Merit Order [MW]	RPM, without EV [MW]	RPM, with EV [MW]
1012	-105.80	-105.80	-105.80
1014	-31.80	-31.80	-12.70
4072 (EV)	-	-	-6.40
1013 (EV)	-	-	-6.40
1022 (EV)	-	-	-6.40
ΔP	-137.60 MW	-137.60 MW	-137.70 MW
ΔP_{loss}	-10.30 MW	-10.30 MW	-10.20 MW

Table 4.6: Result: Down regulating power prices at hour 18

Bus [$No.$]	Merit Order [€/MWh]	RPM, without EV [€/MWh]	RPM, with EV [€/MWh]
1012	17.60	17.60	17.600
1014	21.33	21.33	21.264
4072 (EV)	-	-	18.519
1013 (EV)	-	-	16.898
1022 (EV)	-	-	17.757

Table 4.7: Result: Total down regulation cost at hour 18

Merit Order[€]	RPM, without EV [€]	RPM, with EV [€]
-2540.37	-2540.37	-2472.45

4.7 Summary

A regulating power market model considering the participation of EV aggregator was developed. The model was used to activate regulating power by re-valuating the marginal cost of regulating power using a penalty factor calculated from ACOPF to account for their influence on active power losses on the transmission lines. A case study was performed on a modified Nordic 32-bus system considering two regulating power activation scenarios. Within the scope of this study it could be seen that the system could benefit from the aggregated regulating power provided by EVs. Considering the effect of regulating power on transmission line losses also results in slightly different set of regulating power activation when compared to the merit order list while also resulting in lower total balancing costs. This is clearly noticeable in the case study when up regulating power scenarios are considered. However, it should be mentioned that the activation of EVs for active power regulation would be very much dependent on their position to perform arbitrage and a thorough analysis regarding this needs to be done.

As a business entity, the EV aggregator encounters a degree of uncertainty associated with participation in day-ahead and regulating power markets. The risks associated

with price and demand uncertainty in the day-ahead market could be hedged against in the forward/futures market. If an electricity retailer assumes a secondary role of an EV aggregator, they would need a framework to plan for their participation in forward market. Furthermore, they would need to decide on retail prices for their customers while accounting for the flexibility offered by owners of EV. The upcoming chapter tries to address this issue by outlining a framework and corresponding mathematical models for an electricity retailer to hedge their risks in the forward market.

Chapter 5

EV Energy and Electricity Retailer Planning

This chapter provides an energy portfolio optimization model for an EV aggregator or electricity retailer incorporating the market functions of an EV aggregator. The retailer could use this model for making decisions regarding purchase of power contracts from forward markets as well as for setting prices for customers entering into fixed and variable retail contracts. The proposed retailer planning (RP) model is used in a case study involving a typical retailer in Sweden assuming the role of an EV aggregator in the market. Results from the case study indicate that variable retail contracts could prove to be beneficial to both the vehicle owners and the retailer in the presence of complete EV energy scheduling flexibility.

5.1 Related Work

An electricity retailer performs the task of a "middleman" between the wholesale electricity market and small/medium end-users. The retailer faces two major issues during the planning stage. Firstly, the cost of purchasing electricity will depend on its price in the spot market at a future point in time and the corresponding demand of its customers, both of which are uncertain. Secondly, the retailer has to determine competitive retail prices for its customers. To alleviate the risks associated with uncertain prices, the retailer can procure part of the end-user demand through forward power contracts, where the price for electricity is fixed over the contract period [40]. Recently, various models have been proposed for forward contract portfolio optimization of an electricity retailer while accounting for the stochastic behavior of electricity price and demand [90], [91]. In [90], a stochastic model was developed with a cost minimization objective to manage the forward contracting decision accounting for the involved risk. In [91], the proposed stochastic

model maximizes the profits of the retailer while determining forward contracts to be signed and the selling prices for its customers.

Emerging technologies such as EVs provide an added possibility of short-term response from the demand side. The opportunities for exploiting EVs as flexible demand have been discussed in [25], [92]. In [93], the elasticity of electric vehicle demand is considered and a short-term model is proposed that optimizes the portfolio of an EV aggregator through its participation in the day-ahead and secondary reserves markets. An electricity retailer has a good possibility of transitioning into the role of an EV aggregator. In such an environment, it becomes imperative for the retailer to accommodate the needs and short-term flexibility of EVs while managing its portfolio over a longer time frame.

In this chapter, a stochastic programming approach (see e.g., [94], [95]) is proposed that manages the portfolio of an electricity retailer who additionally assumes the role of an EV aggregator. The model presented in [91] was adopted and further developed by considering a price-taking retailer that optimizes its portfolio over a medium-term horizon with hourly discretization while scheduling the EV demand. The retailer considers the possibility to enter into power contracts in the forward electricity market and offers fixed and variable price contracts to its customers. In a fixed retail contract, it is assumed that the retailer determines and sells electricity at a constant price per MWh whereas, in a variable retail contract, the customer is charged based on the volume weighted average of the electricity price at the spot market. The objective of the retailer is to maximize its expected profits while considering the risks associated with spot price and demand uncertainties.

In the proposed approach, a retailer would perform the following functions: i) optimize the EV charging demand using expected spot price signals, ii) determine its yearly, quarterly and monthly forward contracts to be entered into, iii) determine the selling price for its existing customers with fixed and variable retail contracts. With this arrangement, the benefit for flexibility offered by EV customers would be the possibility to charge their vehicles during periods of low electricity price. The retailer is considered to aid the customers by suggesting a charging profile based on their charging requirements one day in advance. By following the charging profile provided by the retailer, EV customers would pay a discounted retail price for vehicle charging and help the retailer adhere to its plan thereby reducing the imbalance costs.

5.2 Electricity Market Framework

5.2.1 Market Structure

The proposed price-taker retailer planning model is set in the context of the Nordic electricity market, Nordpool [37]. The retailer is considered to purchase power from two main power markets namely, the spot and the forward markets and resell power to end-users through retail contracts. The forward contract to be entered into by the retailer can be yearly, quarterly or monthly base load contracts [40]. The retailer is assumed to offer two types of retail contracts to its customers namely, fixed and variable price

contracts. The total user demand of the retailer is assumed to consist of an inflexible conventional demand and a flexible EV demand. The total demand of the customers is assumed to be satisfied by the retailer through the purchase of power from either the spot and/or the forward markets. Figure 5.1 describes the main elements in the proposed planning framework.

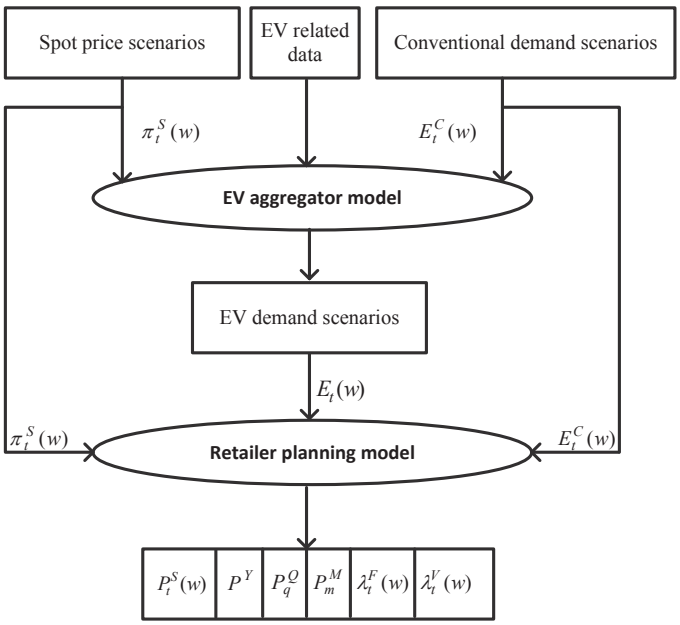

Figure 5.1: Electricity market framework for the retailer

In a forward power contract, a buyer and a seller enter into a financial agreement on the lock-in price for a certain quantity of electric power over a pre-determined future time period. Therefore, the power contracted in the forward market and the corresponding price remains constant over the delivery period. The delivery period indicates the time period over which the forward contract is put into effect. Based on the type, forward contracts can be classified as base load and peak load contracts. In the Nordpool forward market, base load contracts are traded round the clock while peak load contracts are traded for the 08:00-20:00 time horizon. Additionally, base load and peak load contracts are traded as yearly, quarterly and monthly contracts depending on the time period of maturity [40]. Only base load yearly, quarterly and monthly contracts are considered in the retailer planning model described in this chapter although peak load contracts can be similarly incorporated. The base forward prices in this chapter are calculated as described in Section 5.3.2.

The EV aggregator demand scheduling model developed [87] reflects the charging and discharging operation of an aggregated battery in accordance with the needs of all the

catered EV owner, while respecting the restrictions imposed by driving needs and the battery's energy limits. The discharging of the batteries is considered to occur only when the EVs are driving. The model takes the estimated spot price, conventional demand and EV related data as input and outputs the optimal charging schedule for the EVs based on a least charging cost objective. The charging schedule from the EV aggregator model is then provided as an input to the retailer planning (RP) model along with the estimated conventional demand and spot price. The optimized results from the RP model outputs the power contracts to be entered into by the retailer in the forward market while also determining the retail prices to be set by it.

5.3 Retailer Planning Model

It is assumed that the EV demand is responsive to the spot price and is scheduled by the EV aggregator model which has an objective of minimizing the total electricity charging cost. For each scenario of spot price and conventional demand, the aggregator model provides an EV demand scenario. The EV demand scenarios are then provided to the retailer planning model as parameters along with spot price and conventional demand scenarios. A scenario tree representing the decisions made is shown in Figure 5.2. The forward prices can be estimated at the time when purchase plans are to be made in the forward market and are called *here-and-now* decisions. The conventional demand and EV demand traded in spot market is a *wait-and-see* decision since it is highly uncertain until the clearing of the spot market and the announcement of spot prices.

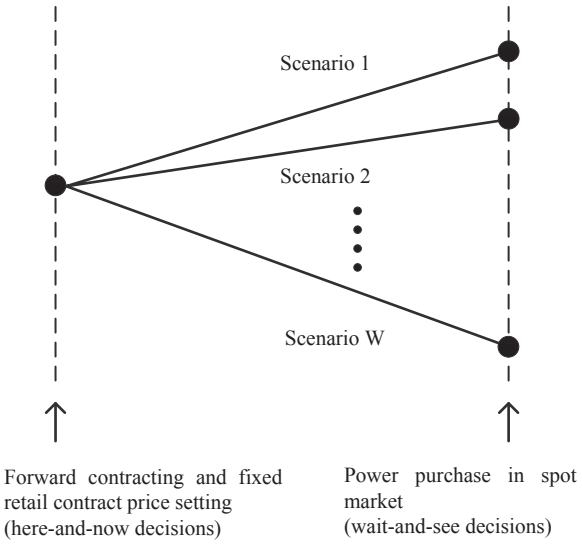

Figure 5.2: Scenario tree used in the RP model [91]

5.3.1 EV Aggregator Model

The EV aggregator model can be used by the electricity retailer to utilize the short-term elasticity offered by the EVs owned by its customers. As described in Figure 5.1, the model inputs are the estimated spot price and conventional demand along with the EV related data. The output from the model is a least cost schedule for EV battery charging. Note that this approach inherently considers the correlation between spot price and conventional demand while scheduling the aggregated EV demand.

The optimization horizon for the EV aggregator model is considered to be H hours and is performed repeatedly to cover the planning horizon of T hours and scenarios subsequently generated in the RP model. The EV aggregator model is mathematically formulated as described below.

5.3.1.1 Objective Function of EV Aggregator

The objective function of the EV aggregator model is to minimize the total charging cost over the scheduling time horizon. This can be formulated as,

$$Minimize \;\; ACC = \sum_{h \in H} \pi_h^S E_h \tag{5.1}$$

This objective of the EV aggregator is subject to the constraints presented in (5.2)-(5.5). The charging schedule obtained from this model is then utilized by the retailer to estimate its total end user demand as will be described in Section 5.3.4. It should be noted from (5.1) that all EV owners are assumed to enter into a variable price retail contract. Through this scheduling, the EV owners would pay for the amount of energy they consume during periods of relatively low prices in the spot market.

5.3.1.2 Minimum Energy Requirement

The retailer estimates the amount of energy that the EVs would need for travel during the battery charge scheduling horizon. Based on this, the batteries are charged only that amount of energy necessary over their initial state. Note that vehicles may travel more or less than the average distance considered. SOC^{min} is utilized to provide a possibility of reserve energy in case the distance traveled needs to be higher than the average distance as shown in (5.2).

$$SOC^{ini} + \sum_{h=1}^{H} E_h = SOC^{min} + \sum_{h=1}^{H} E_h^{next} \tag{5.2}$$

5.3.1.3 The Charging Period Limit

The retailer needs to schedule the charging of the EVs in such a way that the battery is charged before the travel during hour h as shown in (5.3).

$$\sum_{hf=1}^{h-1} E_{hf} - E_{hf}^{next} \geq E_{h}^{next}; \quad \forall h \in H \tag{5.3}$$

5.3.1.4 The Battery State

Charging and discharging of the battery during consecutive hours results in a change in its energy level. This is formulated as shown in (5.4).

$$SOC_h = \begin{cases} SOC^{ini} + E_h - E_h^{next} & \forall h \in \{1\} \\ SOC_{h-1} + E_h - E_h^{next} & \forall h \in \{2, 3..., H\} \end{cases} \tag{5.4}$$

5.3.1.5 Battery Energy Limits

The energy level in the battery should remain within its minimum and maximum limits as shown in (5.5).

$$SOC^{min} \leq SOC_h \leq SOC^{max}; \quad \forall h \in H \tag{5.5}$$

5.3.2 Forward Contract Cost

The costs associated with contracting power from the forward market by an electricity retailer consists of yearly, quarterly and monthly contracts. The total cost incurred by the retailer from forward contracts over a time period can be formulated as in (5.6).

$$C_t^F = (\pi_t^{FY} P_t^{FY}) + (\pi_t^{FQ} P_t^{FQ}) + (\pi_t^{FM} P_t^{FM}); \quad \forall t \in T \tag{5.6}$$

The contract price in the forward market is modeled as a linear function of the amount contracted to consider the fact that there is limited forward contracts accessible to the retailer. This is shown in (5.7)-(5.9). The base price for each of the forward contracts π^{Ybase}, π^{Qbase}, π^{Mbase} is calculated using the estimated average spot price over the delivery period of the contract. The forward price function is assumed to be linear to make the problem simple and limit the order of the objective function to be quadratic in nature.

$$\pi_t^{FY} = \pi_t^{Ybase} + \rho^Y P_t^{FY}; \quad \forall t \in T \tag{5.7}$$
$$\pi_t^{FQ} = \pi_t^{Qbase} + \rho^Q P_t^{FQ}; \quad \forall t \in T \tag{5.8}$$
$$\pi_t^{FM} = \pi_t^{Mbase} + \rho^M P_t^{FM}; \quad \forall t \in T \tag{5.9}$$

The constraints (5.10)-(5.12) maintain the value of power purchased from each of the forward contracts over their delivery periods.

$$P_t^{FY} = PY_y v_{yt}; \quad \forall t \in T, y \in Y \tag{5.10}$$
$$P_t^{FQ} = PQ_q v_{qt}; \quad \forall t \in T, q \in Q \tag{5.11}$$
$$P_t^{FM} = PM_m v_{mt}; \quad \forall t \in T, m \in M \tag{5.12}$$

The constraint formulated in (5.13) denotes the non-negative nature of the power purchased.

$$P_t^{FY}, PY_y, P_t^{FQ}, PQ_q, P_t^{FM}, PM_m \geq 0; \quad \forall t \in T, y \in Y, q \in Q, m \in M \tag{5.13}$$

Decisions made in the forward market include the amount of power to be purchased from each of the base load contracts considering the scenarios associated with the uncertainty in spot prices and customer demand.

5.3.3 Cost of Purchase from Spot Market

In this proposed model, a part or all of the end user demand may be purchased by the retailer from the spot market. The prices in the spot market are uncertain in nature at the time when forward contract decisions are made and are modeled to be stochastic. The equation (5.14) denotes the cost arising from the purchase of energy from the spot market. The constraint (5.15) denoted the non-negative nature of the purchased power.

$$C_t^S(w) = \pi_t^S(w) P_t^S(w); \quad \forall w \in W \tag{5.14}$$
$$P_t^S(w) \geq 0; \quad \forall w \in W \tag{5.15}$$

5.3.4 The Power Balance

It is imperative that there is a balance between the energy bought and sold by the retailer. For every time period, the power balance is given as shown in (5.16):

$$P_t^D(w) = P_t^S(w) + P_t^{FY} + P_t^{FQ} + P_t^{FM}; \quad \forall w \in W \tag{5.16}$$

The retailer supplies the total demand through purchase of power from the spot and forward markets. From the expression (5.16), the total demand of the end users is the sum of conventional and EV demands as shown in (5.17):

$$P_t^D(w) = E_t(w) + E_t^C(w); \quad \forall w \in W \tag{5.17}$$

5.3.5 Revenue of the Retailer

The retailer obtains its revenue by selling electrical energy to end-users through fixed price and variable price contracts as shown in (5.18) and (5.20), respectively. Based on the retailer's estimated cost for a particular level of consumption, the customers are informed of the price for electricity over the lock-in period before they enter into a contract with the retailer. The determination of this price by the retailer can be formulated as,

$$R_t^F(w) = \lambda_t^F(w) P_t^D(w) \nu^F; \quad \forall w \in W \tag{5.18}$$
$$\lambda_t^F(w) = \pi_t^{FY} + \theta^F [\nu^F P_t^D(w) - P^{maxF}]; \quad \forall w \in W \tag{5.19}$$

From (5.18), the retail price for customers with fixed price contract is modeled to be dependent on the end-user demand as shown in (5.19). It is further considered that the retailer provides a "discount" on the pricing to its customers depending on their consumption level. Thus, the higher the consumption of customers, greater is the "discount" offered by the retailer.

In variable price contracts, the retailer charges the customers for their consumption over a period of time, e.g., one month. The pricing for variable price contracts are based on the spot price for electricity volume-weighed over a specified period of time, plus a markup [96] considering other costs incurred by the retailer such as imbalance cost. The determination of this price by the retailer is formulated as,

$$R_t^V(w) = \lambda_t^V(w) P_t^D(w) \nu^V; \quad \forall w \in W \tag{5.20}$$
$$\lambda_t^V(w) = \pi_t^S(w) + \theta^V [\nu^V P_t^D(w) - P^{maxV}]; \quad \forall w \in W \tag{5.21}$$

From (5.20), the retail price for customers with variable price contract is modeled to be dependent on the end-user demand as shown in (5.21). Similar to the case of a fixed price contract, it is further considered that the retailer provides a discount on the pricing to its variable price contract customers depending on their consumption level. Additionally, the discount provided by the retailer to variable price contract customers is assumed to be higher when compared to fixed price contract customers. This stems from the idea that the retailer assumes a higher risk from fixed price contracts as opposed to variable price contracts.

5.3.6 The Retailer's Expected Profit

The expected profit of the retailer is equal to the difference between the revenue expected to be obtained from selling electricity to end-users and the cost of purchasing this electricity from the spot and forward markets. This can be expressed as a risk neutral problem as shown in (5.22).

$$Exp[z] = \sum_{w \in W} prob(w) \sum_{t \in T} [R_t^F(w) + R_t^V(w) - C_t^S(w) - C_t^F] \tag{5.22}$$

Expression (5.22) clearly expresses the problem faced by an electricity retailer. It can be seen that the revenue of the retailer from selling electricity and the cost of buying electricity from the spot market are uncertain and scenario dependent. To alleviate this level of uncertainty, the retailer can purchase part of the electricity from the forward market where the prices are relatively more stable [97].

5.3.7 The Risk Management Constraint

There are numerous methods for measuring risk that have been proposed in literature and have been compared in [98]. The method used in this chapter is $CVaR$ [91], [99]. $CVaR$ for a profit function at a certain confidence level $\alpha \in (0,1)$ is the expected value of profit based on the condition that the profit is less than or equal to VaR. VaR is the highest possible profit value with a probability of $(1-\alpha)$. The advantage of $CVaR$ is that it also accounts for the low profit scenarios that occur past the VaR risk threshold that is selected. For a profit function z, $CVaR$ can be obtained as,

$$prob(z \leq VaR_\alpha) = 1 - \alpha \tag{5.23}$$

$$CVaR_\alpha = Exp[z|z \leq VaR_\alpha] \tag{5.24}$$

For the profit function of the retailer, $CVaR$ calculation at a confidence level α can be translated into solving the following optimization problem [91],

$$Maximize_{\xi,\eta(w)} \;\; CVO = \left(\xi - \frac{1}{1-\alpha}\sum_{w\in W} prob(w) \quad \eta(w)\right) \tag{5.25}$$

Subject to,

$$\xi - \left(\sum_{t\in T} R_t^F(w) + R_t^V(w) - C_t^S(w) - C_t^F\right) \leq \eta(w); \quad \forall w \in W \tag{5.26}$$

$$\eta(w) \geq 0; \quad \forall w \in W \tag{5.27}$$

5.3.8 Objective Function of Retailer Planning Model

The objective function of the retailer considering the $\alpha - CVaR$ risk measure can now be formulated as,

$$\begin{aligned} Maximize \;\; RPO = \beta\Bigg(\sum_{w\in W} prob(w)\Bigg(\sum_{t\in T} R_t^F(w) + R_t^V(w) - C_t^S(w) - C_t^F\Bigg)\Bigg) \\ + (1-\beta)CVO \end{aligned} \tag{5.28}$$

The objective function in (5.28) is subject to the core problem constraints (5.6) through (5.21) and the constraints imposed by the risk measure (5.26)-(5.27). The RP model

described above is a non-linear optimization problem to be solved by the retailer. Optionally, a risk weight factor is introduced to give the electricity retailer consideration over the extreme risks associated with the planning problem. The risk weight factor $0 \leq \beta \leq 1$ allows the retailer to follow a risk neutral plan when $\beta = 1$ or a risk-averse plan when $\beta = 0$.

5.4 Case Study

5.4.1 Description of the Case Study

A case study was performed to illustrate the proposed model using the data from a typical electricity retailer in Sweden. The case study considers that the retailer participates in the Nordpool forward and spot markets.

Three main sets of input data were used in this case study:

1. Spot market prices from NordpoolSpot
2. Electricity demand of the retailer's customers from a specific bidding area
3. Estimated EV demand based on customer statistics and data available for conventional vehicles in the area covered by the retailer.

The system spot price data was obtained from NordpoolSpot [100] for a period of one year available with an hourly resolution and used as the expected value in the model as shown in Figure 5.3. The base prices for yearly, quarterly and monthly forward contracts were subsequently estimated using the average spot price over the maturity periods.

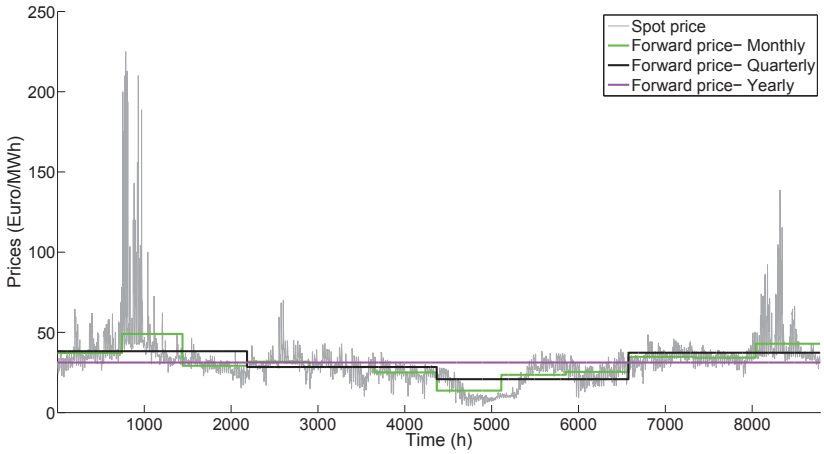

Figure 5.3: Spot market price and corresponding estimated base forward contract prices

The uncertainty associated with spot market prices was then modeled using a set of

scenarios that were generated by adding a random term to the expected spot prices as shown in (5.29). Note that advanced techniques for forecasting model building and scenario generation could be easily used and integrated with the proposed approach.

$$\pi_t^S(w) = Exp[\pi_t^S] + G(\mu, \sigma); \quad \forall w \in W \tag{5.29}$$

The hourly conventional electricity demand of customers of a typical retailer in Sweden was obtained for a period of one year. The conventional demand data obtained corresponds to the same time period as that of the spot prices and was used as the expected demand. This is shown in Figure 5.4. The uncertainty associated with conventional demand was modeled in a manner similar to that of spot prices. A set of scenarios were generated by adding a random term to the expected conventional demand as shown in (5.30).

$$P_t^C(w) = Exp[P_t^C] + G(\mu, \sigma); \quad \forall w \in W \tag{5.30}$$

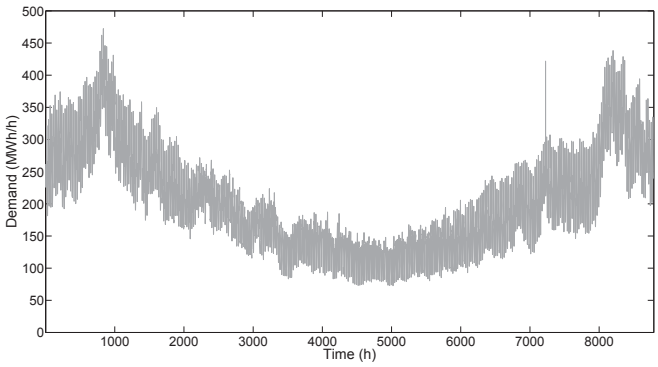

Figure 5.4: Estimated conventional demand of retailer's customers

Some of the EV related data has been derived from existing data on conventional fossil fueled vehicles. The total number of existing household cars has been obtained using statistical data available in [101] for the city of Gothenburg. The penetration level of EVs is then defined as the ratio of number of EVs to the total number of vehicles in the system, expressed in percentage.

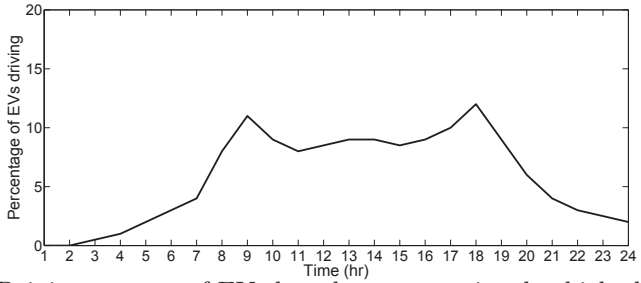

Figure 5.5: Driving pattern of EVs based on conventional vehicle data [62], [87]

The driving pattern of EVs is further derived based on conventional vehicle user pattern as shown in Figure 5.5. It is based on the assumption that human behavior will be independent of the type of vehicle driven. It is also assumed that the driving pattern is the same for all the days in the optimization horizon and the batteries of EVs not driving during any hour are available to the aggregator for scheduling. A 230 V single phase ac supply with a 16 A fuse that provides a maximum connection power of 3.68 kW is considered. This is the most widespread type of supply infrastructure available to the customers in Sweden [88]. The main EV parameter inputs to the EV aggregator model are shown in Table 5.1.

Table 5.1: EV Aggregator Model Input Parameters [62], [87]

Battery Capacity	24 kWh
Energy Consumption	0.192 kWh/km
Distance Travelled	40 km/day
Energy Consumption per Day	7.68 kWh/day
Charging Power	3.68 kWh/h

The value of SOC^{min} was fixed at 20% of battery capacity to allow for a reserve in case the distance traveled needs to be higher than 40 km. Similarly, SOC^{max} was fixed at 85% of battery capacity to account for the changes in aggregated battery capacity limits when a significant number of vehicles are unavailable to the aggregator while traveling.

The parameter values used in the case study are shown in Table 5.2.

Table 5.2: Parameter values used in the case study

α	0.95	θ^F	0.0004 [€/MW^{2}h]
ρ^Y	0.3 [€/MW^{2}h]	θ^V	0.0002 [€/MW^{2}h]
ρ^Q	0.32 [€/MW^{2}h]	P^{maxF}	500 MW
ρ^M	0.34 [€/MW^{2}h]	P^{maxV}	500 MW

The RP model described in Section 5.3 was implemented in General Algebraic Modeling System (GAMS) using MINOS solver [102] that resulted in 298633 constraints, 298651 real variables 1150605 non-zero elements for a case with 10 scenarios.

5.4.2 Results and Discussions

5.4.2.1 Scheduled EV demand

Various levels of EV penetration in the end-user market have been considered in this chapter and are based on studies conducted by [88], where an introduction of 600000 EVs has been estimated. This would result in approximately 13% EV penetration in Sweden. It is reasonable to consider that the penetration level of EVs might differ between regions

and might be higher in cities and lower in smaller towns. Hence, an EV penetration level of 10-30 % has been considered in the case study. The resulting EV demand for an EV penetration level of 10%, over a period of one week for ten scenarios of the spot market price and conventional demand, is shown in Figure 5.6.

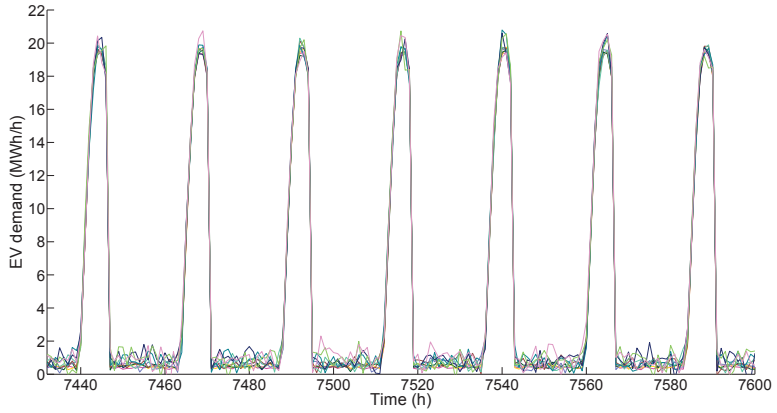

Figure 5.6: Demand scenarios generated by EV aggregator over one week for 10% EV penetration

5.4.2.2 Forward contract decision by retailer

Figure 5.7 depicts the forward contract decisions made by the retailer when it is risk neutral ($\beta = 1$) and risk averse ($\beta = 0.1$). It can be observed that a risk averse retailer would purchase more power from the forward markets when the spot market prices are high.

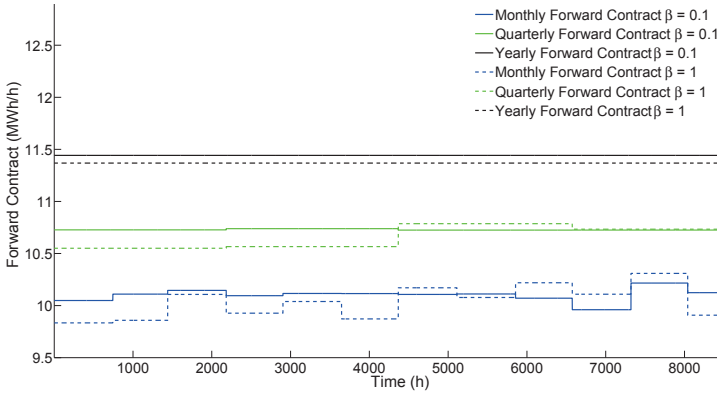

Figure 5.7: Forward contract decisions by the retailer when risk neutral and risk averse

5.4.2.3 Retailer's profit

Figure 5.8 shows the expected profit versus the standard deviation of profit for various levels of fixed price contract chosen by the end users. It can be noted that for the same total demand served, the expected profit of the retailer would increase if the fraction of end-user demand contracting fixed price contracts decreases. The opposite holds true for the corresponding standard deviation. With the increasing penetration of EVs, the standard deviation increases. The spread of standard deviation becomes larger as more customers of the retailer sign up for fixed price contracts at increasing EV penetration levels. This can be anticipated because with fixed price contracts, the retailer completely shields its customers from the price variations in the spot market, thereby incurring additional financial risks.

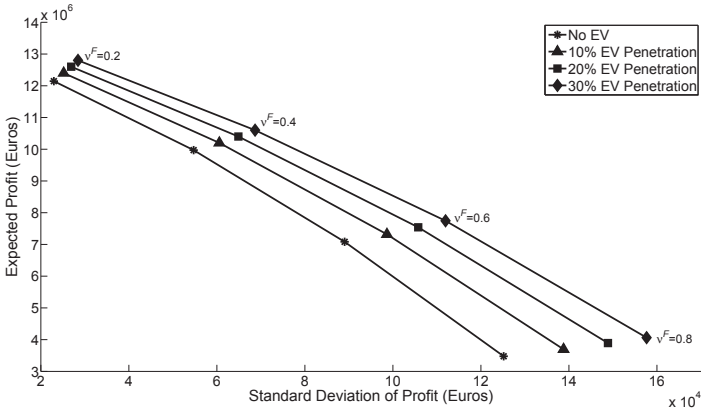

Figure 5.8: Expected profit versus standard deviation

5.4.2.4 Retail contract prices

Figure 5.9 shows the retail price offered by the retailer with increasing ratio of its customers opting for variable price contracts at 10% EV penetration. It can be seen that with increasing ratio of the retailer's customers opting for variable price contracts, the retail price offered by the retailer on fixed price contract increases. This can be accounted for by observing that the discount offered by the retailer on fixed retail contracts is volume weighed over the total contracted power by the fixed retail contract customers as shown in (5.19). In the case of variable price contracts, the retail prices offered are volume weighed based on the individual customer's demand profile.

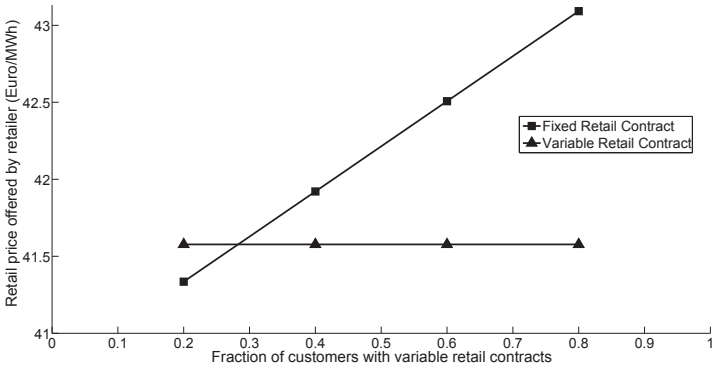

Figure 5.9: Price offered by the retailer with increasing ratio of customers opting for variable retail contracts at 10% EV penetration

5.4.2.5 Savings in charging cost by EV customers

Figure 5.10 shows the total charging cost saving by the EV owners with increasing ratio of the retailer's customers opting for variable price contracts at different levels of EV penetration. The cost savings is calculated as the difference between the costs incurred by EV owners in case they entered a fixed price contract and the costs incurred by them in case they entered into a variable price contract. Considering a pricing structure described in Section 5.3.5, for a lower fraction of customers with variable retail contract, it can be seen that the EV owners would end up paying more by entering into a variable retail contract as opposed to a case when the majority of the retailer's customers have entered into a variable contract. It is interesting to note that this is advantageous to both the retailer and the EV customers because, with variable price contracts, the EV owners would transfer less financial risk to the retailer while attaining additional savings. At the same time, it can be noted that the profits of the retailer would be relatively increased with increasing number of its customers opting for a variable price contract. Additionally, at higher variable price contract ratios, these savings would be increased with increasing levels of EV penetration in the system.

5.5 Summary

A stochastic programming based planning model of an electricity retailer that maximizes its expected profit while considering uncertainty in EV charge scheduling has been proposed in this chapter. The solution from the model yielded the forward contract decisions, retail price setting for customers, and the EV demand scheduling. The price setting for retail contracts was determined by the RP model based on two types of contract signed with the retailer. From the case study, it could be concluded that the total cost savings for EV customers would increase with the EV penetration level and also with increasing number of customers opting for variable price contracts with the retailer as opposed to

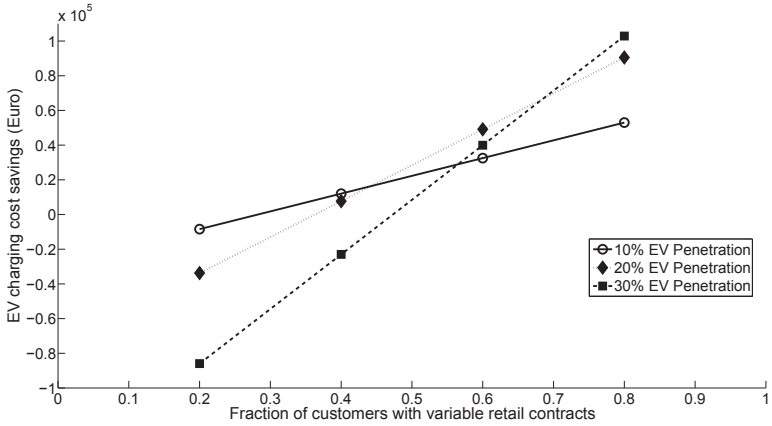

Figure 5.10: EV charging cost savings with increasing variable price contracts

fixed price contracts. This was found to benefit the retailer as its expected profit was found to increase with a greater share of customers opting for variable price contracts. However, it should be mentioned that neglecting power imbalance cost would represent an ideal situation and due to uncertainties involved in customer demand, a more practical approach would necessitate the inclusion of imbalance costs.

So far in the thesis, only the active power aspects have been addressed. This is the component that has monetary value when trading power. The other aspect is that of reactive power, which helps in maintaining voltage levels within power systems. Since, batteries of EVs are interfaced with the distribution system though power electronic converters, they are able to control active and reactive power independently and hence, can also provide voltage control support. The upcoming chapter deals with optimally controlling distributed energy resources, including battery energy storage and solar photovoltaic systems, to control the voltage in distribution networks in a coordinated manner.

Part III

Voltage Control Perspective

Chapter 6

Coordinated Voltage Control with Distributed Energy Resources

This chapter compares traditional local voltage control strategy with coordinated, optimization-based ones in LV distribution systems with photovoltaics and battery energy storage systems. Optimization-based strategies are formulated within a model predictive control (MPC) framework. Three strategies based on MPC offering differing advantages and disadvantages are proposed and implemented, namely, centralized, decentralized and distributed MPC. The formulated strategies for voltage control are compared in a case study using a modified CIGRÉ European 3-area low-voltage network.

6.1 Previous Work

Higher penetration of DGs could bring about new challenges to the DSO when it comes to performing voltage control in such LV active distribution systems since they were traditionally not designed to host local generation [103], [104]. Currently, voltage monitoring at the LV network is not common in distribution systems. This makes the DSO unaware of voltage variation occurring at the customers' side. With large PV penetration, this factor coupled with the variable nature of PV generation based on the time of day, season and cloud effect could pose limitations in effectively regulating LV bus voltages using traditional methods involving tap-changing transformers and capacitors banks at MV substations.

Through grid codes for distribution systems, requirements could be imposed that DGs, such as PV and BESS connecting to distribution system, be able to provide local voltage support [11], [105]. With very high penetration of PVs and the possible increase in

voltage measurements and communication in future distribution systems, coordinating the voltage regulation operation over the entire LV distribution system by utilizing an optimization-based strategy might become a feasible option. This type of coordinated control could be achieved using just one central controller regulating all the devices or through many decentralized controllers, each controlling few devices at a time [12], [15]. An additional possibility is to use communication links to exchange information so that a distributed controller in one area has knowledge on the actions to be taken by other distributed controllers before it could make its own decision. By utilizing MPC [16], the effectiveness of distributed controllers could be enhanced, since prediction of possible future actions is also implicitly obtained. In order to decide on the most suitable control strategy for a distribution system, it is necessary to understand the advantages and disadvantages of utilizing these strategies.

Automating the coordination with the help of optimization-based control strategies could offer a greater advantage because of two main reasons: one, the number of DGs could potentially be extremely large to manually determine and vary the ideal setpoint for each device and two, it would be possible to readily define a new objective, augment the model to include components in the system and hence, additional control variables to the optimization problem.

In [14], local control strategies to regulate active and reactive power output from PVs to increase their hosting capacity into LV distribution system are investigated. Strategies already available commercially along with other advanced LVC techniques yet to be made available commercially for PV connected to LV distribution systems have been compared. The authors in [17] have proposed a central MPC-based controller is used to regulate active and reactive power response from PVs to maintain bus voltages in MV distribution system within acceptable limits. Centralized, decentralized and distributed MPC strategies to regulate active power of a BESS for power market participation have been studied in [20]. However, research work on a distributed MPC-based strategy for voltage control in distribution system and also, its comparison with local, centralized and decentralized control strategies has not been carried out.

In this chapter, mathematical formulation of centralized, decentralized and distributed MPC-based strategies for voltage control in LV power systems have been proposed and their performance have been compared to the traditional local voltage control strategy. Models of PV and BESS active/reactive power controllers have been utilized and time domain simulations have been carried out to observe dynamic responses of the investigated optimization-based controllers to sudden voltage variations in the modified CIGRÉ European LV distribution system. The main highlights of this chapter can be summarized as follows:

- Local voltage control strategy has been compared with coordinated MPC-based optimization strategies for LV distribution systems with BESS and large amounts of PV.
- A novel formulation of coordinated voltage control problem for LV distribution systems based on sequential and iterative cooperative distributed MPC has been proposed and implemented in the case study. Architecturally, in iterative distributed

MPC, the distributed optimizers exchange information simultaneously at every time step and hence, the term *parallel* has been preferred instead of iterative in this chapter and is referred to as P-PDiVC. In case of sequential distributed MPC, individual optimizers exchange information with only their neighboring optimizer in a particular sequence and is henceforth referred to as S-PDiVC.

- A formulation for decentralized MPC strategy called PDVC is formulated wherein the optimizers do not communicate with each other regarding the actions they take.
- The mathematical formulation for PDVC, S-PDiVC and P-PDiVC strategies can be readily derived from the mathematical model of a centralized MPC-based controller called PCVC as will be described in the following sections.
- The optimization-based controllers have been implemented using MATLAB and the time domain simulation has been performed with the help of DIgSILENT Powerfactory, which are both commonly available simulation platforms. Hence, DSOs and researchers can readily adopt the proposed MPC controllers within their simulation framework without significant effort.

6.2 Local Voltage Control (LVC)

Multi-loop PI controllers are most commonly used for local control at the equipment level. For full power converters, there is typically an inner PI current control loop and an outer PI control loop where active and reactive power or voltage at PCC can be regulated as shown in Figure 6.1 and Figure 6.2 for BESS and PV, respectively. Their control structure is described more in detail below.

6.2.1 BESS Local Control Structure

The battery is assumed to be interfaced with the network through a full power converter. With this converter, it is possible to independently control both the active and reactive power output from the battery. The overall structure is henceforth referred to as BESS in this chapter and its model adapted from [106] is shown in Figure 6.1. The active power P_{meas} and reactive power Q_{meas} output from the BESS are controlled independently by controlling the (d, q) axes current references to the full power converter, i^*_{dref} and i^*_{qref}, respectively. i^*_{dref} is obtained from the charge/discharge control block that controls the charging and discharging of the battery based on the present value of its state-of-charge SOC and the current reference signal from the active power control block i_{pref}. At any point in time, i^*_{qref} can receive signals from either the LVC block or the reactive power control block of the BESS. And at any time, either the optimization-based control block including active and reactive power control block or the LVC alone can be operational. Additionally, the active and reactive power control blocks receive auxiliary signals P_b and Q_b from the optimization-based controller which could be based on either the PCVC, PDVC, S-PDiVC or P-PDiVC strategy that vary the set-point based on an objective that

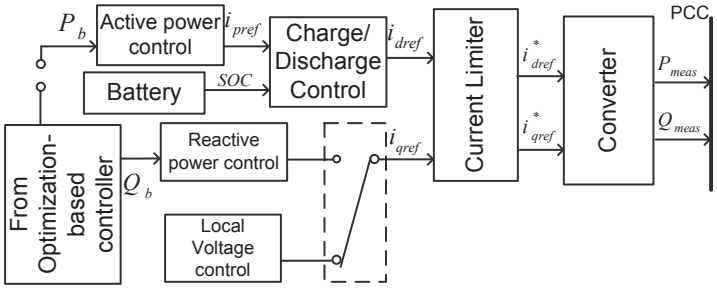

Figure 6.1: BESS local controllers for dynamic studies [106]

effectively coordinates the bus voltages across the network. Both i^*_{dref} and i^*_{qref} signals are limited values to ensure that the total current output does not exceed the rated value of the converter. It should be noted that the state-of-charge and hence, the energy within the battery, is limited to its maximum and minimum values at all times k. This can be ensured using (6.1).

$$SOC^{min} \leq SOC(k) \leq SOC^{max} \tag{6.1}$$

The LVC block consists of a PI controller that maintains the voltage at the PCC of BESS. A voltage deadband between is implemented which means that the PI controller will be active only if the PCC voltage deviates from beyond the deadband. The value of this deadband corresponds to the acceptable voltage values defined for MPC-based controllers that will be described in Section 6.4.2.

6.2.2 PV Local Control Structure

The PV local controller model is similar to that of BESS shown previously without the battery model and the charge/discharge control. This is shown in Figure 6.2. The PV

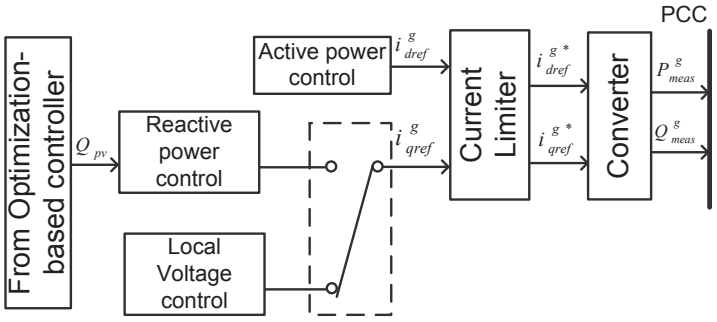

Figure 6.2: PV local controllers for dynamic studies

model also consists of a LVC block which is only operational when the optimization-based

control block and reactive power control block are inactive. The LVC block for PV has the same characteristics as that of the BESS model and maintains the PV's PCC voltage between $[0.975, 1.025]$ p.u.

6.3 Coordinated Voltage Control using MPC

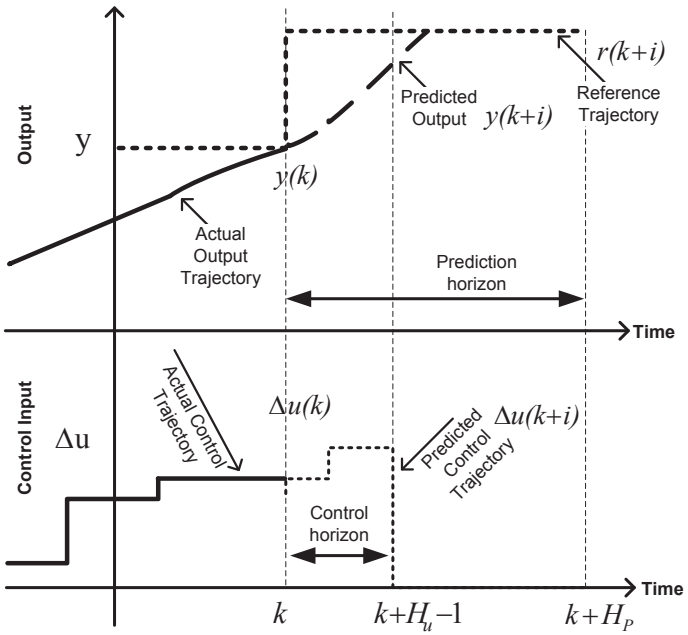

Figure 6.3: Basic idea of MPC

The basic idea of MPC is to find a sequence of control actions over the control horizon H_u considering the response of the system to these actions over the prediction horizon H_p based on a certain objective function [16]. MPC could be further explained with the help of Figure 6.3. At any time instant k, the controller determines the predicted control trajectory using the latest available measurements over the next $k + H_u - 1$ time steps in order to meet the required target trajectory $\mathbf{r}(k)$ for the output $\mathbf{y}(k)$ by time $k + H_p$. However, the predictive control utilizes the receding horizon idea. This means that only the first control action $\Delta\mathbf{u}(k)$ determined by the controller at time k is applied. Then the controller's internal clock is updated to time $k + 1$ with new sets of measurements to reflect the updated states based on the previous control action $\Delta\mathbf{u}(k)$ taken. The steps to determine the optimal control action and state updates are then repeated for time

$k+1$ in a manner similar to that described for time instant k. It should be noted that H_p should be chosen such that it is able to account for the control actions taken over H_u time steps. Hence, the length of the prediction horizon should be greater than or equal to the length of the control horizon, i.e., $H_p \geq H_u$.

In this thesis, state-space model of the system is considered to be linear, time-invariant and the objective function is quadratic in nature. It is also important to note that the constraints are considered to be linear. This way, a linear quadratic optimization problem with a convex nature is obtained.

6.3.1 Predictive Centralized Voltage Control (PCVC)

The PCVC consists of a single optimizer that handles a central model of the whole system consisting of all the monitored bus voltage measurement feedback and control variables available with the objective function being the objective function of the whole system. This architecture is shown in Figure 6.4.

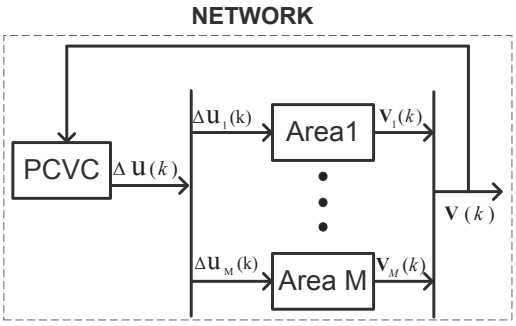

Figure 6.4: PCVC architecture

Given the voltage measurement and control inputs at time k (henceforth indicated using $|k$), the main objective of the PCVC optimizer is to minimize the control actions $\mathbf{\Delta u}(k+i|k)$ taken over the control horizon, $i \in [0, H_u - 1]$. The change in setpoint $\mathbf{u}(k) = \mathbf{u}(k-1) + \mathbf{\Delta u}(k)$ is then sent by the PCVC optimizer to the local controller at every time instant k. The overall optimization problem of PCVC with an objective function Φ can be expressed in its standard quadratic form as shown in (6.2). The objective function is subjected to the constraints (6.3)-(6.7).

$$\Phi = min \sum_{i=0}^{H_u-1} ||\mathbf{\Delta u}(k+i|k)||^2_{\mathbf{R}} + \sum_{i=1}^{H_p} \rho\epsilon(k+i|k) \tag{6.2}$$

Subject to,

$$\mathbf{V}(k+i+1|k) = \mathbf{V}(k+i|k) + \frac{\partial \mathbf{V}}{\partial \mathbf{u}} \Delta \mathbf{u}(k+i|k) \tag{6.3}$$

$$\mathbf{V}(k+i|k) \geq \mathbf{V}^{min}(k+i) - \epsilon_1(k+i|k)\mathbf{1} \tag{6.4}$$

$$\mathbf{V}(k+i|k) \leq \mathbf{V}^{max}(k+i) + \epsilon_2(k+i|k)\mathbf{1} \tag{6.5}$$

$$\mathbf{u}^{min}(k+i|k) \leq \mathbf{u}(k+i|k) \leq \mathbf{u}^{max}(k+i|k) \tag{6.6}$$

$$\Delta \mathbf{u}^{min} \leq \Delta \mathbf{u}(k+i|k) \leq \Delta \mathbf{u}^{max} \tag{6.7}$$

6.3.1.1 Constraint Relaxation

The PCVC should also account for situations where the optimization problem becomes infeasible. This is done with the help of a non-negative scalar slack variable $\epsilon(k+i|k)$ that is penalized with a user-defined, non-negative scalar parameter ρ [16].

6.3.1.2 Bus Voltage Evolution

The evolution of bus voltages is predicted using the information available at time k. It is assumed within the formulation that we have complete state information from voltage measurements at time instant k. The evolution of bus voltages over the prediction horizon H_p is predicted based on a linearized state-space model of the power system that can be obtained by linearizing the power flow equations around the operating point. We get an updated value of the voltage vector $\mathbf{V}(k+i+1)$ as a function of its previous value $\mathbf{V}(k+i)$, the sensitivity gains $\frac{\partial \mathbf{V}}{\partial \mathbf{u}}$ and the active and reactive power changes as shown by (6.3).

6.3.1.3 Limits on State and Control Variables

The objective function (6.2) is subject to constraints on the bus voltages that need to be kept within the minimum $\mathbf{V}^{min}(k+i)$ and maximum $\mathbf{V}^{max}(k+i)$ limits as shown in (6.4) and (6.5), respectively,where $\mathbf{1}$ is vector with each element equal to 1. This constraint is softened with the help of slack variables $\epsilon = [\epsilon_1^T, \epsilon_2^T]^T$ that are penalized with a large scalar parameter ρ in the objective function. The objective function is also subject to maximum and minimum limits that are applied on the control inputs and changes in control inputs as shown in (6.6) and (6.7), respectively.

6.3.1.4 Selection of Control Variables

The control variables are chosen to be a combination of all the vectors of active and reactive power set-points ($\mathbf{P_b}, \mathbf{Q_b}$) of BESS and vector of reactive power set-points of all PVs ($\mathbf{Q_{pv}}$) in the network. Correspondingly, the changes in control variables at any time

instant k can be denoted as a single column vector $\Delta\mathbf{u}$:

$$\Delta\mathbf{u} = \left[\Delta\mathbf{P_b}^T, \Delta\mathbf{Q_b}^T, \Delta\mathbf{Q_{pv}}^T\right]^T \tag{6.8}$$

6.3.1.5 Dynamic Constraints on Control Variables

The maximum and minimum limits vary dynamically according to (6.6). For all the local controllers of PV and BESS, it is considered that the priority is assigned to active power control loop. This means that PV and BESS active powers are allowed to vary according to the availability of solar power and needs of the battery owner, respectively. Based on the active power output at any time, limits for reactive power are calculated. For a PV, maximum Q_{pv}^{max} and minimum Q_{pv}^{min} reactive power limit at time $k+1$ are calculated based on the active power output $P_{meas}^{g}(k)$ of the PV at time k and the MVA rating of its converter S_{conv} as given by (6.9) and (6.10), respectively.

$$Q_{pv}^{max}(k+1|k) = +\sqrt{S_{conv}^2 - (P_{meas}^{g}(k))^2} \tag{6.9}$$

$$Q_{pv}^{min}(k+1|k) = -\sqrt{S_{conv}^2 - (P_{meas}^{g}(k))^2} \tag{6.10}$$

A similar procedure is used to obtain the reactive power limits for the BESS.

6.3.1.6 PCVC Algorithm

A PCVC designed for a distribution network utilizes the following algorithm:

1. At time k, the PCVC receives the measurements of all the monitored bus voltages $\mathbf{V}$ in the network.
2. PCVC calculates its optimal control variables trajectory and sends the first value $\mathbf{u}(k)$ to the local controllers.
3. At next time step $k+1$, go to Step 1 and repeat.

6.3.2 Predictive Decentralized Voltage Control (PDVC)

PDVC strategy consists of as many optimizers as there are subsystems/areas in the distribution system under consideration. If there are $\mathbf{M}$ areas then there would be one PDVC optimizer for each area $j = [1, 2, ..., M]$. This has the advantage of faster and relatively more independent calculations by the optimizers. Communication within an area exists between the control devices and the optimizer in that area. However, as there is no communication between optimizers, each of them are not aware of the decisions taken by the other optimizers. This could result in more reactive power use in certain area than required, especially when there is significant interaction between areas. An overview of PDVC architecture is shown in Figure 6.5.

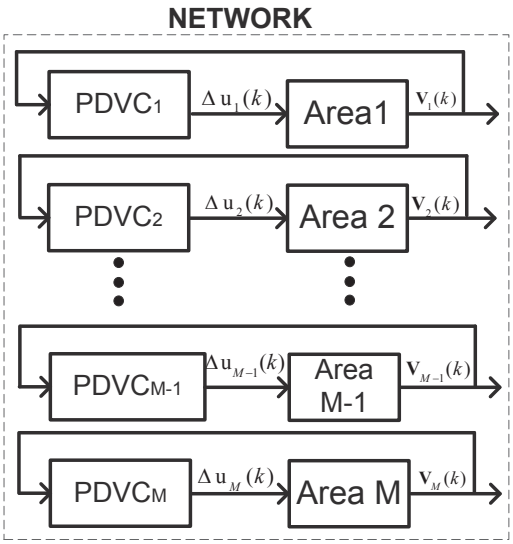

Figure 6.5: PDVC architecture

The objective function of PDVC optimizer in area j is the individual objective function for the area Φ_j consisting of monitored bus voltages ($\mathbf{V}_j$), control variables ($\mathbf{u}_j$) and change in control variables ($\Delta\mathbf{u}_j$) belonging to that area alone. Hence, the design of PDVC ignores all the interactions that could happen between control variables in one area with states in other areas. The mathematical model for the PDVC can be obtained from model of PCVC for every area $j = [1, 2, ..., M]$ in the complete distribution network under consideration by grouping the equations (6.2)-(6.7) based on area and ignoring all the equations denoting the interaction between the areas. The equations (6.2)-(6.7) can be modified for every area j and equivalent set of equations for a PDVC optimizer can be obtained. The objective function Φ_j of each PDVC optimizer can be expressed as in (6.11),

$$\Phi_j = min \sum_{i=0}^{H_u-1} ||\Delta\mathbf{u}_j(k+i|k)||^2_{\mathbf{R}_j} + \sum_{i=1}^{H_p} \rho\epsilon_j(k+i|k) \tag{6.11}$$

and is subject to constraints on monitored bus voltages denoted by (6.12)-(6.13) and constraints on control variables (6.14)-(6.15).

$$\mathbf{V}_j(k+i|k) \geq \mathbf{V}_j^{min}(k+i) - \epsilon_{1j}(k+i|k)\mathbf{1} \tag{6.12}$$
$$\mathbf{V}_j(k+i|k) \leq \mathbf{V}_j^{max}(k+i) + \epsilon_{2j}(k+i|k)\mathbf{1} \tag{6.13}$$
$$\mathbf{u}_j^{min}(k+i|k) \leq \mathbf{u}_j(k+i|k) \leq \mathbf{u}_j^{max}(k+i|k) \tag{6.14}$$
$$\Delta\mathbf{u}_j^{min} \leq \Delta\mathbf{u}_j(k+i|k) \leq \Delta\mathbf{u}_j^{max} \tag{6.15}$$

The evolution of voltage vector for area j over time can be expressed using (6.16).

$$\mathbf{V}_j(k+i+1|k) = \mathbf{V}_j(k+i|k) + \frac{\partial \mathbf{V}_j}{\partial \mathbf{u}_j}\Delta \mathbf{u}_j(k+i|k) \tag{6.16}$$

The control variables of PDVC optimizer consists of all the (P, Q) of BESS and Q of PV in area $j \in [1, M]$ as shown in (6.17).

$$\Delta \mathbf{u}_j = \left[\Delta \mathbf{P_b}_j^T, \Delta \mathbf{Q_b}_j^T, \Delta \mathbf{Q_{pv}}_j^T\right]^T \tag{6.17}$$

In short, for $j = 1$ to M, every PDVC j utilizes the following algorithm:

1. At time k, the PDVC j receives the measurements of all the monitored bus voltages $\mathbf{V}_j$ in that area alone.
2. PDVC j calculates the optimal control variables trajectory for all the devices in area j and sends the first value $\mathbf{u}_j(k)$ to the local controllers.
3. At next time step $k+1$, go to Step 1 and repeat.

6.3.3 Sequential Predictive Distributed Voltage Controller (S-PDiVC)

In this section, a method known as sequential cooperative distributed MPC [19] is adapted to the coordinated voltage control problem in distribution systems. It is henceforth referred to as S-PDiVC. The overall architecture of this control strategy is shown in Figure 6.6.

Similar to PDVC, S-PDiVC, in general, consists of as many optimizers as there are subsystems/areas in the network and an optimizer in an area is communicating with control devices in that area. However, it also has similarities to PCVC:

- All the S-PDiVC optimizers get voltage measurements from all the monitored buses at every optimization time step k
- There is communication between optimizers- each of the S-PDiVC optimizer gets the trajectory of optimal input of all the other S-PDiVC optimizers from the previous or current time step depending on the position of the concerned S-PDiVC controller in the sequence $j = [1, 2, ..., M]$
- S-PDiVC$_1$ communicates only with its nearest neighbor, S-PDiVC$_2$. S-PDiVC$_2$ only with S-PDiVC$_3$ and so on. However, as seen in Figure 6.6, S-PDiVC$_{M-1}$ not only communicates its own trajectory with S-PDiVC$_M$ but the optimal input trajectories of all S-PDiVC before it in the sequence.

The mathematical model for the S-PDiVC can, in general, also be obtained from model of PCVC [18]. For the application of the strategy for voltage control in LV distribution systems, the formulation proposed below is used for a S-PDiVC controller in every area

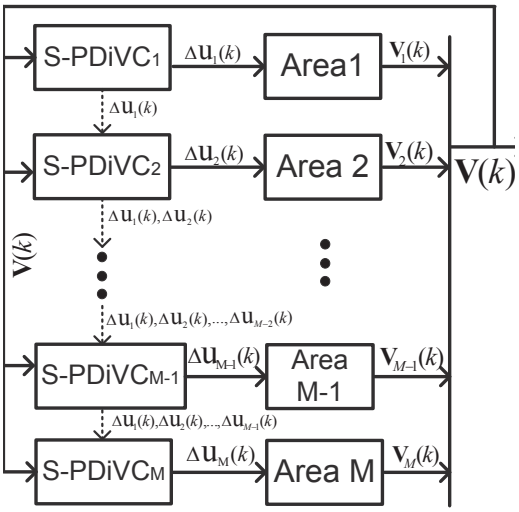

Figure 6.6: S-PDiVC architecture

$j \in [1, M]$ in the complete distribution network under consideration. The equations (6.2)-(6.7) can be modified for every area j and equivalent set of equations for S-PDiVC can be obtained. The objective function Φ_j of each S-PDiVC is a copy of the global objective function in PCVC and can be expressed as in (6.18),

$$\Phi_j = min \sum_{i=0}^{H_u-1} ||\Delta \mathbf{u}_j(k+i|k)||^2_{\tau_\mathbf{j}\mathbf{R}_j} + \sum_{i=1}^{H_p} \rho\epsilon(k+i|k) \tag{6.18}$$

Subjected to,

$$\mathbf{V}(k+i|k) \geq \mathbf{V}^{min}(k+i) - \epsilon_1(k+i|k)\mathbf{1} \tag{6.19}$$

$$\mathbf{V}(k+i|k) \leq \mathbf{V}^{max}(k+i) + \epsilon_2(k+i|k)\mathbf{1} \tag{6.20}$$

$$\mathbf{u}_j^{min}(k+i|k) \leq \mathbf{u}_j(k+i|k) \leq \mathbf{u}_j^{max}(k+i|k) \tag{6.21}$$

$$\Delta\mathbf{u}_j^{min} \leq \Delta\mathbf{u}_j(k+i|k) \leq \Delta\mathbf{u}_j^{max} \tag{6.22}$$

$$\Delta\mathbf{u}_j = \left[\Delta{\mathbf{P}_\mathbf{b}}_j^T, \Delta{\mathbf{Q}_\mathbf{b}}_j^T, \Delta{\mathbf{Q}_\mathbf{pv}}_j^T\right]^T \tag{6.23}$$

$$\begin{aligned}\mathbf{V}(k+i+1|k) = \mathbf{V}(k+i|k) &+ \frac{\partial\mathbf{V}}{\partial\mathbf{u}_j}\Delta\mathbf{u}_j(k+i|k) \\ &+ \sum_{l=1,l\neq j}^{j-1} \frac{\partial\mathbf{V}}{\partial\mathbf{u}_l}\Delta\mathbf{u}_l(k+i|k) \\ &+ \sum_{l=j+1,l\neq j}^{M} \frac{\partial\mathbf{V}}{\partial\mathbf{u}_l}\Delta\mathbf{u}_l(k+i|k-1)\end{aligned} \tag{6.24}$$

Similar to $\mathbf{R_j}$ which represents a vector of relative weights on control variable change of control devices within an area j, $\tau = [\tau_1, ...\tau_j, ...\tau_M]$ is a vector denoting the relative weights between all the S-PDiVC present in the distribution system under consideration. The objective function in (6.25) is subject to the constraints on monitored bus voltages (6.19)-(6.20) and on control variables (6.21)-(6.22). The control variables of S-PDiVC in area j is selected as in (6.23) and the evolution of voltage vector over time can be expressed using (6.24) for every $j = 1, 2, ..., M$.

It is to be noted that for all $l \neq j$ the value of $\mathbf{u}_l$ is given as an input to the S-PDiVC in area j and this is done sequentially as expressed in (6.30). In short, S-PDiVC utilizes the following steps:

1. At time k all the M S-PDiVC receive the measurements of all the monitored bus voltages $\mathbf{V}$ in the network.
2. For $j = 1$ to M
   (a) S-PDiVC j receives the value of control variable trajectories $\forall l = [j+1, ..., M], l \neq j$ of $\Delta\mathbf{u}_l(k+i)$ calculated at time step $k-1$.
   (b) S-PDiVC j also receives the control variable trajectories $\forall l = [1, ..., j-1], l \neq j, i = [0, ..., H_u - 1]$ of $\Delta\mathbf{u}_l(k+i)$ calculated at time step k.
   (c) S-PDiVC j calculates its optimal control variables trajectory and sends the first value $\mathbf{u}_j(k)$ to the local controllers. The calculated trajectory $\mathbf{u}_j(k+i), \forall i = [0, ..., H_u - 1]$ is sent to S-PDiVC $j+1$ and the above Steps (a) and (b) are repeated for all $j \in M$.
3. At next time step $k+1$, go to Step 1 and repeat.

6.3.4 Parallel Predictive Distributed Voltage Controller (P-PDiVC)

In this section, a method known as iterative cooperative distributed MPC is adapted to the voltage control problem in distribution systems. It is henceforth referred to as P-PDiVC. It retains an architecture similar to PDVC, i.e., P-PDiVC in general consists of as many optimizers as there are subsystems/areas in the network. This has the advantage of faster and relatively independent calculations by the optimizers but require more complex communication infrastructure. An overview of P-PDiVC architecture is shown in Figure 6.7.

It also has similarities to PCVC as described by the following points:

- The objective function for P-PDiVC is part of the objective function of the PCVC.
- All the P-PDiVC optimizers get voltage measurements from all the monitored buses at every optimization time step k.

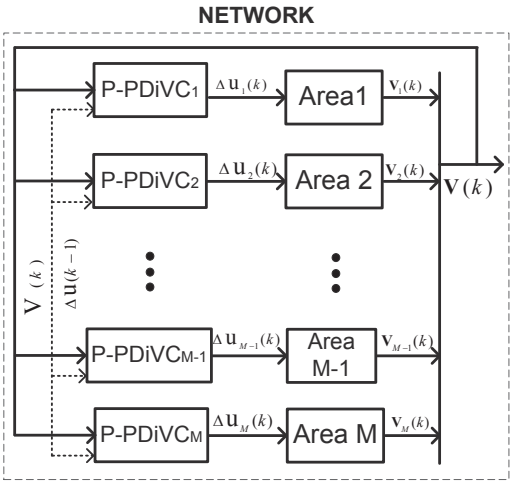

Figure 6.7: P-PDiVC architecture

- There is communication between optimizers- unlike S-PDiVC, all the P-PDiVC optimizers get the trajectory of optimal input of *all* the other P-PDiVC optimizers from the previous time step.

The mathematical model for the P-PDiVC can also be obtained from model of PCVC [18]. For the application of this strategy to voltage control in LV distribution systems, the formulation proposed below for a P-PDiVC controller in every area $j \in [1, M]$ in the complete distribution network under consideration is used. The equations (6.2)-(6.7) can be modified for every area j and equivalent set of equations for P-PDiVC can be obtained similar to that described for PDVC. The objective function Φ_j of each P-PDiVC is a copy of the global objective function in PCVC and can be expressed as in (6.25),

$$\Phi_j = min \sum_{i=0}^{H_u-1} ||\Delta \mathbf{u}_j(k+i|k)||^2_{\tau_\mathbf{j}\mathbf{R}_j} + \sum_{i=1}^{H_p} \rho\epsilon(k+i|k) \tag{6.25}$$

The objective function in (6.25) is subject to the constraints on monitored bus voltages (6.26)-(6.27) and on control variables (6.28)-(6.29).

$$\mathbf{V}(k+i|k) \geq \mathbf{V}^{min}(k+i) - \epsilon_1(k+i|k)\mathbf{1} \tag{6.26}$$
$$\mathbf{V}(k+i|k) \leq \mathbf{V}^{max}(k+i) + \epsilon_2(k+i|k)\mathbf{1} \tag{6.27}$$
$$\mathbf{u}_j^{min}(k+i|k) \leq \mathbf{u}_j(k+i|k) \leq \mathbf{u}_j^{max}(k+i|k) \tag{6.28}$$
$$\Delta\mathbf{u}_j^{min} \leq \Delta\mathbf{u}_j(k+i|k) \leq \Delta\mathbf{u}_j^{max} \tag{6.29}$$

The control variables of P-PDiVC, similar to PDVC, consist of all the (P, Q) of BESS and Q of PV in area j as shown in (6.17). The evolution of voltage vector over time can

be expressed using (6.30) for every $j = 1, 2, ...M$.

$$\mathbf{V}(k+i+1|k) = \mathbf{V}(k+i|k) + \frac{\partial \mathbf{V}}{\partial \mathbf{u}_j}\Delta \mathbf{u}_j(k+i|k) + \sum_{l=1, l\neq j}^{M} \frac{\partial \mathbf{V}}{\partial \mathbf{u}_l}\Delta \mathbf{u}_l(k+i|k-1) \quad (6.30)$$

It is to be noted that $\forall l \neq j$ the value of $\mathbf{u}_l$ is given as input to the P-PDiVC in area j and this is done simultaneously as expressed in (6.30). Also, the optimizer in area j has a model of the interactions occurring due to changes in $\mathbf{u}_l$ with the help of the sensitivity term $\frac{\partial \mathbf{V}}{\partial \mathbf{u}_l}$. In short, P-PDiVC utilizes the following steps:

1. At time k all the M P-PDiVC receive the measurements of all the monitored bus voltages $\mathbf{V}$ in the network.
2. For $j = 1$ to M
   (a) P-PDiVC j receives the value of control variable trajectories $\forall l = [1, ..., M], l \neq j$ of $\Delta \mathbf{u}_l(k+i)$ calculated at time step $k-1$.
   (b) P-PDiVC j calculates its optimal control variables trajectory and sends the first value $\mathbf{u}_j(k)$ to the local controllers. The calculated trajectory $\mathbf{u}_j(k+i), \forall i = [0, ..., H_u - 1]$ is sent to all other P-PDiVC optimizers $l \in [1, M], l \neq j$ and the above Steps (a) and (b) are repeated for all $j \in [1, M]$.
3. At next time step $k+1$, go to Step 1 and repeat.

A termination criterion described in [18] where the optimization problem is solved only for a pre-defined number of iterations could also be utilized if the processing delay is critical for performance.

6.4 Test System and Simulation Setup

This section describes the modified CIGRÉ European LV network [107] that has been used for the study and corresponding setup for simulations.

6.4.1 Test System

A single line diagram of the modified CIGRÉ European LV network is shown in Figure 6.8. The network is connected to the external grid with 10 MVA short circuit capacity. The network consists of three areas- residential, industrial and commercial, the buses of whom are denoted using letters R, I and C, respectively. Each area is connected to the external grid through a 20/0.4 kV, 125 kVA transformer. All the BESS and PV in the network are assumed to be interfaced with the grid through a full power converter with a rating of 25 kVA. The PV panels are located at buses R_{15b}, R_{16}, R_{17}, C_{12}, C_{14}, C_{17} and C_{19}, while the BESS are located at buses R_{6a} and I_2. Converters of the devices are assumed to be available to all the optimizers for voltage control. Also, a constant power

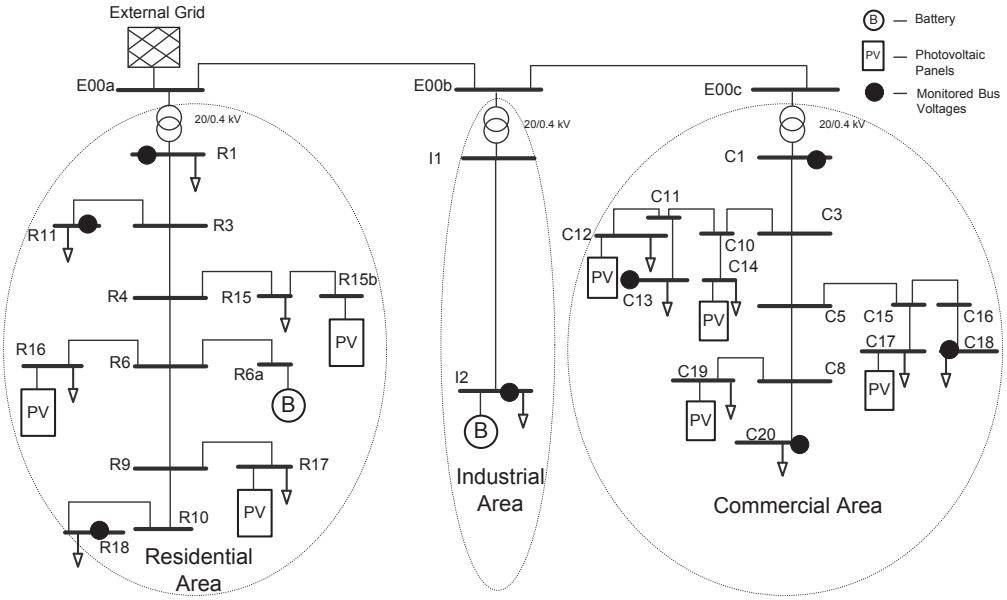

Figure 6.8: Modified CIGRÉ European LV Network

model was utilized for the loads in order to capture the true response from the various controllers. All the PVs are supplying 77% of the total active power requirements of the loads in the network.

6.4.2 Simulation Setup

6.4.2.1 Voltage Measurements

It is considered that voltage measurements are available to MPC from the monitored buses R_1, R_{11}, R_{18} in residential area, I_2 in industrial area and C_1, C_{13}, C_{18}, C_{20} in commercial area of the system as shown in Figure 6.8. Additionally, it is considered that the active and reactive power outputs from BESS and PV are also measured. With coordinated control, it is expected that the DSO would want to maintain stricter voltage limits than the typical bound values used today, which lie in the range $[0.9, 1.06]$. Hence, the acceptable voltage values for all monitored buses are assumed to lie within the range i.e., $[V^{min}, V^{max}] = [0.975, 1.025]$, but can also be chosen according to other desired values.

6.4.2.2 Communication Setup

The local controllers are considered to have a faster response time compared to the PCVC, PDVC and P-PDiVC. In order to not react too quickly, the optimization-based controllers are configured to send a control signal to the PV and BESS every 10s after an initial delay of 30s. The controllers do not react immediately (but still react ahead of MV transformer tap changes with typical settings between 45-120 s) after being activated with the 30s initial delay while the 10s time resolution for the control signal ensures that sufficient time delay is accounted for due to measurement collection, predictive controller calculations and control signal communication.

6.4.2.3 MPC Controller Settings

The sensitivity gains in (6.3) were calculated as described in the self-publication [108] based on a static power flow solution of the network for loading conditions given in the CIGRÉ reference document. Constant gain values were used because the loading condition did not vary significantly in the whole system over the simulation period and hence, the gains were observed to be relatively constant. Furthermore, it is expected that the MPC-based controllers would handle the errors in sensitivity gains as it continuously obtains voltage measurement feedback from the system. It is also to be noted that limitations on changes in control inputs were imposed. The active power and reactive powers from PV and BESS were limited to change at subsequent time steps by up to 50%, 80% and 40% of their individual capacities in residential, industrial and commercial area, respectively. This was chosen randomly to demonstrate that the constraints on changes in control variables are being observed by the optimization-based controllers while simultaneously showing clarity within the resulting plots. For all the simulations, the prediction horizon of the controller was set at $H_p = 6$ and the control horizon was set to $H_u = 6$. This means that the predictive voltage controller is able to foresee the effects of changes in control variables 6 steps ahead in time, or in absolute time, 60 seconds ahead. Finally,the weight on slack variable ρ in (6.2), (6.11) and (6.25) is chosen to be equal to 10^6, a significantly large number when compared to the values in $\mathbf{R}$ and/or $\mathbf{R_j}$ that are assumed to be equal for all j. τ_j in (6.25) is also assumed to be equal to 1 for all control areas $j \in M$, which would mean that there is no specific preference to utilize more/less reactive power from a particular area.

6.5 Results and Discussions

Simulations were performed using the above described test system. The active power profile for all the PVs in the test system is assumed to be the same. It was obtained from measurements done by us at one of the PVs at Chalmers University of Technology and was scaled accordingly for use with the CIGRÉ test system. The profile essentially represents a scenario where the active power output from PV decreases due to the cloud coverage between 50s-70s and thereafter, remains at its lower output value. Consequently, this also

results in bus voltage drops across the network due to the relatively large penetration of PVs in the test system. Subsequently, there occurs at fault upstream of the LV network at 75s that results in a uniformly large drop in bus voltages. The resulting response using LVC, PCVC, PDVC, S-PDiVC and P-PDiVC strategies is shown below.

6.5.1 LVC Strategy Results

The results from simulations using LVC is shown in this section. In Figure 6.9, the active and reactive power output of all the PVs and BESS is plotted. The sequence of events described above can be readily seen. From 50s, the cloud cover appears due to which there is a drop in active power output of all PVs (denoted by $P_{pv_{all}}$). Correspondingly, all three areas experience a drop in voltages as seen in Figure 6.10-6.12. As expected,

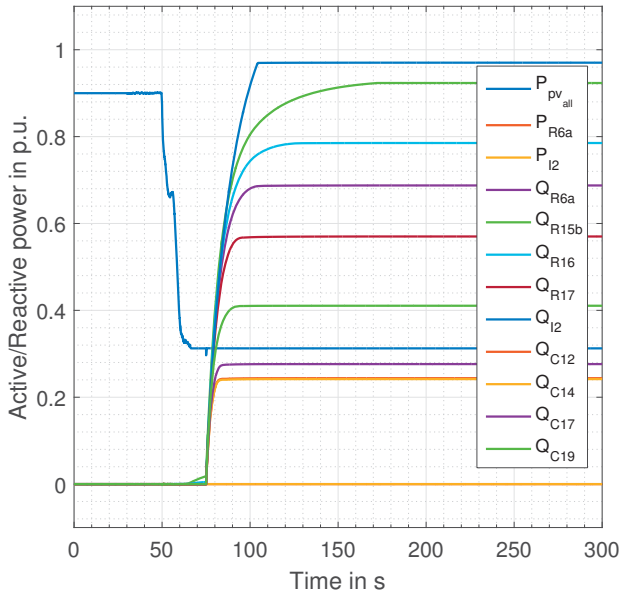

Figure 6.9: LVC- Active and reactive power output of all control devices in the network

the drop is larger in areas that have a higher penetration of PVs, i.e., residential and commercial. At time 75s, the external event occurs upstream of the LV network that results in a sudden drop in voltages across all three areas.

Figure 6.10 shows the voltages across the monitored, PV and BESS buses in the area. Due to the external event, the voltages at PCC of PVs and BESS drop below the acceptable limit of 0.975 p.u. This results in all the PVs and BESS regulating their reactive power output in order to bring the voltages back above the limit. All the control device succeed in achieving this goal. However, the inherent limitation of LVC can also be observed, which is the failure to regulate buses at which no PV or BESS is connected- in this case, bus R_{11}.

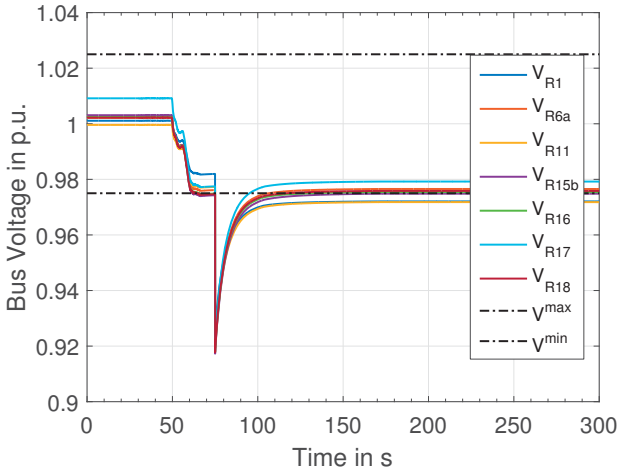

Figure 6.10: LVC- Bus voltages in the residential area

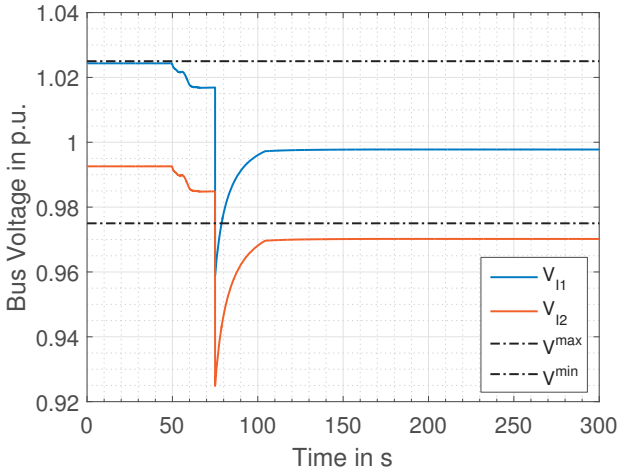

Figure 6.11: LVC- Bus voltages in the industrial area

The voltages changes in the industrial area can be seen in Figure 6.11. From the plot, it can be easily deduced that there is insufficient reactive power reserves in the area to bring the bus I_2 voltage within the acceptable voltage bound.

Figure 6.12 shows the voltage plots for the commercial area. The PVs successfully bring their PCC voltages within the acceptable limits. However, the uncontrolled nature of non-PV and non-BESS buses is more pronounced in this case. Hence, it could be concluded that LVC has two main drawbacks- one, uncontrolled non-PV and non-BESS bus voltages and two, the drawback to not have the control possibility to import reactive power from other areas in case of insufficient reserves within an area.

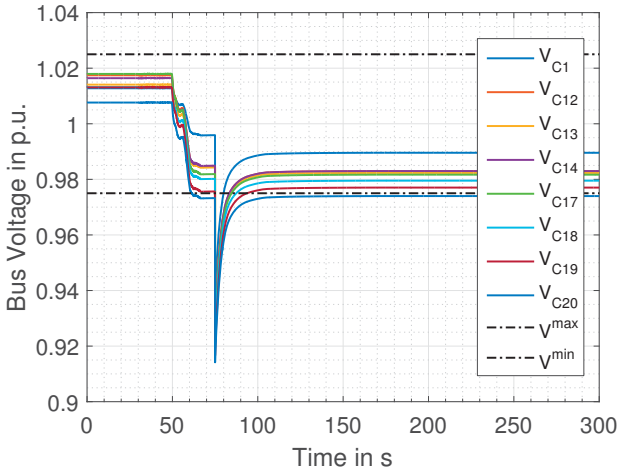

Figure 6.12: LVC- Bus voltages in the commercial area

6.5.2 PDVC Results

As seen with LVC, the some buses are not directly controlled. This could be resolved by placing an optimizer in each area and coordinating the response from all PV and BESS to regulate voltages at selected monitored buses, which, at the discretion of a DSO could be either PV, BESS or other load buses. This is the fundamental idea of PDVC. There is one PDVC for each area that regulates monitored bus voltages in that area using control devices in that area alone. The results using PDVC optimizers is shown below starting with Figure 6.13 that depicts the active and reactive power outputs of all the control devices in the three areas. After the occurrence of the external event at 75s, the PDVC optimizers receive bus voltage measurements 5s later and the optimizers send the necessary set-point changes to the individual PV and BESS local controllers. The change is subsequently reflected in the power outputs of BESS and PV.

The corresponding impact on bus voltages in the residential area is shown in Figure 6.14. In this case, all monitored buses are brought within the acceptable voltage bound.

The bus voltages in the industrial area are shown in Figure 6.15. It can be seen that bus I_2 is brought to the same voltage level when compared to the case with LVC. This can be attributed to the lack of sufficient reactive reserves in the area to compensate for the overall drop in bus voltage. Ultimately, the PDVC also suffers from the same drawback as LVC when it comes to running out of reactive reserves in that area and not being able to import from other area due to the non-interacting nature of the controllers.

Figure 6.16 shows the bus voltages in the commercial area. Compared to LVC, it can be seen that the non-generator bus voltages are successfully brought within the voltage bound in this case. However, observing more carefully, it can be seen that the optimizers are bringing the voltages in the commercial area to a higher than necessary value of 0.975 p.u. The main reason could be attributed to the existing interactions between changes in

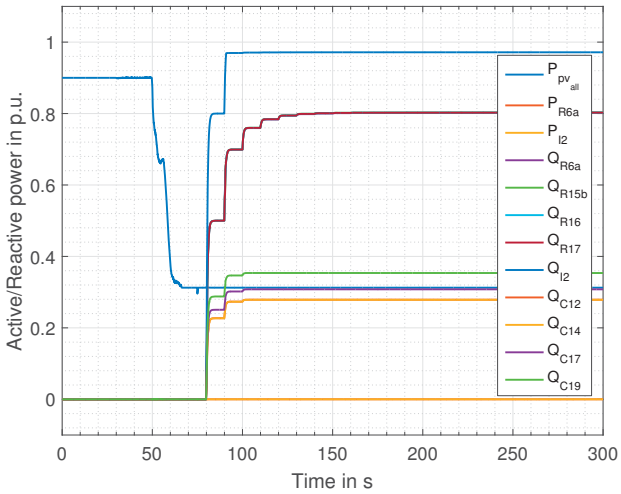

Figure 6.13: PDVC- Active power output of all control devices in the network

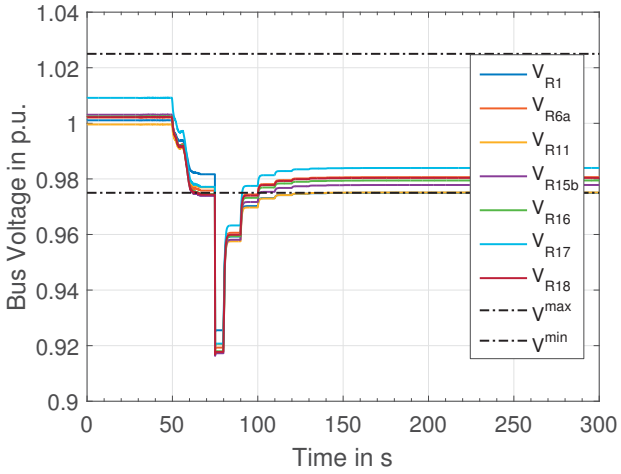

Figure 6.14: PDVC- Bus voltages in the residential area

control variable in one area to bus voltages in another area and blindness of the optimizers to see the effect of these interactions. In other words, reactive power change from PVs in commercial area have an effect on bus voltages in residential area but take a decision without accounting for this fact and vice-versa.

6.5.3 PCVC Results

In the previous section, it was observed that PDVC is able to regulate all the monitored buses voltages but faces the same issues as LVC when the reserves within an area for

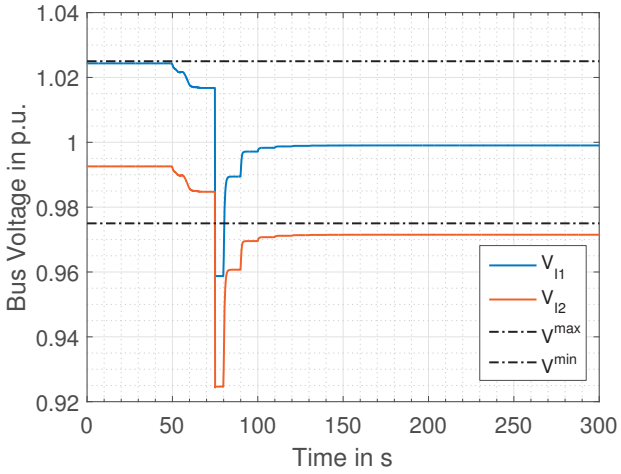

Figure 6.15: PDVC- Bus voltages in the industrial area

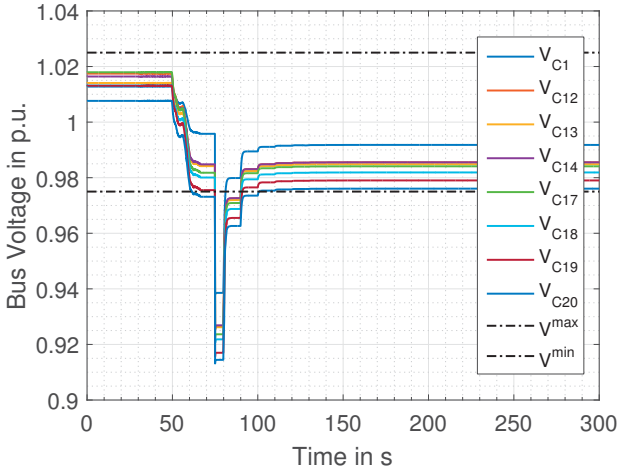

Figure 6.16: PDVC- Bus voltages in the commercial area

regulation are insufficient. This can be overcome with the help of PCVC strategy. The active/reactive power outputs of all the PVs can be seen in Figure 6.17. It can be seen that the amount of reactive reserves utilized in all three areas in this case is higher than the PDVC case. This is because the PCVC optimizer tries to bring bus I_2 within the voltage bound and utilizes additional reserves from residential and commercial areas to achieve this.

The bus voltages in the residential area is shown in Figure 6.18 and it can be observed that they are brought to a slightly higher voltage level than the lowest bound value of 0.975 p.u. due to the extra compensation required to regulate the bus voltage at I_2. This can be seen in Figure 6.19.

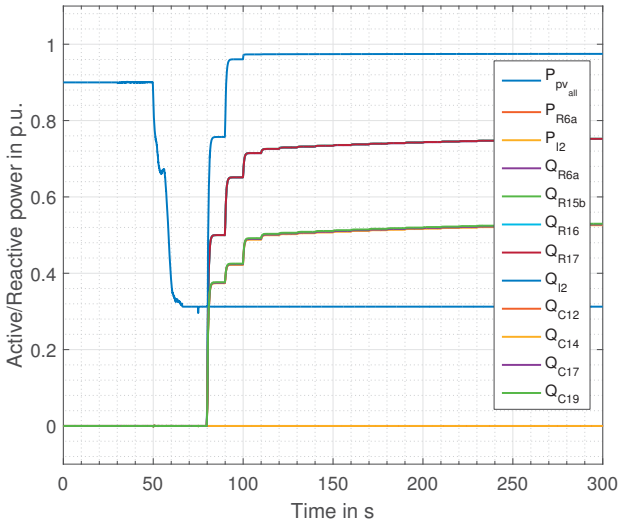

Figure 6.17: PCVC- Active and reactive power output of all control devices in the network

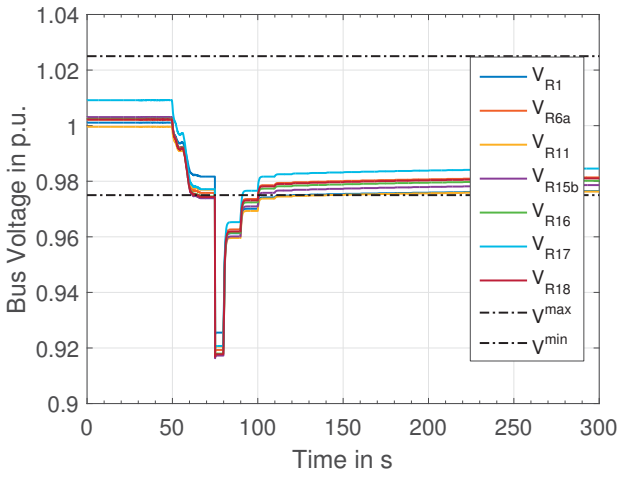

Figure 6.18: PCVC- Bus voltages in the residential area

Bus voltages in the commercial area is depicted in Figure 6.19 and as expected, all the bus voltages in this area also are brought to a level higher than necessary due to the extra reactive support needed for the industrial area.

6.5.4 S-PDiVC Results

The active/reactive power output with S-PDiVC is shown in Figure 6.21. S-PDiVC utilizes more reactive power than the PCVC case. Furthermore, the utilization of reactive

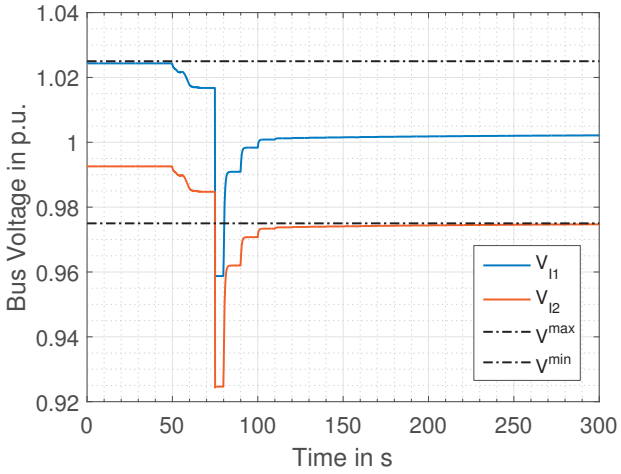

Figure 6.19: PCVC- Bus voltages in the industrial area

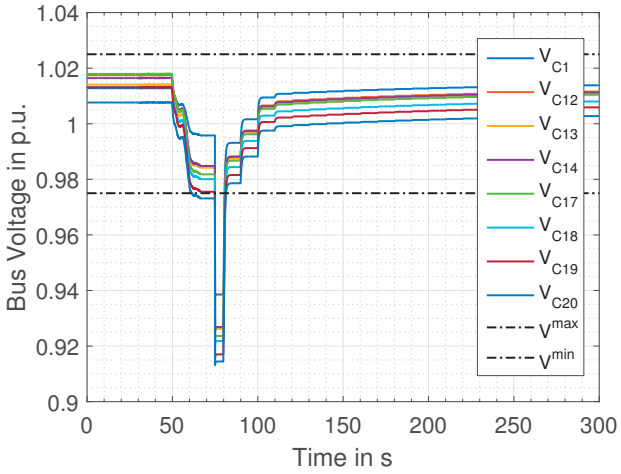

Figure 6.20: PCVC- Bus voltages in the commercial area

reserves differs between areas with more being utilized in the residential area by S-PDiVC optimizer. This also results in a difference in active power losses as will be seen in Section 6.5.6.

The bus voltages in the residential area are shown in Figure 6.22 and are at a slightly higher level because of the overcompensation compared to PCVC case. The effect over the industrial area bus voltage can be seen in Figure 6.23 which shows that bus I_2 voltage is just within the defined bounds. Finally, the commercial area bus voltages shown in Figure 6.24 settle at a slightly lower value compared to PCVC due to the lower reserves utilized from this area.

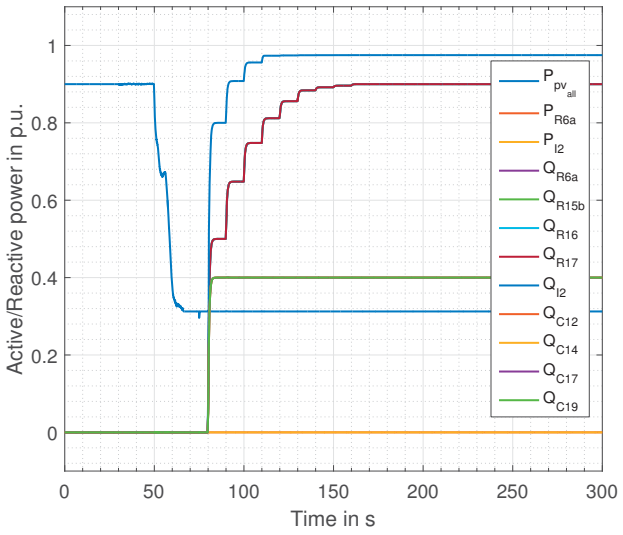

Figure 6.21: S-PDiVC- Active and reactive power output of all control devices in the network

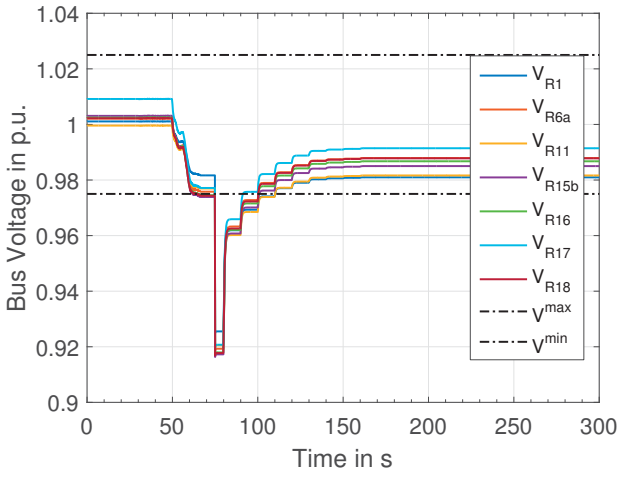

Figure 6.22: S-PDiVC- Bus voltages in the residential area

6.5.5 P-PDiVC Results

The biggest obstacle with PCVC is the complexity in practical implementation and loss of reliability with optimizer or communication channel malfunction. To maintain the architectural advantage of PDVC and the consideration of interaction models in PCVC, a compromise is made in the form of P-PDiVC strategy as detailed in Section 6.3.4. The resulting plots below try to compare the performance of P-PDiVC with PCVC, since the

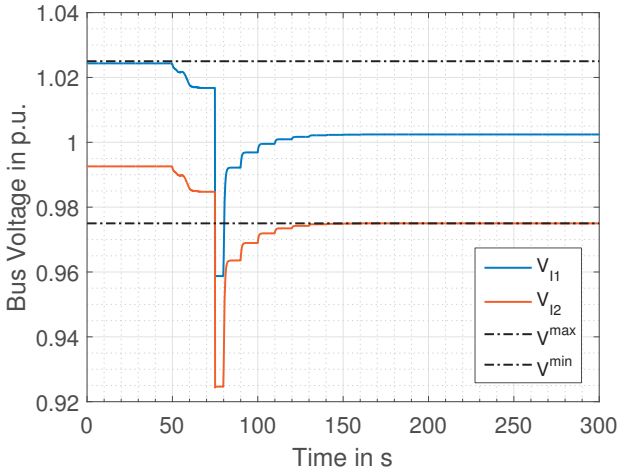

Figure 6.23: S-PDiVC- Bus voltages in the industrial area

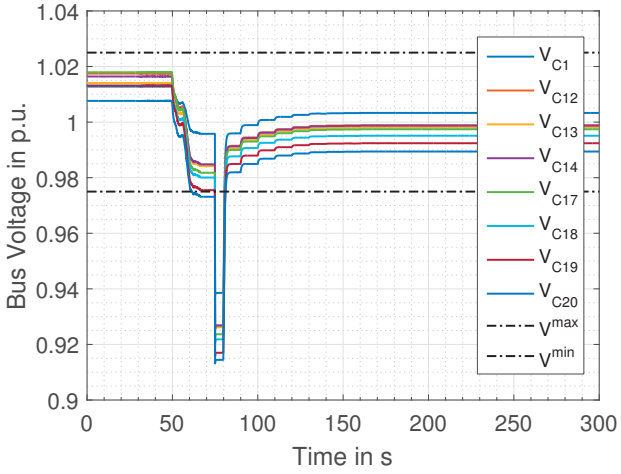

Figure 6.24: S-PDiVC- Bus voltages in the commercial area

latter gives a desired system-wide optimal response. The active/reactive power output with P-PDiVC is shown in Figure 6.25. P-PDiVC gives an overall response similar to PCVC but on closer inspection it can be seen that the total reactive power utilized is slightly higher than the PCVC case. All the devices in residential area output the same amount of reactive power in their final state. This is due to the fact that the relative weights on control changes $\mathbf{R_j}$ is kept the same for all j. Hence, the reserves are equally distributed between the devices in the commercial area as well.

The voltages in the residential area is shown in Figure 6.26 and are at a slightly higher level because of the suboptimal overcompensation compared to PCVC. It can be seen in Figure 6.27 that P-PDiVC optimizers take just enough control action to bring bus I_2

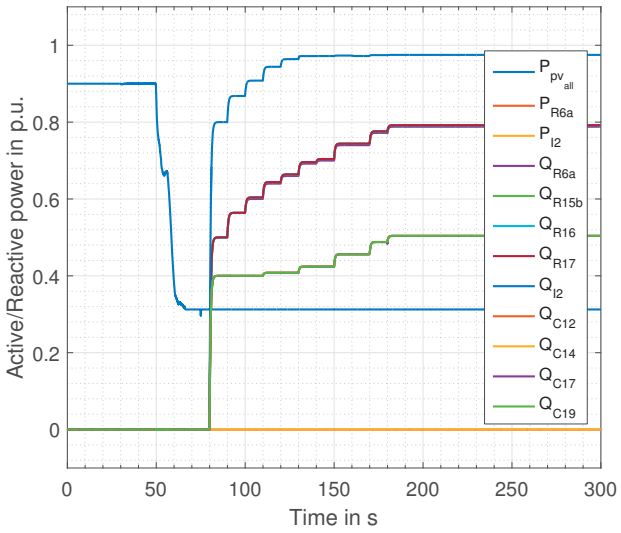

Figure 6.25: P-PDiVC- Active and reactive power output of all control devices in the network

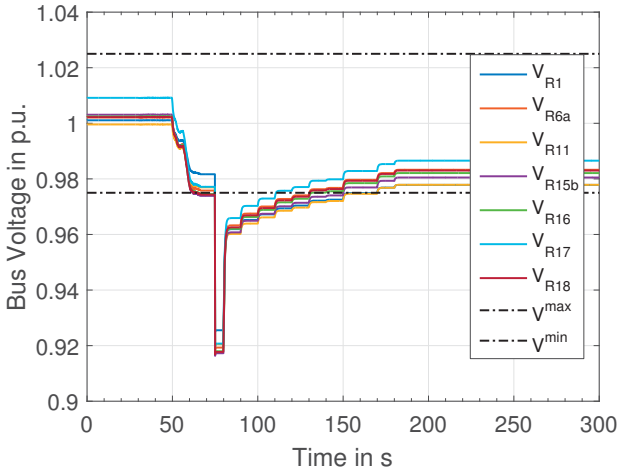

Figure 6.26: P-PDiVC- Bus voltages in the residential area

voltage within the bounds.

The commercial area bus voltages shown in Figure 6.28 settles at a lower value compared to PCVC due to the overcompensating solution by the optimizer at residential area.

Finally, it can also be seen that the voltages in this case with P-PDiVC optimizers settle to their final values after the external disturbance slower than PCVC. This could be because

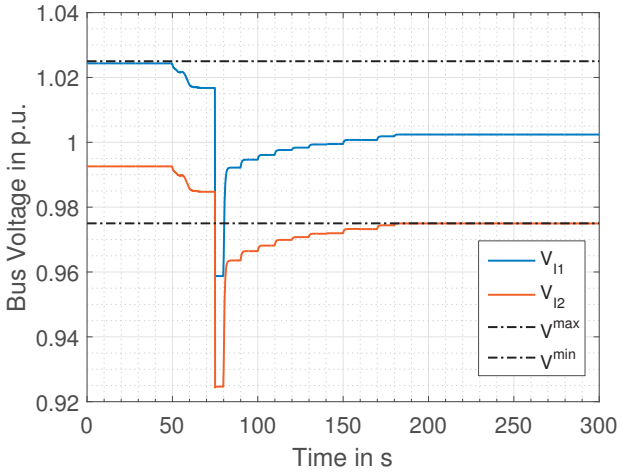

Figure 6.27: P-PDiVC- Bus voltages in the industrial area

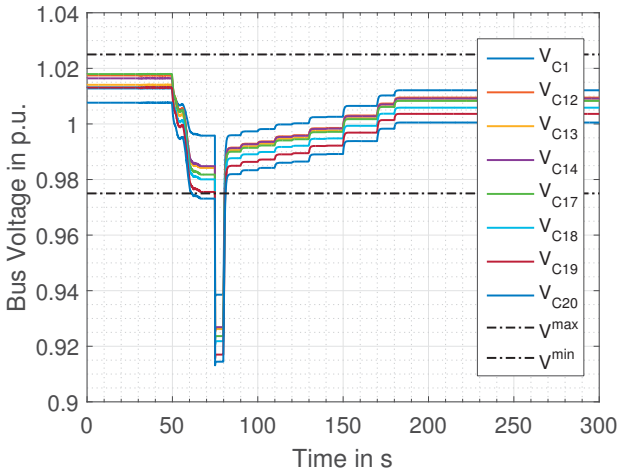

Figure 6.28: P-PDiVC- Bus voltages in the commercial area

the P-PDiVC optimizers receive the decision of other optimizer only in the subsequent time step and take longer to correct the corresponding errors.

6.5.6 Result comparison of all strategies

LVC and the three MPC strategies have also been compared based on the total reactive power utilized for voltage support after the external event Q_{total}, the percentage change in active power losses at the final simulation state when compared to the initial state (ΔP_{loss}) and the average time it takes for processing the solution with optimization-based

control strategies at every time step. The comparison is shown in Table 6.1.

Table 6.1: Comparison of control strategies

Control Strategy	Q_{total} (p.u)	$\Delta P_{loss}(\%)$	$T_{sim}(s)$
No Control	0.000	+12.4	-
LVC	0.840	-4.7	-
PDVC	0.870	-2.1	0.055
PCVC	1.000	-1.9	0.060
S-PDiVC	1.014	+2.5	0.135
P-PDiVC	1.013	-0.8	0.140

The following observations could be made from the results:

- As can be seen, LVC utilizes 16% less reactive power when compared to 1 p.u (153kVAr) using PCVC, the least amount in order to just regulate the PCC voltage. PDVC utilizes slightly more reactive power that LVC but still 13% lower when compared to PCVC in order to bring not just the PCC bus voltage (the bus to which the PV and BESS is connected to in the distribution system), but also the monitored buses within the voltage bounds. However, for the industrial area, the insufficient reactive power reserves limits its usage. In comparison, PCVC manages to also bring the industrial area bus I_2 voltage within bounds by utilizing additional reactive power from residential and commercial areas. P-PDiVC and S-PDiVC perform similar to PCVC, the difference being that they utilize 1.3% and 1.4% more reactive power reserves than PCVC, respectively.

- Comparing the change in total system active power loss, it can be seen that having no voltage control in the network results in an overall increase by 12.4% as more active and hence, reactive power needs to be imported from the external grid. However, some form of voltage control within the network greatly reduces the losses. LVC performs the best by only regulating the generator PCC voltages resulting in 4.7% lower losses when compared to 1.9% by PCVC and 0.8% by P-PDiVC in the final state that compensate for limited reactive resources in the industrial area by utilizing more reserves from the residential and commercial areas. Loss reduction is slightly lower with P-PDiVC as it over-compensates by utilizing more reactive reserves from the residential area than necessary, thus resulting in increased losses over the transformer in that area. S-PDiVC brings the system to a final state where the overall losses have increased by 2.5% when compared to the initial state. The main difference lies in where the reactive power compensation is coming from. In S-PDiVC, there is more reactive power compensation from residential area when compared to P-PDiVC case, which seems to utilize more reactive power from the commercial area. The latter provides a better output because the losses over the transformer in the residential area is higher than over the transformer in the commercial area.

- Looking at the average processing times, PCVC and PDVC solve the problem at approximately the same time. P-PDiVC is much slower compared to PDVC and PCVC due to the exchange in information required by each optimizer. P-PDiVC is also slower than S-PDiVC by almost 5ms as information that needs to be exchanged between all the optimizers at every time step. However, it should be noted that the size of the system simulated is comparatively small. With a much larger distribution system, greater number of areas and more control variables, the solution time for PCVC would increase considerably [16].

6.5.7 Discussions

It must be mentioned that should an optimization-based controller fail, the fall-back are local controllers. However, P-PDiVC, S-PDiVC and PDVC offer a significant practical advantage as the chances of multiple optimizers failing are much lower and can be compensated for relatively easily than a single optimizer failure in the case of PCVC.

Finally, looking at the results, it could be clearly seen that optimization-based control strategies utilize the available resources more efficiently to meet a defined criteria. Through such comparison studies, DSO has to make a decision on the worth of using one strategy over another, e.g., utilizing 1.013 p.u reactive reserves with P-PDiVC compared to 0.84 p.u with LVC in order to maintain strict voltage levels across the network. Furthermore, the DSO also has to decide on how the control architecture in their distribution system would look like in the future. Would they prefer to retrofit cables and tune multi-loop PI controllers to regulate voltages in the network when more PVs are integrated or invest in efficient, automated, optimization-based control over the next few years by regularly investigating renewable integration trajectory within their system? In short, DSOs would need to make informed decisions through extensive studies and compare various strategies for their distribution systems as demonstrated in this chapter.

6.6 Summary

This chapter compared LVC with coordinating, optimization-based strategies for distribution systems hosting large amounts of PV and BESS. It should be noted that the investigated strategies were carried out under the main assumption that there is communication and monitoring infrastructure available in the future distribution systems in the smart grid era. The formulated strategies for voltage control were compared with the help of a case study using a modified CIGRÉ European 3-area LV network. It could be concluded that all of the optimization-based strategies perform better than the LVC strategy in terms of achieving the objective, which is to bring all the monitored bus voltages within bounds. Among the MPC-based strategies, PCVC provided the optimal results but utilized relatively higher reactive power from the control devices when compared to PDVC in order to achieve the objective of also controlling the non-PV and non-BESS bus voltages. The latter performed well so long as the reactive power reserves

within an area are sufficient but faced drawbacks similar to that of LVC strategy when the reactive reserves within an area were insufficient. P-PDiVC strategy was found to provide results comparable to the optimal PCVC while also providing an architectural advantage of PDVC. S-PDiVC performed slightly worse than P-PDiVC in terms of change in total active power loss. Based on the studies performed, it would be recommended to use P-PDiVC strategy for coordinated voltage control within distribution systems with large number of renewable-based generation.

After developing a theoretical model of the MPC controller, the next step is to test whether this controller functions according to its design criterion within a real distribution system. The next chapter addresses this challenge by thoroughly outlining the steps involved in design-to-implementation of an MPC-based controller for a voltage source converter used to control a remote bus voltage. Furthermore, it also details the experience and lessons learned from the field tests performed using the MPC controller.

Chapter 7

Field Test Using Model Predictive Voltage Controller

This chapter documents the experience from field test performed to verify the functioning of a model predictive control-based voltage controller in distribution systems. A voltage controller was formulated and implemented within the model predictive control framework. The objective of the controller is to maintain the remote bus voltage within a pre-defined bound while respecting the reactive power output constraints from the voltage source converter with the least amount of reference value changes given to the local reactive power controller. The field test was carried out in Gothenburg, Sweden at a location where an 8 MVA voltage source converter can inject or absorb up to 4 MVAr reactive power. This changes the voltage magnitude of a remote bus located within the same distribution system.

7.1 Background

Due to the various advantages that it offers, MPC is becoming popular and is being applied to many facets of power system control. The authors in [109] propose an MPC controller for load-frequency control in a meshed network. In [110], the authors have applied MPC to control transformer tap changers, capacitor banks and load shedding in order to maintain system bus voltages in transmission networks during emergency conditions. In [17], an MPC-based central voltage controller is developed that coordinates the response of transformer tap control and PVs in a medium voltage distribution network, while the authors in [108] have developed a controller to coordinate the response of BESS and transformer tap control within a low voltage distribution network. All of these

controllers have been tested within a simulation environment. There is a real need to understand how these MPC controllers perform on the field, in real-time. This chapter attempts to address that need to understand the practical challenges faced when utilizing optimization-based control algorithms such as MPC in distribution system to control bus voltages.

In this chapter, development to field test implementation of an MPC-based voltage controller for distribution systems is described in detail. Field tests were performed using the developed MPC voltage controller for a single-input-single-output system due to limitations in the available practical resources. The output of the system under consideration is the monitored remote bus voltage while its input is the reactive power output from a voltage source converter (VSC). Wireless communication was used to feed back the measured voltage values close to the physical location of the MPC controller, which then calculates the optimal setpoint change to the local reactive power controller of the VSC in order to maintain the remote bus voltage within pre-defined limits. The optimization-based control is performed in real-time and corresponding results obtained are presented in this chapter.

The main contribution from this work are as follows:

- A mathematical model for implementing an MPC controller for voltage control has been developed.
- The process of realizing the controller model for field test has been described in detail.
- Field tests using the developed controller have been performed to control a remote bus voltage by optimally regulating the setpoint to the local reactive power controller of a VSC.

7.2 MPC Voltage Controller Design

MPC is used to find a sequence of control actions over the control horizon H_u considering the response of the system model to these actions over the prediction horizon H_p based on a certain objective function and corresponding constraints [111]. At any time instant k, the controller uses the latest available remote bus voltage measurements to calculate the reactive power output sequence over the next H_u time steps in order to bring the bus voltage within acceptable limits over the prediction horizon $k + H_p$. However, the predictive control utilizes the receding horizon idea. This means that only the first control action $\Delta u(k)$ determined by the controller at time k is actually sent to the local reactive power controller. Then the MPC controller's internal clock is updated to time $k + 1$ with new sets of measurements to reflect the updated states based on the previous control action $\Delta u(k)$ taken. The steps to determine the optimal control sequence and state updates are then repeated for time instant $k + 1$ in a manner similar to that described for time instant k.

For designing the predictive voltage controller, a discretized state-space linear model of the power system is used. Remote bus voltage is considered as the state and reactive power output change from the VSC is the input in the model. This model indicates how $V(k)$, the given voltage at the remote bus at time k (henceforth denoted as $|k$) evolves to $V(k+1)$ at time $k+1$ with changes in $\Delta u(k)$, the reactive power output from the VSC at time k depending on $\frac{\partial V}{\partial u}$, the sensitivity gain that could be obtained either from power flow solution or by performing on-site step-response tests. This discrete model could be expressed using (7.1).

$$V(k+1) = V(k) + \frac{\partial V}{\partial u}\Delta u(k) \tag{7.1}$$

The above discrete model could then be used to predict the evolution of states over the next H_p time steps given that the reactive power change occurs over the next H_u time steps. This could be expressed using (7.2).

$$\begin{bmatrix} V(k+1|k) \\ V(k+2|k) \\ \vdots \\ V(K+H_p|k) \end{bmatrix} = V(k) + \frac{\partial \mathbf{V}}{\partial \mathbf{u}} \begin{bmatrix} \Delta u(k|k) \\ \Delta u(k+1|k) \\ \vdots \\ \Delta u(k+H_u-1|k) \end{bmatrix} \tag{7.2}$$

The H_pxH_u matrix $\frac{\partial \mathbf{V}}{\partial \mathbf{u}}$ describes how the voltages at the remote bus is affected at various time steps depending on the control action taken during previous time steps as shown in (7.3).

$$\frac{\partial \mathbf{V}}{\partial \mathbf{u}} = \begin{bmatrix} \frac{\partial V}{\partial u} & 0 & 0 & \dots & 0 \\ \frac{\partial V}{\partial u} & \frac{\partial V}{\partial u} & 0 & \dots & 0 \\ \frac{\partial V}{\partial u} & \frac{\partial V}{\partial u} & \frac{\partial V}{\partial u} & \dots & 0 \\ \vdots & \vdots & \vdots & \ddots & \vdots \\ \frac{\partial V}{\partial u} & \frac{\partial V}{\partial u} & \frac{\partial V}{\partial u} & \dots & \frac{\partial V}{\partial u} \\ \frac{\partial V}{\partial u} & \frac{\partial V}{\partial u} & \frac{\partial V}{\partial u} & \dots & \frac{\partial V}{\partial u} \\ \vdots & \vdots & \vdots & \vdots & \vdots \\ \frac{\partial V}{\partial u} & \frac{\partial V}{\partial u} & \frac{\partial V}{\partial u} & \dots & \frac{\partial V}{\partial u} \end{bmatrix} \tag{7.3}$$

Since, the mathematical model is that of a single-input-single-output system, the matrix $\frac{\partial \mathbf{V}}{\partial \mathbf{u}}$ consists of only one sensitivity gain value as its non-zero elements. After obtaining the prediction model shown in (7.2), the MPC problem can be formulated using a quadratic objective function (7.4) Φ, which requires that the control problem be solved with the least amount of changes in reactive power based on $V(k)$, the voltage measurement available at time k.

$$\Phi = \min_{\Delta u} \sum_{i=0}^{H_u-1} \Delta u(k+i|k)^2 \tag{7.4}$$

The objective function Φ in (7.4) is subject to minimum and maximum limits on the reactive power output from the VSC as well as the changes in reactive power output as shown in (7.5) and (7.6), respectively for all values of $i \in [0, H_u - 1]$.

$$u^{min} \leq u(k+i|k) \leq u^{max} \tag{7.5}$$

$$\Delta u^{min} \leq \Delta u(k+i|k) \leq \Delta u^{max} \tag{7.6}$$

The objective function (7.4) is also subjected to constraints on the remote bus voltage as shown in (7.7), whose magnitude needs to be maintained within the defined minimum and maximum limits of V^{min} and V^{max}, respectively for all values of $i \in [1, H_p]$.

$$V^{min} \leq V(k+i|k) \leq V^{max} \tag{7.7}$$

Now, there could be situations when the limits on reactive power has been reached and the optimization problem becomes infeasible. In such situations, it should be ensured that the MPC controller is able provide the best possible solution, albeit constraints on bus voltage magnitude is violated. To achieve this, a linear penalty on the maximum of the possible bus voltage constraint violations (∞-norm) has been imposed with the help of non-negative scalar slack variables $\epsilon_1(k+i|k)$ and $\epsilon_2(k+i|k)$ that are penalized with a user-defined, non-negative scalar parameter ρ [16]. Hence, the objective function Φ in (7.4) is modified to include the penalty as shown in (7.8).

$$\begin{aligned}\Phi = \underset{\Delta u, \epsilon_1, \epsilon_2}{min} & \sum_{i=0}^{H_u-1} \Delta u(k+i|k)^2 + \sum_{i=1}^{H_p} \rho\epsilon_1(k+i|k) \\ & + \sum_{i=1}^{H_p} \rho\epsilon_2(k+i|k)\end{aligned} \tag{7.8}$$

To reflect the fact that constraints on remote bus voltage magnitude is relaxed, (7.7) is updated to include the slack variable as shown in (7.9), where $i \in [1, H_p]$.

$$\begin{aligned}V^{min} - \epsilon_1(k+i|k) &\leq V(k+i|k) \\ &\leq V^{max} + \epsilon_2(k+i|k)\end{aligned} \tag{7.9}$$

Hence, the final optimization problem for the MPC controller is the objective function in (7.8) subjected to constraints, (7.2),(7.5),(7.6) and (7.9). This optimization problem, expressed in a standard form, can then be solved using well known quadratic programming algorithms such as interior-point convex method to obtain the optimal solution.

7.3 Field Test Setup

7.3.1 Geographical Setup

A geographical map depicting the location of the VSC close to the wind farm (red marker on left) and substation where voltage measurement is made at remote bus K4 (red marker

on right) is shown in Figure 7.1. An approximate outline of the cable connecting the two is also shown with a thick black line. The length of the cable connecting the VSC to the remote bus is approximately 3.4 kilometers.

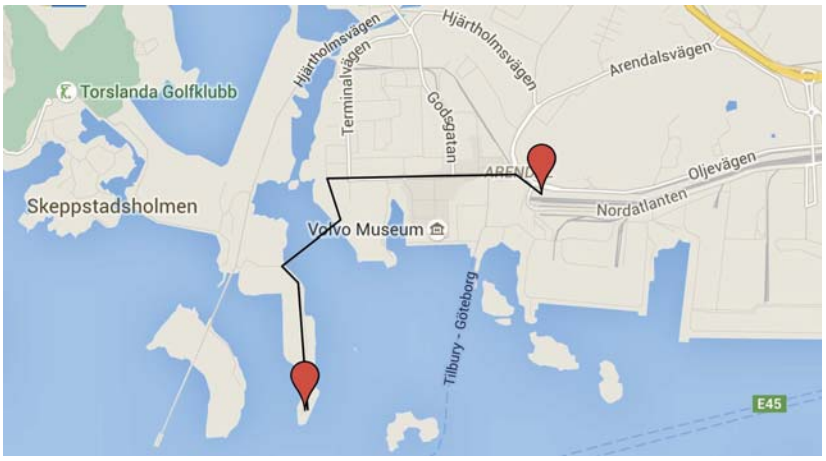

Figure 7.1: Geographical location of VSC (left red marker) and remote bus (right red marker) (maps courtesy: Google Maps).

7.3.2 Voltage Measurement Setup

In this setup, the reactive power from the VSC close to the wind farm is controlled to maintain the voltage at bus K4 between acceptable limits. The voltage measurement unit at K4 can sense values between 0-12.5 kV that are provided as scaled down voltage input to the MPC controller between a corresponding 1-5 V range. As shown by the dotted red line in Figure 7.2, voltage measurement is done at bus K4 and then transferred via ethernet using a Beckhoff CX8090 and finally transmitted to the VSC using a Teltonika RUT950G wireless router communicating over a 4G channel, the fourth generation of wireless mobile communications technology. At the MPC controller's end, the measurement signals are captured wirelessly using another Teltonika RUT950G wireless router that is connected to a Beckhoff CX8090 via ethernet, which then communicates the signals in real-time to the MPC controller, which is located close to the VSC. The sampling rate of the measurement device was given to be 10 samples per second with a total delay for wireless transmission of these voltage signals to be approximately 450 ms. The measurement delay however, was very small compared to the time resolution of the MPC controller, which was set to be 10 seconds. Hence, the delay was small enough to not affect the functioning of the control algorithm- especially after smoothening the measured voltage values as described

in Section 7.4.2.

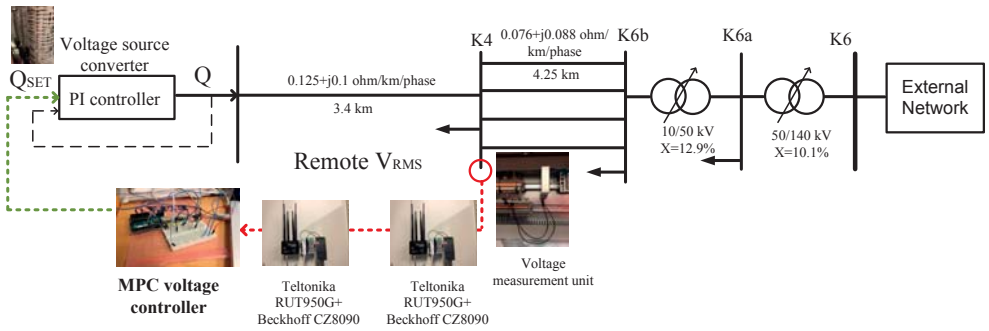

Figure 7.2: Measurement and Communication Setup.

According to historical voltage measurement data, continuous voltage variations could occur in the range of ±0.1 kV at the remote bus and is considered to be normal operation. This could also be observed from the measurements done by the authors and can be seen in Figure 7.4.

7.3.3 Voltage Source Converter

The VSC [112], whose geographical location is shown in Figure 7.1 is utilized for remote bus voltage control. It essentially consists of multiple modules of insulate-gate bipolar transistors (IGBT) that are connected together as shown in Figure 7.3. The VSC consists of a local controller that can be utilized either in reactive power or voltage control mode. For the field tests, the reactive power control mode for the local controller was activated. The setpoint to this local controller was provided from the MPC controller. It should be noted that even though the VSC is rated at 8 MVA, its actual reactive power output is limited to ±4 MVAr by the local controller due to current limitations imposed by the protection system. Furthermore, a positive value of reactive power output from the VSC is considered to be injection and a negative value, absorption.

7.3.4 Upstream Transformer

Within the considered network, there is a 50/10 kV tap changing transformer upstream of bus K4 that also tries to maintain the voltage within certain limits and could interact adversely with the MPC controller. By changing the reactive power output from the VSC, the remote bus voltage was forcibly varied to identify the voltage limits when the tap controller of the transformer is activated. Results from one instance of this test performed is shown in Figure 7.4.

Figure 7.3: Voltage source converter. IGBT stacks for the 10kV converter.

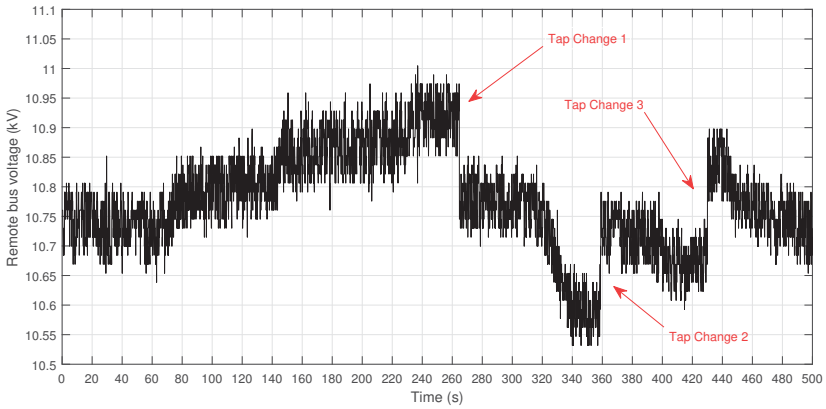

Figure 7.4: Measured remote bus voltage denoting instances of transformer tap activation.

Specifically, as seen from the figure, the tap controller was found to be activated when the bus voltage at K4 went beyond the limits of $[10.7, 10.9]$ kV for more than 40 seconds. Using these values as a base, the bus voltage limits for the MPC controllers were chosen to be within a narrower band to avoid any form of hunting. By modifying one tap step, the transformer is able to boost or reduce the K4 bus voltage by 1.67%, which in this case translates into a voltage change of 0.17 kV.

7.3.5 MPC Controller Setup

An Arduino Uno [113], a single-board microcontroller was used to translate the input voltage signals between 1-5 V into digital data that could be processed by a computer. Hence, the Arduino Uno, along with a computer, formed the MPC controller in this setup as shown in Figure 7.5. The MPC algorithm is implemented within the MATLAB

environment [114] in the computer. Output from the MPC controller is the optimal setpoint value to the local proportional-integral(PI) reactive power controller of the VSC (dotted green line in Figure 7.2). This reactive power setpoint is given as a voltage signal between 0-5 V that is then translated into corresponding reactive power value using a lookup table, which was provided by the operators of the VSC, i.e., Göteborg Energi AB in conjunction with Protrol AB.

Even though the VSC is rated at 8 MVA, its actual reactive power output is limited to ±4 MVAr by the local controller due to current limitations imposed by the protection system. Furthermore, the reactive limits for the MPC controller is considered to be $u^{min} = -3$MVAr and $u^{max} = +3$MVAr in order to clearly differentiate the limits observed by the MPC controller and the current limits imposed by the local reactive power controller.

The limits on changes in reactive power output was kept to be $\Delta u^{min} = -2$MVAr and $\Delta u^{max} = +2$MVAr as large variations in reactive power output was not desired. It was desired for the MPC controller to finish its control actions before a tap changer action could occur. Since, the tap controller was found to be inactive for at least 40 seconds after voltage deviation from the bounds, the prediction horizon H_p for the field test was considered to be 4 steps and the control horizon H_u was considered to be equal to 2 steps, which correspond to 40 seconds and 20 seconds in absolute time, respectively.

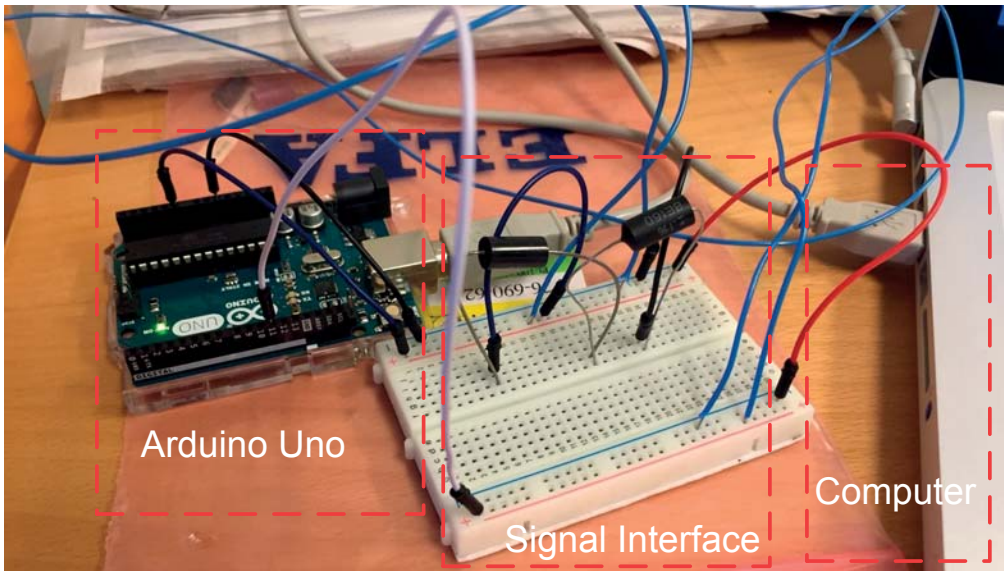

Figure 7.5: Overview of MPC Controller Setup.

7.3.6 Local Reactive Power Controller

It must be noted that there is a local reactive power controller. It is a PI controller with a rise time less than 1 second that is able to maintain the reactive output from the VSC based on a given setpoint value. Hence, for the purpose of this field test, it could be considered that the output from the VSC equals the setpoint value provided by the MPC controller almost instantly. This setpoint value is optimally modulated by the MPC controller in order to regulate the remote bus voltage. The latter, however, takes a few seconds to settle down to its new value after a change in reactive power output from the VSC as shown in Figure 7.7.

7.3.7 Model Sensitivity Gain Estimation

The sensitivity gain in (7.1) needs to be estimated and provided to the model as an input parameter. This gain depends on the system under investigation and its operating conditions. For a network with multiple control devices, the gains can be obtained from the linearized power flow solution performed at the control center. To verify this, power flow solution for the system shown in Figure 7.2 was obtained using DIgSILENT Powerfactory [106]. To obtain the sensitivity gain, the reactive power output from the VSC was changed by 1 MVAr and the effect of its change on the remote bus voltage was observed. The results of the simulations performed is shown in Figure 7.6

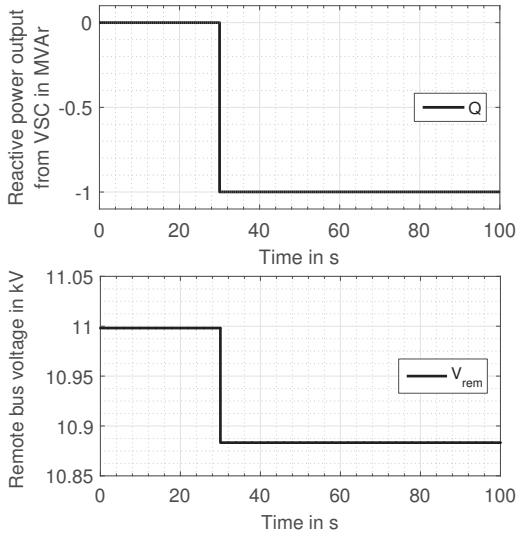

Figure 7.6: Results from simulation studies. Upper plot is reactive power output from VSC. Lower plot is remote bus voltage

From the simulations, the sensitivity gain $\frac{\partial V}{\partial u}$ for the system under consideration can be found out to be 0.115 kV/MVAr. The simulated values could also be compared with

step-response tests performed within the practical setup. Hence, repeated step response tests were performed by manually varying the reactive power output in multiple steps of 1 MVAr from the VSC and observing changes on the remote bus voltage magnitude. One instance when the 2 MVAr more reactive power was injected by the VSC and its effect on remote bus voltage is shown in Figure 7.7. The bus voltage changes from an initial value of 10.8 kV to a final value of 11.02 kV. The sensitivity gain $\frac{\partial V}{\partial u}$ was thus, found to be 0.11 kV/MVAr for this setup. This is slightly lower than the value found using simulations with the error being less than 5% between the theoretical estimation and its practical counterpart.

In comparison, a tap change by the tap controller of the transformer resulted in the remote bus voltage magnitude changing by 0.17 kV. Hence, actions of reactive power change by VSC can be differentiated from that of the tap controller by observing the magnitude change in the remote bus voltage. However, it should be noted that the VSC has only a marginal, but observable, influence on the remote bus voltage and the latter's magnitude is continuously varying due to switching of loads and operational changes in other parts of the distribution system.

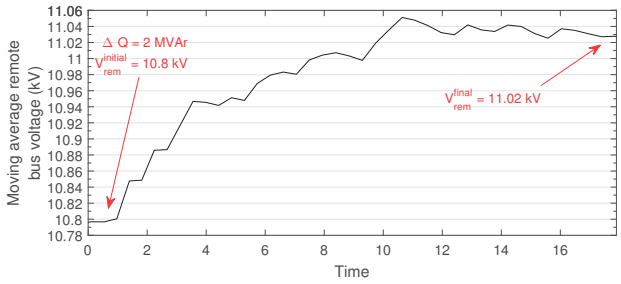

Figure 7.7: Result from step response tests.

7.4 Results

Field tests were performed using the designed MPC controller for a number of cases. Three cases of interest are reported, namely:

- Case 01: In the first case, initial trials with the controller were performed by utilizing the unaltered voltage measurement available and response action by the controller at the instant it was activated for voltage control.
- Case 02: From the lessons learned, modifications were made in the second case to provide smoothened voltage measurements to the controller and to let it begin its functioning after an initial time delay.
- Case 03: In the third case, an error in the sensitivity gain was introduced and also, the voltage bounds were shifted to lower values to observe if the MPC controller respects the constraints on reactive power from the VSC.

7.4.1 Case 1- Initial Trials

In this case, measured remote bus voltage was provided to the MPC controller every 10 seconds. The voltage bound for the controller is considered to be less than that of the transformer as explained in Section 7.3.4. Hence, the voltage limits were assigned as $V^{max} = 10.84$ and $V^{min} = 10.76$ kV. The voltage measurements obtained from the setup was left unaltered. This means that the voltages available to the controller looked like that depicted in Figure 7.4 with a normal variation in voltages around ± 0.1kV. Moreover, the MPC controller was instantly available for voltage control when it was activated. The resulting remote bus voltage as seen by the MPC controller is shown in Figure 7.8. It can be observed readily that, one, the controller only sees snapshots of the bus voltage and two, as the bus voltage is provided unaltered, the voltage bound assigned is lower than the possible normal variation in its magnitude. This could result in the controller reacting every 10 seconds, i.e., every time it receives a snapshot of the voltage measurement as seen in Figure 7.9. This is unnecessary and needs to be avoided. Hence, the proper functioning of the MPC controller depends heavily on the quality of the voltage measurement feedback provided to it. In this case, smoothening the voltage measurements and then providing the values to the MPC controller could potentially improve its response.

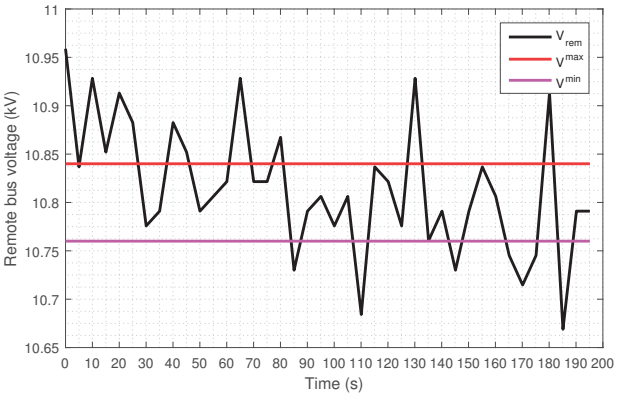

Figure 7.8: Case 01- Remote bus voltage.

The second observation to be made is that the MPC controller takes an action immediately after it is activated at time 0 seconds in Figure 7.9 where it has reacted to voltage being out of bounds by changing the reactive power setpoint by 0.75 MVAr to the local controller of the VSC. Coupled with unaltered voltage measurements, this also results in unnecessary control actions by the MPC controller that should also be avoided. Hence, a time delay should be provided from the time the controller is activated till the time it is made available for voltage control.

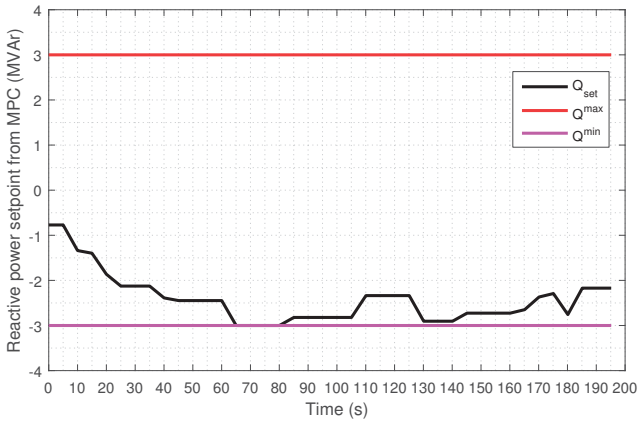

Figure 7.9: Case 01- Reactive power setpoint from MPC controller.

7.4.2 Case 2- Smoothened voltage measurements and initial time delay before controller activation

This case provides results after the two important challenges highlighted in Section 7.4.1 were addressed. So, the voltage values received from the remote measurement units were smoothened over a 5-second interval using a robust local regression smoothening. This resulted in much smoother voltage values made available to the MPC controller. Moreover, the controller was re-designed to not begin with voltage control actions at the instant it was activated by introducing a 30 seconds initial delay. E.g., the controller activated at 0^{th} second will begin to control the remote bus voltage at the 30^{th} second. This can be seen in Figure 7.10 and Figure 7.11. It should be noted that for Case 2, the voltage bound is defined to be slightly higher than for Case 1. This is due to the fact that the remote bus voltage was observed to be operating close to an average of 10.85 kV. Moreover, reactive power from the VSC has a marginal, but observable, influence over the voltage of remote bus in the network. This can also be inferred from the value of the sensitivity gain, which essentially reflects how much influence the reactive power change from the VSC has on the remote bus voltage. In this setup, the gain translates into a 0.01 p.u. voltage change for every 1 MVAr change in reactive power output from the VSC.

From Figure 7.10, it can be seen that the remote bus voltage V_{rem} is brought within the defined limits of $V^{max} = 10.89$ and $V^{min} = 10.81$ kV. The biggest change in voltage occurs at 40 seconds when there is a large deviation of the voltage from the maximum defined limit. This forces the MPC controller to take action by changing the reactive power setpoint Q_{set} to around 1.25 MVAr as seen in Figure 7.11. The voltage mostly remains within bounds for the rest of the test period. A small deviation from V^{max} occurs between 120 seconds and 140 seconds, which the MPC controller senses at 130 seconds and request a corresponding minor change in VSC reactive power setpoint.

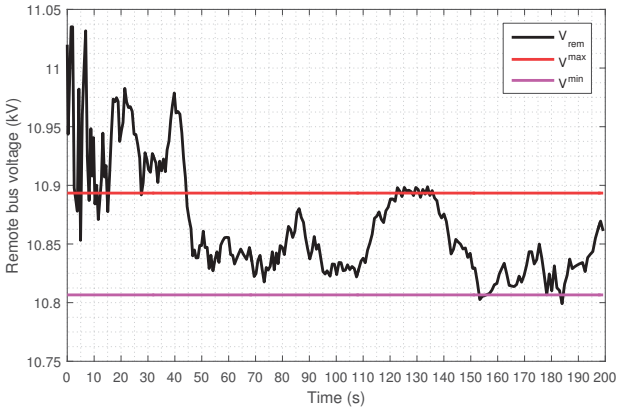

Figure 7.10: Case 02- Remote bus voltage.

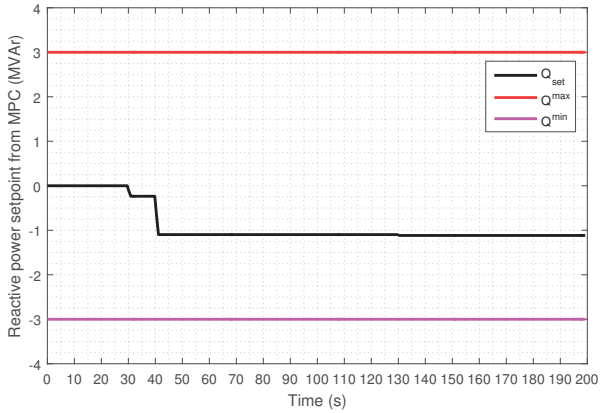

Figure 7.11: Case 02- Reactive power setpoint from MPC controller.

7.4.3 Case 3- Error in prediction model

It is clear from Case 2 that the MPC controller respects the limits on bus voltage limits at every time instance that voltage measurement is provided to it. Now, it would be interesting to see if the controller respects the limits on reactive power setpoint as well considering the changes made in terms of smoothening of voltage measurements and the initial delay provided to the controller. It would also be interesting to see if the MPC controller is able to compensate for errors in the sensitivity gain of the prediction model in (7.2) that was found using step response test. This is achieved in this case by changing the voltage limit band to the same that of Case 1 and by reducing the sensitivity gain to a value of 0.08 kV/MVAr, thereby introducing an error of 20% in the sensitivity gain.

The remote bus voltage results from this test case is shown in Figure 7.12, which shows

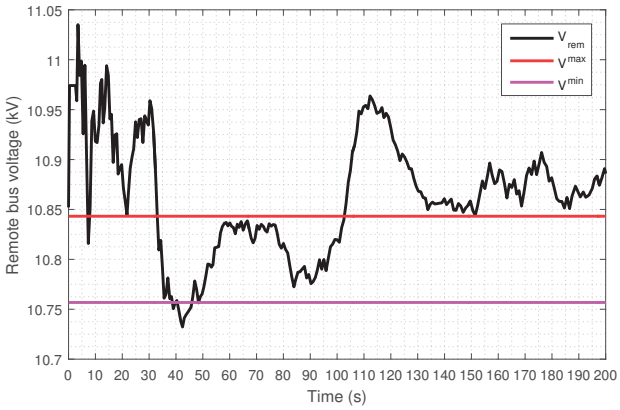

Figure 7.12: Case 03- Remote bus voltage.

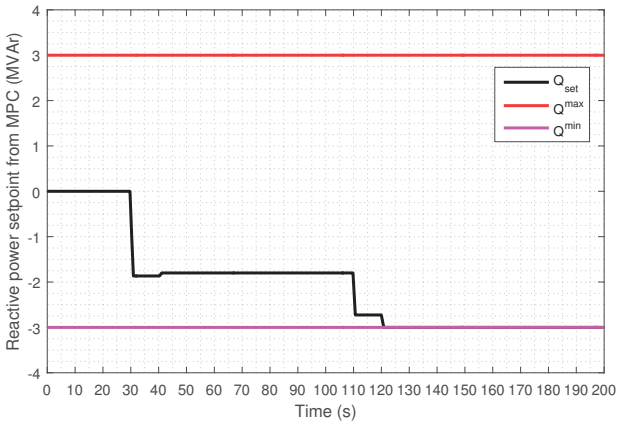

Figure 7.13: Case 03- Reactive power setpoint from MPC controller.

that there is a huge voltage change occurring at the 30^{th} second, i.e., at the instant that MPC controller starts to perform voltage control. Looking at Figure 7.13, the reason for this can be explained. Due to the error in the sensitivity gain provided to the model of the controller, it estimates more than necessary reactive power setpoint change. This is also reflected in the corresponding voltage change. Hence, the MPC controller still functions acceptably with slight errors in sensitivity gain values. However, it should be noted that if the sensitivity gain values were higher, i.e., if the reactive power change would have more influence over remote bus voltage change, then even small errors in sensitivity gains could result in unacceptably large deviations in reactive power setpoint change and remote bus voltage magnitudes.

Furthermore, the voltage varies continuously due to other events in the distribution network and subsequently increases to a value higher than maximum limit observed by the controller. This results in further control actions at time 110 and 120 seconds, after

which the minimum reactive power limit is reached. Hence, as seen in Figure 7.13, another point to note from the results of this case is that the limits on reactive power is observed by the MPC controller even after the changes made in smoothening voltage measurements and the initial time delay.

7.5 Summary

In this chapter, an MPC controller was mathematically developed for a single-input-single-output system. The aim of the work was to test whether an optimization-based voltage controller using the MPC algorithm functions as designed in a practical setting. Hence, an MPC controller was implemented and its real-time functioning was verified through field tests wherein a remote bus voltage was controlled by changing the reactive power output from a VSC located close to a wind farm.

Results from the test cases indicated that quality of voltage measurements given to the controller is pivotal in a well-functioning MPC controller. It was also found that a time delay provided to the controller between the time it is activated and the time it is made available for voltage control could help in avoiding unnecessary changes to reactive power output by the VSC. Small errors in estimated sensitivity gain values resulted in much greater changes in reactive power output by the controller than necessary. However, the performance was still acceptable since the bus that was being controlled was marginally influenced by VSC reactive power change.

Finally, a PI controller could also be used to perform this function for a single-input-single-output system that would perform as well, if not better, than an MPC controller. This work dealt with a controller with single input and single output due to limitations in the resources available for control. The real advantage of MPC could be obtained in cases when voltages at many buses in the network need to be controlled using multiple distributed energy sources such as PV and BESS. In such cases, the controller mathematical model described in this chapter could be readily extended to multi-input-multi-output systems as well, which would be an interesting future work to test on the field. Also, small disturbance in voltage measurements could occur all the time. Modeling of this disturbance and its subsequent rejection by the MPC controller would also be an essential part of future work.

Part IV

Conclusions

Chapter 8

Conclusions and Future Work

This chapter presents the main conclusions from this thesis. Possible ideas for future work that could meaningfully extend the work done in this thesis are also presented.

8.1 Conclusions

In this thesis, mathematical models have been proposed to study the impacts of large scale penetration of grid connected EVs on the demand profile within the test system, price of electricity in the day-ahead and regulating power markets and the changes in regulation cost due to demand response from EVs. Also, a framework for long-term energy portfolio optimization of an electricity retailer, who also assumes the market functions of an aggregator, has been proposed. Furthermore, coordinated voltage control in distribution systems with PV and BESS using centralized, decentralized and distributed MPC strategies have been developed and their performance compared against each other and local voltage control. Functioning of the developed MPC-based voltage control algorithm has also been verified through field tests. The main conclusions from various studies performed as part of this thesis are listed below.

8.1.1 Electricity Markets Perspective

Regarding the effects of EVs on day-ahead market, the following conclusions could be made:

- The proposed joint scheduling method assumes that there is a central dispatch of both generators and vehicle batteries thereby resulting in better utilization of both

the production resources and consumption side flexibilities. Whereas, the aggregator scheduling method reflects a more realistic scenario considering the Nordic market framework, with possibility for less efficient use of scheduling resources by aggregator due to errors in estimation of day-ahead market price.

- Case studies performed using a Nordic test system indicated that day-ahead price increase due to vehicle integration could be low at lower penetration of EVs. Electricity price increase was found to occur at higher levels of around 100% vehicle penetration, at which point, advanced methods of scheduling of EV charging could be needed to limit the increase.

- Transmission network constraints can directly influence the penetration level of the EVs that can be accommodated in the system before a significant increase in market price. This was observed in the constrained case where power transmission limit between different bidding areas resulted in price leveling within bidding area DK2 at 100% EV penetration when compared to the leveling at 300% in the unconstrained case.

- Changes in market price are also affected by other factors such as conventional load profile, bidding strategies by various players, state and availability of the production units, intra-area network constraints etc. Hence, more analysis would need to be done in order to observe the effects of these factors on a particular system and arrive at concrete conclusions.

From the case study of EV aggregator participation in the regulating power market, the following points were observed:

- Simulation results indicated that the system could benefit from the aggregated regulating power provided by EVs. The system gain was mostly found to occur in the form of lower regulation costs when EV aggregator bid competitively at lower marginal costs.

- Accounting for the effect of regulating power injection or withdrawal on transmission line losses resulted in a slightly different set of regulating power activation when compared to the merit-order list. The case study with up regulating power scenarios indicated lower regulation costs mostly due to lower up-regulating power prices offered by the EV aggregator.

- In the studies performed, it was assumed that the EV aggregator could predict the direction of regulation during a particular delivery hour, which is not entirely accurate. While, there might be indicators that could point to the direction of regulation, predicting it with a high degree of accuracy could prove extremely difficult, if not impossible, in a well functioning market.

- Activation of EVs for power regulation would be very much dependent on the aggregator's position to perform arbitrage just prior to the delivery hour, which is not entirely accounted for and hence, imposes limitations on the results from the study.

- Implementing the proposed activation method for RPM using re-valuation of bids could result in the activation of extremely small power output variations from generators at different buses. This might necessitate automatic control to be implemented by producers and aggregators as opposed to the manual control used today.

The following inferences could be made from the retailer planning model incorporating EV scheduling:

- The model was found to yield the necessary forward contract decisions, retail price setting for customers with two types of contracts, and EV demand scheduling as outputs. The price setting for retail contracts was assumed to be determined by the retailer based on the type of contract signed.
- An overall conclusion was that the total cost savings of EV owners could increase with EV penetration and also with the increasing number of customers signing variable price contracts with the retailer as opposed to fixed price contracts. This was also found to benefit the retailer, as the retailer's expected profit was found to increase with a greater share of customers opting for variable price contracts.
- The studies performed in this work have not accounted for imbalance costs faced by the retailer. This could have an impact on the profit margin of the retailer, the corresponding retail price set and the cost savings of EV owners. Hence, studies accounting for imbalance costs also need to be performed.

8.1.2 Voltage Control Perspective

The following conclusions can be drawn from the MPC voltage controller studies:

- Centralized MPC strategy provides the optimal solution in terms of system-wide voltage regulation. System losses and the reactive power utilized could be higher in the case of centralized MPC when compared to local voltage control due to the additional requirement on it to maintain monitored buses within voltage limits.
- Decentralized MPC strategy could be used in distribution system areas where there is a localized voltage issue due to high amounts of DGs in that area.
- Parallel distributed MPC strategy was found to provide results comparable to that of centralized MPC. It is the recommended strategy as it also provides the architectural advantage of decentralized MPC.

Based on the field tests performed using the MPC voltage controller, the following points could be deduced:

- Field tests indicate that the MPC-based voltage controller works in real-time within a practical setting.
- Smoothened voltage measurement feedback should be provided to the MPC controller for it to function satisfactorily and, according to its design criterion.

- It would be recommended to provide an initial delay between the time MPC controller is brought online and the time it begins to actively perform voltage control.

8.2 Future Work

The following ideas regarding electricity markets participation by the aggregator could be identified for future work:

- Intraday markets: the aggregator has the possibility of trading in the intra-day market such as Elbas that is cleared continuously between the day-ahead market clearing and the delivery hour. If deviations are known prior to the hour of delivery, this market could be valuable in correcting these deviations on time; possibly for a cost lower than that incurred in the regulating power market. It is also possible for the aggregator to perform arbitrage in this market and increase its profits. Furthermore, this continuous market could be used to co-optimize its energy bids in the intra-day and regulating power markets.
- Primary and Secondary reserve market: the aggregator could also participate in markets organized by the TSO in order to provide primary and secondary reserves. These reserves could prove useful to improve the frequency quality deterioration caused by large scale integration of variable and intermittent sources of power such as wind and solar.

With regards to challenges in the distribution network, the following could be addressed as an extension of this thesis:

- A field test using the MPC voltage controller with multiple devices in the network controlling numerous bus voltages could be done. This might provide further insights regarding practical issues encountered during implementation of the control strategy.
- With the help of multiple devices, it could also be possible to practically implement the parallel distributed MPC algorithm, which could then open up the possible challenges related to aspects of communication and its failure.
- It would be interesting to compare other optimization techniques with MPC-based strategies to deduce the best possible strategy for voltage control in distribution systems.
- Considering the market and power system operation framework, a unified model could be developed to simulate the scheduling of EVs for market participation and their subsequent control for power system support, e.g., voltage regulation and congestion management.

Bibliography

[1] *Technology roadmap: Electric and plug-in hybrid electric vehicles (ev/phev).* International Energy Agency, 2011.

[2] *Technology roadmap: Wind energy.* International Energy Agency, 2013.

[3] *Technology roadmap: Energy storage.* International Energy Agency, 2014.

[4] *Technology roadmap: Solar photovoltaic energy - 2014 edition.* International Energy Agency, 2014.

[5] "Renewable Capacity Statistics 2016", International Renewable Energy Agency, Tech. Rep. [Online]. Available: http://www.irena.org/DocumentDownloads/Publications/IRENA_RE_Capacity_Statistics_2016.pdf (visited on 09/28/2016).

[6] Pedro S. Moura and Aníbal T. de Almeida, "Large Scale Integration of Wind Power Generation", *Handbook of Power Systems I*, M. Panos Pardalos, Steffen Rebennack, F. Mario V. Pereira, and A. Niko Iliadis, Eds., Berlin, Heidelberg: Springer Berlin Heidelberg, 2010, pp. 95–119. [Online]. Available: http://dx.doi.org/10.1007/978-3-642-02493-1_5.

[7] *The 50.2 Hz problem.* Association for Electrical Electronic & Information Technologies (VDE). [Online]. Available: https://www.vde.com/en/ (visited on 08/29/2016).

[8] J. A. Peças Lopes, N. Hatziargyriou, J. Mutale, P. Djapic, and N. Jenkins, "Integrating distributed generation into electric power systems: A review of drivers, challenges and opportunities", *Electric power systems research*, vol. 77, no. 9, 1189–1203, Jul. 2007. DOI: 10.1016/j.epsr.2006.08.016. [Online]. Available: http://www.sciencedirect.com/science/article/pii/S0378779606001908 (visited on 09/28/2016).

[9] *Conclusion of the study on the 50.2 Hz shutdown of PV systems in the low voltage distribution network.* Association for Electrical Electronic & Information Technologies (VDE). [Online]. Available: https://www.vde.com/en/fnn/pages/50-2-hz-study.aspx (visited on 08/29/2016).

[10] F. Katiraei and J.R. Agüero, "Solar PV Integration Challenges", *Ieee power and energy magazine*, vol. 9, no. 3, 62–71, 2011. DOI: 10.1109/MPE.2011.940579.

[11] *VDE-AR-N 4105:2011-08 Power generation systems connected to the low-voltage distribution network - Technical minimum requirements for the connection to and parallel operation with low-voltage distribution networks.* Association for Electrical Electronic & Information Technologies (VDE), 2011.

[12] I. Leisse, O. Samuelsson, and J. Svensson, "Coordinated voltage control in medium and low voltage distribution networks with wind power and photovoltaics", *PowerTech (POWERTECH), 2013 IEEE Grenoble*, Jun. 2013. DOI: 10.1109/PTC.2013.6652349.

[13] James B. Rawlings and Brett T. Stewart, "Coordinating multiple optimization-based controllers: New opportunities and challenges", *Journal of process control*, Selected Papers From Two Joint Conferences: 8th International Symposium on Dynamics and Control of Process Systems and the 10th Conference Applications in Biotechnology8th International Symposium on Dynamics and Control of Process Systems and the 10th Conference Applications in Biotechnology, vol. 18, no. 9, 839–845, Oct. 2008. DOI: 10.1016/j.jprocont.2008.06.005. [Online]. Available: http://www.sciencedirect.com/science/article/pii/S0959152408001054 (visited on 07/02/2016).

[14] T. Stetz, F. Marten, and M. Braun, "Improved Low Voltage Grid-Integration of Photovoltaic Systems in Germany", *Ieee transactions on sustainable energy*, vol. 4, no. 2, 534–542, Apr. 2013. DOI: 10.1109/TSTE.2012.2198925.

[15] S. N. Salih and P. Chen, "On Coordinated Control of OLTC and Reactive Power Compensation for Voltage Regulation in Distribution Systems With Wind Power", *Ieee transactions on power systems*, vol. 31, no. 5, 4026–4035, Sep. 2016. DOI: 10.1109/TPWRS.2015.2501433.

[16] Jan Marian Maciejowski, *Predictive control: With constraints*. Pearson education, 2002.

[17] G. Valverde and T. Van Cutsem, "Model Predictive Control of Voltages in Active Distribution Networks", *Ieee transactions on smart grid*, no. 4, Dec. 2013.

[18] Brett T. Stewart, Aswin N. Venkat, James B. Rawlings, Stephen J. Wright, and Gabriele Pannocchia, "Cooperative distributed model predictive control", *Systems & control letters*, vol. 59, no. 8, 460–469, Aug. 2010. DOI: 10.1016/j.sysconle.2010.06.005. (visited on 08/11/2016).

[19] Jinfeng Liu, David Muñoz de la Peña, and Panagiotis D. Christofides, "Distributed model predictive control of nonlinear process systems", en, *Aiche journal*, vol. 55, no. 5, 1171–1184, May 2009. DOI: 10.1002/aic.11801. [Online]. Available: http://onlinelibrary.wiley.com/doi/10.1002/aic.11801/abstract (visited on 08/09/2016).

[20] K. Worthmann, C. M. Kellett, P. Braun, L. Grüne, and S. R. Weller, "Distributed and Decentralized Control of Residential Energy Systems Incorporating Battery Storage", *Ieee transactions on smart grid*, vol. 6, no. 4, 1914–1923, Jul. 2015. DOI: 10.1109/TSG.2015.2392081.

[21] N.S. Rau and W.D. Short, "Opportunities for the integration of intermittent renewable resources into networks using existing storage", *IEEE transactions on energy conversion*, vol. 11, no. 1, 181–187, Mar. 1996. DOI: 10.1109/60.486594.

[22] P. Richardson, D. Flynn, and A. Keane, "Optimal charging of electric vehicles in low-voltage distribution systems", *IEEE transactions on power systems*, vol. 27, no. 1, 268–279, Feb. 2012. DOI: 10.1109/TPWRS.2011.2158247.

[23] Willett Kempton and Steven E. Letendre, "Electric vehicles as a new power source for electric utilities", *Transportation research part d: Transport and environment*, vol. 2, no. 3, Sep. 1997. DOI: 10.1016/S1361-9209(97)00001-1.

[24] *Global EV Outlook 2016*. International Energy Agency. [Online]. Available: https://www.iea.org/publications/freepublications/publication/Global_EV_Outlook_2016.pdf (visited on 09/28/2016).

[25] J.A.P. Lopes, F.J. Soares, and P.M.R. Almeida, "Integration of electric vehicles in the electric power system", *Proceedings of the IEEE*, vol. 99, no. 1, Jan. 2011. DOI: 10.1109/JPROC.2010.2066250.

[26] Kejun Qian, Chengke Zhou, M. Allan, and Yue Yuan, "Modeling of load demand due to EV battery charging in distribution systems", *IEEE transactions on power systems*, vol. 26, no. 2, May 2011. DOI: 10.1109/TPWRS.2010.2057456.

[27] *Grid-for-vehicles (G4V) project*. [Online]. Available: http://www.g4v.eu/about.html (visited on 09/28/2016).

[28] *EDISON project*. [Online]. Available: http://www.edison-net.dk/About_Edison.aspx (visited on 09/28/2016).

[29] D. Steen, L.A. Tuan, O. Carlson, and L. Bertling, "Assessment of electric vehicle charging scenarios based on demographical data", *IEEE transactions on smart grid*, vol. 3, no. 3, Sep. 2012. DOI: 10.1109/TSG.2012.2195687.

[30] M. Parvania, M. Fotuhi-Firuzabad, and M. Shahidehpour, "Optimal demand response aggregation in wholesale electricity markets", *IEEE transactions on smart grid*, vol. 4, no. 4, Dec. 2013. DOI: 10.1109/TSG.2013.2257894.

[31] R.J. Bessa and M.A. Matos, "Optimization models for EV aggregator participation in a manual reserve market", *IEEE transactions on power systems*, vol. 28, no. 3, 3085–3095, Aug. 2013. DOI: 10.1109/TPWRS.2012.2233222.

[32] R.J. Bessa, M.A. Matos, F.J. Soares, and J.A.P. Lopes, "Optimized bidding of a EV aggregation agent in the electricity market", *IEEE transactions on smart grid*, vol. 3, no. 1, 443–452, Mar. 2012. DOI: 10.1109/TSG.2011.2159632.

[33] S.I. Vagropoulos and A.G. Bakirtzis, "Optimal bidding strategy for electric vehicle aggregators in electricity markets", *IEEE transactions on power systems*, vol. 28, no. 4, 4031–4041, Nov. 2013. DOI: 10.1109/TPWRS.2013.2274673.

[34] M. Gonzalez Vaya and G. Andersson, "Optimal bidding strategy of a plug-in electric vehicle aggregator in day-ahead electricity markets", *European energy market (EEM), 2013 10th international conference on the*, May 2013. DOI: 10.1109/EEM.2013.6607304.

[35] "Case Study: Sweden's Goteborg Energi Successfully rolled out Nuri Telecom's AiMiR RF Mesh AMI Solution to the Entire City of 270,000 Customers", NURI Telecom, Tech. Rep. [Online]. Available: http://www.nuritelecom.co.kr/prcenter/sweden.pdf (visited on 09/30/2016).

[36] Math Bollen, "EI R2011:03 Adapting Electricity Networks to a Sustainable Energy System – Smart metering and smart grids", Energy Markets Inspectorate, Tech. Rep., 2011. [Online]. Available: http://ei.se/Documents/Publikationer/rapporter_och_pm/Rapporter%202011/EI_R2011_03.pdf (visited on 09/30/2016).

[37] "The nordic electricity exchange and the nordic model for a liberalized electricity market", Nord Pool Spot, Tech. Rep. [Online]. Available: http://nordpoolspot.com/globalassets/download-center/rules-and-regulations/the-nordic-electricity-exchange-and-the-nordic-model-for-a-liberalized-electricity-market.pdf (visited on 09/28/2016).

[38] "Directive 2009/72/EC of the european parliament and of the council of 13 july 2009 concerning common rules for the internal market in electricity and repealing directive 2003/54/EC", Official Journal of the European Union, Tech. Rep., Jul. 2009. [Online]. Available: http://eur-lex.europa.eu/LexUriServ/LexUriServ.do?uri=OJ:L:2009:211:0055:0093:EN:PDF (visited on 11/04/2016).

[39] "Nord Pool Spot- Central to European Power Integration: Annual Report 2013", Nord Pool Spot, Tech. Rep. [Online]. Available: http://www.nordpoolspot.com/globalassets/download-center/annual-report/annual-report_nord-pool-spot_2013.pdf (visited on 11/04/2016).

[40] *Contract Specifications: Commodity Derivatives*. [Online]. Available: http://www.nasdaqomx.com/digitalAssets/103/103083_160620-joint-appendix-2---contract-specifications.pdf (visited on 11/04/2016).

[41] "Power Distribution in Europe Facts & Figures", EURELECTRIC, Tech. Rep., 2013. [Online]. Available: http://www.eurelectric.org/media/113155/dso_report-web_final-2013-030-0764-01-e.pdf (visited on 11/04/2016).

[42] "Treatment of Losses by Network Operators ERGEG Position Paper for public consultation", European Regulators Group for Electricity and Gas (ERGEG), Tech. Rep. [Online]. Available: http://www.energy-regulators.eu/portal/page/portal/EER_HOME/EER_CONSULT/CLOSED % 20PUBLIC % 20CONSULTATIONS/ELECTRICITY/Treatment%20of%20Losses/CD/E08-ENM-04-03_Treatment-of-Losses_PC_2008-07-15.pdf (visited on 11/04/2016).

[43] "Road map towards a common harmonised nordic end-user market", NordREG, Tech. Rep. 3-2012. [Online]. Available: http://www.nordicenergyregulators.org/wp-content/uploads/2012/12/Road-map-towards-a-common-harmonised-Nordic-end-user-market.pdf (visited on 11/04/2016).

[44] Iiro Rinta-Jouppi, *Smart meter- a field report from sweden*, Wien, Aug. 2009. [Online]. Available: http://portalapp.e-control.at/portal/page/portal/medienbibliothek/presse/dokumente/pdfs/Vattenfall_experience_in_Smart_Metering_Iiro_Rinta-Joupp.pdf (visited on 11/04/2016).

[45] A. G. Boulanger, A. C. Chu, S. Maxx, and D.L. Waltz, "Vehicle Electrification: Status and Issues", *Proceedings of the IEEE*, vol. 99, Jun. 2011. DOI: 10.1109/JPROC.2011.2112750.

[46] conEdison, *Types of electric vehicles*. [Online]. Available: http://www.coned.com/electricvehicles/types_of_EVs.asp (visited on 11/04/2016).

[47] Kankar Bhattacharya, Math HJ Bollen, and Jaap E. Daalder, *Operation of restructured power systems*. Springer Science and Business Media, LLC, 2001.

[48] "Mapping demand response in europe today", Smart Energy Demand Coalition, Tech. Rep., Apr. 2014. [Online]. Available: http://sedc-coalition.eu/wp-content/uploads/2014/04/SEDC-Mapping_DR_In_Europe-2014-04111.pdf (visited on 11/04/2016).

[49] C Bang, F Fock, and M Togeby, "The existing Nordic regulating power market", Ea Energy Analyses, Tech. Rep., May 2012. [Online]. Available: http://www.ea-energianalyse.dk/reports/1027_the_existing_nordic_regulating_power_market.pdf (visited on 11/11/2016).

[50] Camilla Hay and et. al., "Introducing electric vehicles into the current electricity market", EDISON Project, Tech. Rep., May 2010. [Online]. Available: www.edison-net.dk/~/media/EDISON/Reports/Edison%20Deliverable%202.3%20-%20Version%203.0.ashx (visited on 11/04/2016).

[51] S. L. Andersson, A. K. Elofsson, M. D. Galus, L. Göransson, S. Karlsson, F. Johnsson, and G. Andersson, "Plug-in hybrid electric vehicles as regulating power providers: Case studies of sweden and germany", *Energy policy*, vol. 38, no. 6, Jun. 2010. DOI: 10.1016/j.enpol.2010.01.006. (visited on 11/04/2016).

[52] "Flexibility: The role of DSOs in tomorrow's electricity market", European Distribution System Operators (EDSO), Tech. Rep., 2014. [Online]. Available: http://www.edsoforsmartgrids.eu/wp-content/uploads/public/EDSO-views-on-Flexibility-FINAL-May-5th-2014.pdf (visited on 11/04/2016).

[53] "Technology roadmap: Electric and plug-in hybrid electric vehicles", International Energy Agency (IEA), Tech. Rep., 2011. [Online]. Available: http://www.iea.org/publications/freepublications/publication/EV_PHEV_Roadmap.pdf (visited on 09/28/2016).

[54] Di Wu, D.C. Aliprantis, and K. Gkritza, "Electric energy and power consumption by light-duty plug-in electric vehicles", *IEEE transactions on power systems*, vol. 26, May 2011. DOI: 10.1109/TPWRS.2010.2052375.

[55] R. Rajaraman, J.V. Sarlashkar, and F.L. Alvarado, "The effect of demand elasticity on security prices for the PoolCo and multi-lateral contract models", *IEEE transactions on power systems*, vol. 12, Aug. 1997. DOI: 10.1109/59.630459.

[56] M. Pantos, "Exploitation of electric-drive vehicles in electricity markets", *IEEE transactions on power systems*, vol. 27, no. 2, May 2012. DOI: 10.1109/TPWRS.2011.2172005.

[57] N. Rotering and M. Ilic, "Optimal charge control of plug-in hybrid electric vehicles in deregulated electricity markets", *IEEE transactions on power systems*, vol. 26, Aug. 2011. DOI: 10.1109/TPWRS.2010.2086083.

[58] M. González Vayá, T. Krause, R. A. Waraich, and G. Andersson, "Locational marginal pricing based impact assessment of plug-in hybrid electric vehicles on transmission networks", *Proceedings of the cigre symposium*, 2011. [Online]. Available: http://www.eeh.ee.ethz.ch/uploads/tx_ethpublications/Gonzalez_cigre_2011.pdf (visited on 09/28/2016).

[59] J.R. Pillai and B. Bak-Jensen, "Integration of vehicle-to-grid in the western danish power system", *IEEE transactions on sustainable energy*, vol. 2, Jan. 2011. DOI: 10.1109/TSTE.2010.2072938.

[60] D. Dallinger, D. Krampe, and M. Wietschel, "Vehicle-to-grid regulation reserves based on a dynamic simulation of mobility behavior", *IEEE transactions on smart grid*, vol. 2, Jun. 2011. DOI: 10.1109/TSG.2011.2131692.

[61] J.M. Arroyo and A.J. Conejo, "Multiperiod auction for a pool-based electricity market", *IEEE transactions on power systems*, vol. 17, Nov. 2002. DOI: 10.1109/TPWRS.2002.804952.

[62] V. Silva, "Estimation of innovative operational processes and grid management for the integration of EV", Grid for Vehicles, Tech. Rep., 2011, p. 2. [Online].

Available: http://www.g4v.eu/datas/reports/G4V_WP6_D6_2_grid_management.pdf (visited on 05/28/2014).

[63] *Work package 1.3: Parameter manual*, RWTH Aachen, Dec. 2010. [Online]. Available: http://g4v.eu/downloads.html.

[64] *Charging lithium-ion*, Battery University, Apr. 2014. [Online]. Available: http://batteryuniversity.com/learn/article/charging_lithium_ion_batteries (visited on 09/28/2016).

[65] Mohammad Shahidehpour, Hatim Yamin, and Zuyi Li, *Market operations in electric power systems: Forecasting, scheduling, and risk management*. Wiley Online Library, 2002.

[66] "Statistics and prospects for the european electricity sector- 37th edition-EURPROG 2009", EURELECTRIC, Tech. Rep. [Online]. Available: http://www.eurelectric.org/media/43813/2009-180-0004-2009-180-0004-01-e.pdf (visited on 09/28/2016).

[67] *Power plant units (installed generation capacity greater than 100 MW)*, Nord Pool Spot, 2012. [Online]. Available: http://nordpoolspot.com/Download-Centre (visited on 09/28/2016).

[68] *The energy market 2004*. Swedish Energy Agency, 2004. [Online]. Available: https://energimyndigheten.a-w2m.se/FolderContents.mvc/Download?ResourceId=2163 (visited on 09/28/2016).

[69] *Energy in sweden – facts and figures (excel) 2015*, 2015. [Online]. Available: http://www.energimyndigheten.se/globalassets/statistik/overgripande-rapporter/energy-in-sweden-2015_150826.xlsx (visited on 09/28/2016).

[70] Gerard Doorman, G. H. Kjolle, Kjetil Uhlen, Einar Staale Huse, and Nils Flatabo, "Vulnerability of the nordic power system", *Report to the nordic council of ministers, SINTEF energy research*, 2004. [Online]. Available: https://www.hks.harvard.edu/hepg/Papers/Doorman.vul.nordic.system.0504.pdf (visited on 09/28/2016).

[71] *Stock of vehicles and population, by county*, Statistics Norway, 2012. [Online]. Available: http://www.ssb.no/en/transport-og-reiseliv/statistikker/bilreg/aar/2013-04-24?fane=tabell&sort=nummer&tabell=107760 (visited on 09/28/2016).

[72] *Vehicles in counties and municipalities at the turn of year 2013/2014*, Statistics Sweden, 2013. [Online]. Available: http://www.scb.se/en_/Finding-statistics/Statistics-by-subject-area/Transport-and-communications/Road-traffic/Registered-vehicles (visited on 09/28/2016).

[73] *Stock of vehicles per 1 january*, Statistics Denmark, 2012. [Online]. Available: http://www.statbank.dk/BIL707 (visited on 09/28/2016).

[74] *Motor vehicle stock*, Statistics Finland, 2013. [Online]. Available: https://www.stat.fi/til/mkan/index_en.html (visited on 09/28/2016).

[75] *Maximum NTC*, European Network of Transmission System Operators for Electricity (ENTSO-E), 2016. [Online]. Available: https://www.nordpoolspot.com/globalassets/download-center/tso/max-ntc.pdf (visited on 09/28/2016).

[76] C. Grigg, P. Wong, P. Albrecht, R. Allan, M. Bhavaraju, R. Billinton, Q. Chen, C. Fong, S. Haddad, S. Kuruganty, W. Li, R. Mukerji, D. Patton, N. Rau, D. Reppen, A. Schneider, M. Shahidehpour, and C. Singh, "The IEEE reliability test

system-1996. a report prepared by the reliability test system task force of the application of probability methods subcommittee", *IEEE transactions on power systems*, vol. 14, Aug. 1999. DOI: 10.1109/59.780914.

[77] ENTSOE, *Nordic Automatic FRR Workshop- Introduction and objective of the workshop*, ENTSOE, 2012. [Online]. Available: https : //www . entsoe . eu/fileadmin/user_upload/_library/publications/nordic/operations/Nordic_Automatic_FRR_Workshop.zip.

[78] *Private communication with Elin Broström, Senior Advisor, Market Design*, Svenska Kraftnät, Mar. 2013.

[79] H. Farahmand, S.M.A. Hosseini, G.L. Doorman, and O.B. Fosso, "Flow based activation of reserves in the nordic power system", *2010 IEEE power and energy society general meeting*, Jul. 2010. DOI: 10.1109/PES.2010.5589810.

[80] Pavan Balram, Le Anh Tuan, and Lina Bertling Tjernberg, "Stochastic programming based model of an electricity retailer considering uncertainty associated with electric vehicle charging", *European Energy Market (EEM), 10th International Conference on the*, May 2013. DOI: 10.1109/EEM.2013.6607404.

[81] Allen J. Wood and Bruce F. Wollenberg, *Power generation, operation, and control*, English. Wiley, New York, 1984.

[82] H. Farahmand, T. Aigner, G. L. Doorman, M. Korpas, and D. Huertas-Hernando, "Balancing market integration in the northern european continent: A 2030 case study", *IEEE transactions on sustainable energy*, vol. 3, Oct. 2012. DOI: 10.1109/TSTE.2012.2201185.

[83] Xing Wang, Yong-Hua Song, and Qiang Lu, "A coordinated real-time optimal dispatch method for unbundled electricity markets", *IEEE transactions on power systems*, vol. 17, May 2002. DOI: 10.1109/TPWRS.2002.1007922.

[84] M. Stubbe and et. al, *Long term dynamics: Final report. phase II*. CIGRE, 1995.

[85] Wang Feng, Le Anh Tuan, L.B. Tjernberg, A. Mannikoff, and A. Bergman, "A new approach for benefit evaluation of multiterminal VSC-HVDC using a proposed mixed AC/DC optimal power flow", *IEEE transactions on power delivery*, vol. 29, Feb. 2014. DOI: 10.1109/TPWRD.2013.2267056.

[86] *Historical Market Data- Consumption*, Nord Pool Spot, Dec. 2012. [Online]. Available: http://www.nordpoolspot.com/Market-data1/Downloads/Historical-Data-Download1/Data-Download-Page/ (visited on 06/11/2014).

[87] Pavan Balram, Le Anh Tuan, and Lina Bertling Tjernberg, "Effects of plug-in electric vehicle charge scheduling on the day-ahead electricity market price", *IEEE PES Innovative Smart Grid Technologies (ISGT europe)*, Oct. 2012. DOI: 10.1109/ISGTEurope.2012.6465755.

[88] *Knowledge base for the market in electric vehicles and plug-in hybrids*, English, Swedish Energy Agency, 2009. [Online]. Available: https://energimyndigheten.a-w2m.se/FolderContents.mvc/Download?ResourceId=2508 (visited on 05/28/2014).

[89] Gerard Doorman and Stefan Jaehnert, "Modelling an integrated northern european regulating power market based on a common day-ahead market", eng, IAEE, 2010. (visited on 07/03/2013).

[90] J. Kettunen, A. Salo, and D.W. Bunn, "Optimization of electricity retailer's contract portfolio subject to risk preferences", *IEEE transactions on power systems*, vol. 25, no. 1, Feb. 2010. DOI: 10.1109/TPWRS.2009.2032233.

[91] M. Carrion, A.J. Conejo, and J.M. Arroyo, "Forward contracting and selling price determination for a retailer", *IEEE transactions on power systems*, vol. 22, no. 4, 2105–2114, Nov. 2007. DOI: 10.1109/TPWRS.2007.907397.

[92] Jasna Tomić and Willett Kempton, "Using fleets of electric-drive vehicles for grid support", *Journal of power sources*, vol. 168, no. 2, Jun. 2007. DOI: 10.1016/j.jpowsour.2007.03.010.

[93] R.J. Bessa, F.J. Soares, J.A. Pecas Lopes, and M.A. Matos, "Models for the EV aggregation agent business", *2011 IEEE PowerTech trondheim*, Jun. 2011. DOI: 10.1109/PTC.2011.6019221.

[94] Peter Kall and Stein W. Wallace, *Stochastic programming*. John Wiley & Sons, Chichester, 1994.

[95] Antonio J. Conejo, Miguel Carrión, and Juan M. Morales, *Decision making under uncertainty in electricity markets*. Springer- International Series in Operations Research & Management Science, 2010.

[96] Faisal Mehmood Mirza and Olvar Bergland, "Pass-through of wholesale price to the end user retail price in the norwegian electricity market", *Energy economics*, vol. 34, 2003–2012, Nov. 2012. DOI: 10.1016/j.eneco.2012.08.004. [Online]. Available: http://www.sciencedirect.com/science/article/pii/S0140988312001740 (visited on 06/12/2014).

[97] *Power situation in Sweden*, Svensk Energi, 2013. [Online]. Available: http://www.svenskenergi.se.

[98] D. Paravan, G.B. Sheble, and R. Golob, "Price and volume risk management for power producers", *2004 international conference on probabilistic methods applied to power systems*, Sep. 2004.

[99] R.Tyrrell Rockafellar and Stanislav Uryasev, "Conditional value-at-risk for general loss distributions", *Journal of banking & finance*, vol. 26, no. 7, Jul. 2002. DOI: 10.1016/S0378-4266(02)00271-6.

[100] *Elspot Prices 2012 Hourly EUR*, Nord Pool Spot, Apr. 2013. [Online]. Available: http://nordpoolspot.com/Market-data1/Downloads/Historical-Data-Download1/Data-Download-Page/.

[101] *Vehicles in counties and municipalities at the turn of year 2012/2013*, Statistics Sweden, Feb. 2013. [Online]. Available: http://www.scb.se/Statistik/TK/TK1001/2012A01B/Internet_kommun2012.xls (visited on 04/03/2014).

[102] R. E Rosenthal, "GAMS- A User's Guide", English, Tech. Rep., 2012, p. 304. [Online]. Available: http://www.gams.com/dd/docs/bigdocs/GAMSUsersGuide.pdf (visited on 04/04/2012).

[103] J. von Appen, M. Braun, T. Stetz, K. Diwold, and D. Geibel, "Time in the Sun: The Challenge of High PV Penetration in the German Electric Grid", *Ieee power and energy magazine*, vol. 11, no. 2, 55–64, Mar. 2013. DOI: 10.1109/MPE.2012.2234407.

[104] I. Leisse, O. Samuelsson, and J. Svensson, "Electricity meters for coordinated voltage control in medium voltage networks with wind power", *Innovative Smart*

Grid Technologies Conference Europe (ISGT Europe), 2010 IEEE PES, Oct. 2010. DOI: 10.1109/ISGTEUROPE.2010.5638977.

[105] *Connecting and operating storage units in low voltage networks*. Association for Electrical Electronic & Information Technologies (VDE). [Online]. Available: https://www.vde.com/en/fnn/documents/fnn_connecting-operating-storage-units-in-low-voltage-networks_2013-06.pdf (visited on 09/15/2016).

[106] *User's manual digsilent powerfactory*. DIgSILENT, 2015.

[107] *Benchmark systems for network integration of renewable and distributed energy resources*. CIGRÉ, 2009.

[108] Pavan Balram, Le Anh Tuan, and Ola Carlson, "Predictive voltage control of batteries and tap changers in distribution system with photovoltaics", *Power Systems Computation Conference (PSCC)*, Jun. 2016. DOI: 10.1109/PSCC.2016.7540847.

[109] A. M. Ersdal, L. Imsland, and K. Uhlen, "Model Predictive Load-Frequency Control", *Ieee transactions on power systems*, vol. 31, no. 1, 777–785, Jan. 2016. DOI: 10.1109/TPWRS.2015.2412614.

[110] Mats Larsson, David J. Hill, and Gustaf Olsson, "Emergency voltage control using search and predictive control", *International journal of electrical power & energy systems*, vol. 24, no. 2, Feb. 2002. DOI: 10.1016/S0142-0615(01)00017-5.

[111] James B Rawlings and David Q Mayne, *Model predictive control: Theory and design*. Nob Hill Publishing, LLC, 2009.

[112] Nicolas Espinoza, Massimo Bongiorno, and Ola Carlson, "Frequency Characterization of Type-IV Wind Turbine Systems", *2016 IEEE Energy Conversion Congress and Exposition (ECCE)*, Sep. 2016.

[113] *Arduino UNO*. Arduino, 2016. [Online]. Available: https://www.arduino.cc/en/Main/ArduinoBoardUno.

[114] MATLAB, *Version (r2015a)*. Natick, Massachusetts: The MathWorks Inc., 2015.

[115] Pavan Balram, Le Anh Tuan, and Lina Bertling Tjernberg, "Centralized Charging Control of Plug-in Electric Vehicles and Effects on Day-Ahead Electricity Market Price", *Plug In Electric Vehicles in Smart Grids*, ser. Power Systems, DOI: 10.1007/978-981-287-317-0_9, Springer Singapore, 2015, pp. 267–299.

[116] Pavan Balram, Le Anh Tuan, and Lina Bertling Tjernberg, "Modeling of regulating power market based on AC optimal power flow considering losses and electric vehicles", *IEEE PES Innovative Smart Grid Technologies (ISGT Asia)*, Nov. 2013. DOI: 10.1109/ISGT-Asia.2013.6698740.

[117] David Steen, Pavan Balram, Le Anh Tuan, Lina Reichenberg, and Lina Bertling Tjernberg, "Impact assessment of wind power and demand side management on day-ahead market prices", *IEEE PES Innovative Smart Grid Technologies (ISGT europe)*, Oct. 2014. DOI: 10.1109/ISGTEurope.2014.7028819.

[118] Pavan Balram, Le Anh Tuan, Ola Carlson, Ingmar Leisse, Pierre Andersson-Ek, Demijan Panic, and Malin Johnsson, "Coordinated voltage control in LV distribution systems with photovoltaics using MPC", *Submitted to Journal of Electric Power Systems Research*, 2016.

[119] Pavan Balram, Le Anh Tuan, and Ola Carlson, "Distributed MPC-based coordinated voltage control in multi-area active distribution systems", *Submitted to Journal of Energy Conversion and Management*, 2016.

[120] Pavan Balram, Le Anh Tuan, and Ola Carlson, "Comparative study of MPC based coordinated voltage control in LV distribution systems with photovoltaics and battery storage", *Submitted to International Journal of Electrical Power and Energy Systems*, 2016.

[121] Pavan Balram, Ola Carlson, and Le Anh Tuan, "Demonstration of voltage control in a real distribution system using model predictive control", *Submitted to IET Journal of Generation, Transmission and Distribution*, 2016.